AN ABSTRACT OF THE THESIS OF

Anthony Clinton Schacher for the degree of Master of Science in Electrical and Computer Engineering presented on June 9, 2004.
Title: Investigation and Comparison Of Generators for Dynamic Operation in Ocean Buoys

Abstract approved:

Alan K. Wallace, Annette vonJouanne

A significantly untapped renewable energy source exists in the world's oceans. It is estimated that if 0.2% of the ocean's untapped energy could be harnessed, it could provide power sufficient for the entire world. Ocean energy extraction is an old concept, and it is currently seeing the benefit of advancing support technologies and an increasing awareness of potential future energy deficits.

Girard, in Paris, registered the world's first wave energy device patent in 1799. Over more than 200 years of development, the number of patents has greatly increased and today there are currently more than 1500 ocean wave energy device patents.

This thesis presents and examines the concept of using an ocean wave as the prime mover for a buoy-mounted, directly driven, electrical generator. The primary focus will be on two particular generator types, a Permanent Magnet Synchronous Generator (PMSG) and a Wound Rotor Induction Generator (WRIG), and their reactions to a simulated wave profile.

The simulations were based on the concept of a directly driven screw, either a roller screw or ball screw, and a sinusoidal wave profile.

The development of this thesis moves through four sections: introduction of wave energy, the details of the experimentation that was conducted; the results of those experiments and the comparisons with mathematical models; and finally the conclusion and recommendations for future experimentation in this area.

A number of different experiments have been conducted for this thesis on the directly driven buoy generator scenario. They range from baseline control tests, which establish a characterization of the generators, to intricate multi-directional reciprocating drive research.

The reciprocating drive scenario is used to simulate a unidirectional direct drive, where one half of the stroke is used to generate electrical power and the energy from the other half of the stroke is stored in inertial mass, such as a spring, or some other similar energy storage device.

The experiments were conducted on both the PMSG and the WRIG as was appropriate to their characteristics, to see how each of the platforms reacts to similar prime movers. Experimental data from the PMSG and WRIG investigations will help to home in on which type of generator would be more suitable for a given buoy generator design. The designation will be based on two main factors, the physical generator to drive screw connection, and the power take-off (PTO) system to be implemented between the buoy generators and the electrical utility grid.

Additionally, an over-running clutch connection will be implemented to verify the notion of a partial cycle "free-wheeling" generation scheme based on the inertial force of the generator itself. It has been hypothesized that if the inertial force of the generator were greater than the load force from the output connection, then the

generator would be allowed to "free-wheel" through half of the wave cycle. This will allow the generator to remain rotating in one direction, as opposed to a directly coupled connection which would force the direction of rotation to oscillate from clockwise to counterclockwise as the buoy driving the generator floated over a wave front. By creating a unidirectional rotation, the ability to use a WRIG becomes much more applicable due to the requirement for fairly high rotational speed for generation.

Much like a child's mechanical top, a WRIG will be able to run up to a base speed suitable for generation and then the electrical utility grid connection will be energized.

By contrast, the PMSG would likely be used in a reciprocating scenario thereby taking advantage of the intrinsic constant magnetic field, which will produce a usable output at low rotational speeds.

It is concluded that each of these generators will have a potential niche to fill in Ocean Energy extraction buoys. Due to the reciprocating nature of the ocean waves and the varying periods and magnitudes, some form of the output conditioning will need to be applied if there are plans for a direct grid connection. The WRIG outputs a fairly constant voltage but the current magnitude varies with the wave profile. If some form of current leveling was introduced and the output current magnitude was made more constant the WRIG will be the prime candidate for a direct grid connection. The PMSG, and its ease of output rectification make it the choice for a rectified transmission to shore scheme, where it can then be inverted to undistorted ac power and connected into the electrical utility grid.

Investigation and Comparison of Generators for Dynamic Operation in Ocean Buoys

By

Anthony Clinton Schacher

A THESIS

Submitted to

Oregon State University

In partial fulfillment of
the requirements of the
degree of

Master of Science

Presented June 9, 2004

Commencement June 2005

Master of Science thesis of Anthony Clinton Schacher presented on June 9, 2004.

APPROVED:

Co-Major Professor, representing Electrical and Computer Engineering

Co-Major Professor, representing Electrical and Computer Engineering

Associate Director of the School of Electrical Engineering and Computer Science

Dean of the Graduate School

I understand that my thesis will become part of the permanent collection of Oregon State University libraries. My signature below authorizes release of my thesis to any reader upon request.

Anthony Clinton Schacher, Author

ACKNOWLEDGEMENTS

I wish to thank my co-advisors and major professors, Dr. Alan Wallace and Dr. Annette vonJouanne, for helping to guide me through my research and for keeping me focused on the task at hand. I learned many things from both that I will be able to take with me in my professional career.

I would also like to take a moment to thank my additional committee members, Dr. Jimmy Eggerton and Prof. Robert Schultz for taking the time to show their support, for reviewing my thesis, and participating in my defense.

Additionally, a special thanks goes to all of the guys in the Motor Systems Resource Facility and on the Ocean Energy Senior Design team that have helped me keep a smile on my face. Especially to Manfred Dittrich, Emmanuel Agamloh, Michael Mills-Price, Waylon Bowers, Xiaolin Zhou, and Jifeng Han. Thanks Guys for all of the help.

To my family and friends, thanks for all of the support through these many, many, many years of school. You all thought I was crazy but look what 7 years will get you!

Last, but certainly not least, I want to say thanks to my parents, Kay and Ted Schacher. They have been there for me through it all, to help whenever I needed it and to just be there when I needed someone to bounce ideas off of.

TABLE OF CONTENTS

LIST OF FIGURES

LIST OF FIGURES (CONTINUED)

LIST OF FIGURES (CONTINUED)

Figure Page

LIST OF TABLES

LIST OF TABLES (CONTINUED)

LIST OF APPENDICES

LIST OF APPENDIX FIGURES

LIST OF APPENDIX FIGURES (CONTINUED)

LIST OF APPENDIX FIGURES (CONTINUED)

LIST OF APPENDIX TABLES

LIST OF APPENDIX TABLES (CONTINUED)

1 INTRODUCTION

1.1 Ocean Energy Extraction – Opportunity is Knocking

A significantly untapped renewable energy source exists in the world's oceans: it is estimated that if 0.2% of the ocean's untapped energy could be harnessed, it could provide power sufficient for the entire world [1]. Ocean energy exists in forms of wave, tidal, thermal and salinity, with wave energy, having been studied most extensively.

Previous literature research has shown that the Oregon coast is one of the coastlines that contain the richest ocean energy potentials in North America. Following along those lines it is only a matter of time before some form of Ocean Wave Energy Extraction (OWEE) device is developed for the Oregon Coast.

1.2 Ocean Energy Extraction Techniques

Girard, in Paris, registered the world's first wave energy device patent in 1799. Over more than 200 years of development, the number of patents has greatly increased and today there are currently more than 1500 ocean wave energy device patents.

Within the last fifty years or so there has been two major drives to bring OWEE into the mainstream. The research that was conducted during these boom times was the result of the early 1970's oil crisis and the mid to late 1990's public awareness to an impending shortage of our natural resource reserves and the overall increased pollution from fossil fuel generating plants.

1.2.1 Classification of Ocean Energy Extraction Devices

Ocean energy extraction devices can be classified according to the distance between the devices and the shoreline. The three major classifications are shoreline, nearshore and offshore.

1.2.1.1 Shoreline Devices

Shoreline devices are fixed to or embedded in the shoreline and they utilize the power that is released from the ocean waves as they impact the ocean shore, i.e. on jetties, rock outcroppings, or the beach itself.

Shoreline devices have the distinct advantages of easier access for installation, maintenance, upkeep, and upgrade. They also have no requirements for deep-water moorings or long submersible electrical cable. The disadvantages of shoreline devices is that as a wave travels towards the shoreline it incurs a significant loss of power due to the friction caused by a rough seabed, another caveat is the environmental and aesthetic impact that shoreline devices intrinsically possess.

One of the most extensively studied shoreline devices is the Oscillating Water Column, or OWC. An OWC system has a partially submerged hollow air chamber, which opens to the sea under the water line. A wave enters the air chamber and forces the air in the column to pass through a turbine. As the wave retreats, the air will be drawn back and pass through the turbine again. See Fig. 1.1 for the basic working principle of the OWC. In most applications the unidirectional Wells turbine is used, which is designed to rotate in the same direction regardless of the direction of the airflow past it.

The LIMPET 500 by Wavegen is the first commercially implemented OWC. [2] In the United Kingdom, the LIMPET generates a peak power of 500 kW, enough to run about 400 island homes. The experimental station located on the Island of Islay has successfully fed electricity into the UK's national electrical utility grid since November 2000.

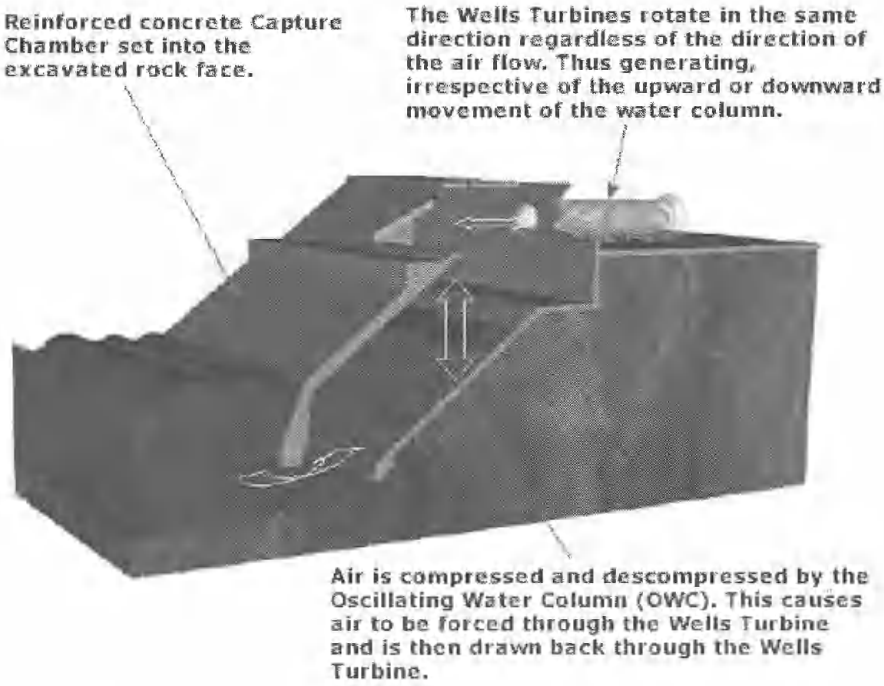

Fig. 1.1: Basic Working Principle of the Oscillating Water Column [2]

The LIMPET design was developed for ease of construction and installation with minimal visual intrusion. [2]

1.2.1.2 Nearshore Devices

The nearshore devices are in between the shoreline devices and the offshore devices. Nearshore devices are characterized by being used to extract the power directly from the breaker zone and the waters immediately beyond the breaker zone.

The depths are relatively shallow (<40m) and the turbidity of the associated water can be quite a bit higher, when compared to offshore devices. Nearshore devices are somewhat of a compromise between shoreline and offshore devices. These nearshore devices have many of the same constraints on them as the offshore devices; they must have an electrical utility grid connection through a submersible electric cable, though considerably shorter in length. They are also prone to many of the same environmental conditions. The nearshore devices will likely require a specific vessel for maintenance and upkeep, though considerably smaller than the vessels required for offshore devices, due to the relative proximity to shore.

An example of a nearshore device is the Pelamis Wave Dragon developed by Ocean Power Delivery in Edinburgh, Scotland. This is a semi-submerged, articulated structure composed of cylindrical sections linked by hinged joints. As the waves peak and trough, the sections of the Pelamis act as a pump and move hydraulic fluid through hydro-turbine generators. The power generated from each segment runs to an underwater substation and then to land via a submersible electric cable. Fig. 1.2 shows an artists rendition of the Pelamis Wave Dragon.

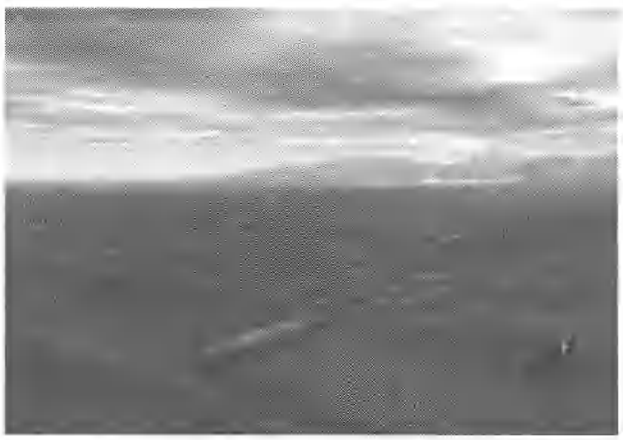

Fig. 1.2: Artists rendition of the Pelamis Wave Dragon [11]

1.2.1.3 Offshore Devices

Offshore devices are the farthest out to sea; they extend well beyond the breaker lines and utilize the high energy densities and higher power wave profiles available in the deep-water (>40m) waves and surge.

In order to extract the maximum amount of energy from the waves, the devices need to be at or near the surface. This makes it a requirement to have flexible moorings. In addition, submersible electrical cables are needed to transmit the generated power onto land where it can be tied into the grid. Maintaining offshore devices is a critical issue, specialized maintenance vessels are necessary to provide for any upkeep or needed repair services to the units. These factors will create difficult cost implications, which must translate into preemptive specifications in construction, maintenance, and overall upkeep.

The AquaBuoy is one such offshore buoy system. The technology was originally patented in Sweden, and is now being promoted by the AquaEnergy Group of Mercer Island, Washington. The up and down motions of ocean waves cause pressure changes which draws seawater into a hose pump. This pressurized water is expelled into a collecting line leading to a turbine, which generates electricity. The individual sizes of the buoys are designed according to the energy content of the prevailing seas at a particular installation site. The capacity of the plant is scalable by using different numbers of buoys. [5] The working principle of the AquaBuoy is shown in Fig. 1.3.

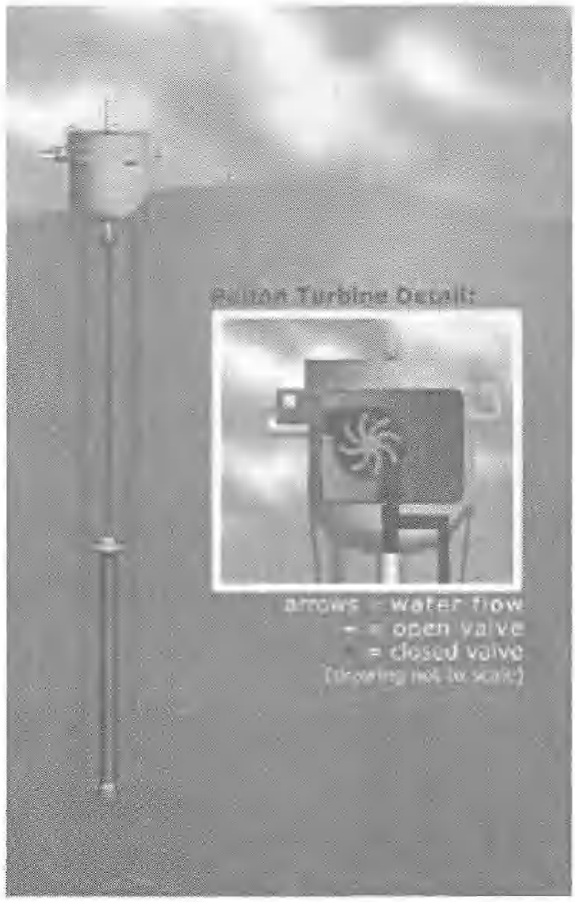

Fig. 1.3: Basic Working Principle Behind the AquaEnergy AquaBuoy [12]

Offshore devices can be designed and installed to have relatively little impact to the environmental and aesthetic regard of coastal communities. The devices can be placed in such a way that they have little visible impact and can actually provide homes for many aquatic creatures, similar to an artificial reef.

NOTE: The nearshore and offshore classification lends itself to being a bit of a grey area, due to the fact that many of the devices being developed for one or the other of the classifications could very easily be implemented into either regime.

1.2.2 A Diversion from the Norm

To date, offshore buoy type devices, with the exception of the Archimedes Wave Swing, and the buoy generator from the Oregon State University Ocean Energy Senior Design Group, have been based on a hydraulic system. Seawater, or some other operating fluid is pumped by the oscillating wave fronts, through a basic fluidic turbine and the resulting rotary motion is coupled with the shaft of an electrical generator. This hydraulic system, though a proven technology, is both inefficient and costly in terms of maintenance, design, and environmental compatibility. There is ample opportunity for hydraulic leaks into the surrounding environment and keeping a pumping system running at its peak in an environment as harsh, and in constant motion, as the sea is nearly impossible without persistent costly supervision.

As a result, the idea of a direct mechanical connection to the generator via a roller screw or ball screw used to convert periodic linear motion to a cyclical rotary motion is proposed. The significance of a directly connected system is that the need for a secondary system, such as the hydraulic components, to convert the linear motion to rotary motion is eliminated. By eliminating these components the need for maintenance greatly decreases, making the overall system more robust. The result is a generation platform that has the potential for improved reliability, survivability, and maintainability. In short it simplifies the generating process.

1.2.2.1 Simulation Investigation of a Directly Connected Generator

The following thesis report covers the investigation and research of a simulated directly connected generator. The purpose of the investigation is to create a characterization of the expected output performance of a generator driven by the

periodicity of an ocean wave. The Motor Systems Resource Facility (MSRF) main test bed and fully programmable drive was used to simulate the driving force of a roller screw or ball screw on an electrical generator. The following two generators were used to compare the output differences of each type to similar prime movers. The first is a 5 hp (3.73 kW) permanent magnet synchronous generator (PMSG), and the second is a 15 hp (11.19 kW) wound rotor induction generator (WRIG).

The PMSG will be used to approximate and simulate the effects of a generator that will have a directly connected oscillating speed from 262.5 rev/min maximum speed through the zero point to -262.5 rev/min minimum operating speed. The resulting output will be indicative of the output that can be expected in a pseudo real-life situation. The main caveat of all of the testing is that in the lab there is the capability to create a near perfect speed profile. It should be realized by the reader that the real life situations, especially at sea, are not likely to meet the same ideal characteristics. However, the output from the testing will be adequate to settle without a doubt the overall proof of concept and allow following researchers the information necessary to continue on with the work that has been started.

1.3 Testing Facilities

The practical investigations were performed in the MSRF at Oregon State University (OSU). In late 1993 the MSRF was initiated by a consortium of the Electric Power Research Institute (EPRI), Bonneville Power Administration (BPA), the U.S. Dept. of Energy (DoE), and Pacific Gas and Electric Company (PG&E). The overall test bed configuration of the MSRF is illustrated in Figure1.4, and its technical data can be viewed in Appendix A.

The MSRF is an independent test laboratory that serves as a regional resource for conducting research and tests on electric motors, generators, and adjustable speed drives (ASD) with ratings up to 300 hp. A regenerative, bi-directional vector-controlled converter with an induction machine as a dynamometer enables both motor and generator tests. The system is designed to operate in an energy recirculation mode in which 80-90% of the demanded energy, depending on the device under test, is circulated back through the internal power system. The MSRF also features a 600A three-phase independent autotransformer with a voltage range of 0 to 600V/phase. The autotransformer phase voltage can be adjusted both manually and by three-phase automatic operation over a driven gear system. This enables testing of single-phase machines besides multiphase machines in balanced, unbalanced, under-voltage, or over-voltage conditions.

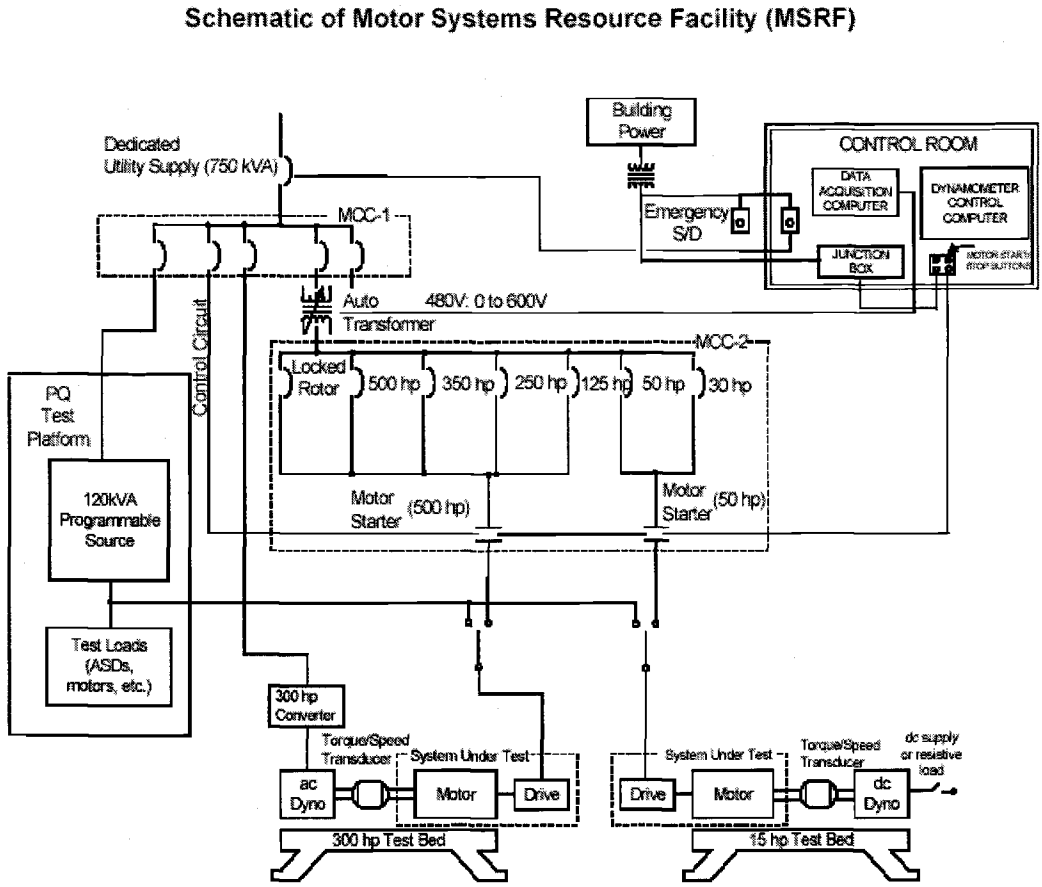

Fig. 1.4: Schematic Representation of the Motor Systems Resource Facility

In keeping with its goal of being a state-of-the art electrical machine research and testing facility, the MSRF includes both steady state operation and programmable dynamic operation. Some of the dynamic operations that the MSRF is capable of performing include the ability to apply a general, predefined torque and speed profile from a generalized polynomial function, a sine wave of torque or speed added to a constant offset, and a general purpose mode which allows the user to specify a typical profile. [7]

2 INVESTIGATION AND RESEARCH

Given the extraordinary nature of the buoy generator system, the required direct connection of the drive screw to a generator, and the maximum dynamic capabilities of the dynamometer in the MSRF, it was proposed that all of the standstill and reciprocating research be done using a 5 hp, 1800 rev/min, 230V PMSG. By using a PMSG, output can be more easily attained at low generator speeds due to a constant magnetic field emanating from the permanent magnets present in the generator.

The research was based on the simulation of a buoy motion on a sinusoidal wave profile with a magnitude of 1.6m and a period of 3.5 sec. This means, from standstill the dynamometer needed to spin up the PMSG to a speed of ~260 rev/min in .875 sec. The overall inertia of the PMSG when compared to the 300hp dynamometer is small therefore implementing this setup does not create any particular mechanical problems.

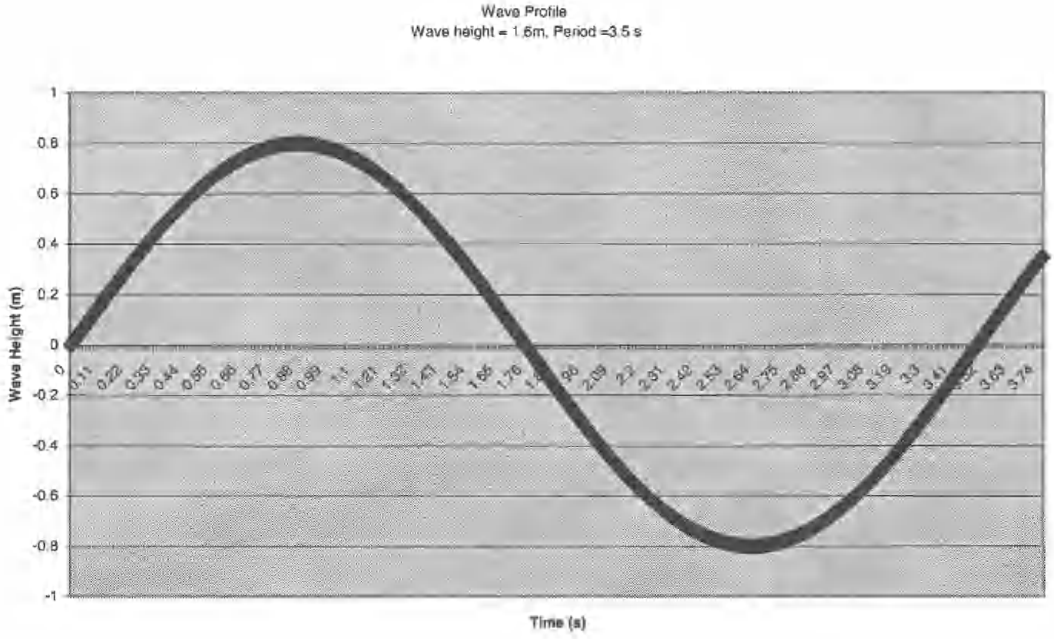

Fig. 2.1: Basic Sinusoidal Wave Profile to be simulated

The velocity of the buoy throughout the wave profile can be found by taking the derivative of the buoy displacement, Fig. 2.1.

One period of the wave profile can be broken down into 4 sections:

1) Initial wave front lifts buoy up; time t = 0s – .875s

   The speed of the directly connected generator will be decreasing in this section to 0 rev/min at the point that the buoy reaches the peak of the wave crest

2) Wave peak to 0m height; time t = .875s – 1.75s

   This coincides with the generator speeding up and reaching a maximum speed at the 0m wave height.

3) 0m height to wave trough; time t = 1.75s – 2.625s

   The generator speed will be decreasing from its maximum speed to 0 rpm

4) Wave trough to 0m wave height; time t = 2.625s – 3.5s

   This coincides with the generator speeding up in the opposite direction and reaching a maximum reverse speed at the 0m wave height

5) Then the entire process will repeat.

The maximum rotation speed of ~260 rev/min is due to the limitations of the dynamometer in the MSRF, the system has a maximum capability of producing an acceleration of 300rev/min/s [7], which means that it is only possible to achieve a speed of 262.5 rev/min in the initial .875s. Therefore all of the required testing will be based on this maximum value.

Additional tests were conducted on a standard 15hp, 1200 rev/min, 230V induction machine to simulate a ratcheting type, unidirectional buoy connection. Unlike the

constant field of the PMSG, the induction generator requires a field to be induced by an electrical utility grid connection. As a result the induction generator was used only above its synchronous speed, 1200 rev/min.

A similar series of tests was conducted on the WRIG and the PMSG. Some of these tests included running the generator up to a base speed, 1462.5 rev/min and then adding a sinusoidal speed fluctuation to the driving dynamometer output, and connecting an over-running clutch to the drive shaft to simulate a unidirectional connection. All of the WRIG experiments included added external impedance into the rotor circuit to enable an operation over a wider speed range than available for the generator alone.

Additionally it is noted that all of the generator loads for the PMSG were entirely resistive, using the water rheostat in the MSRF, whereas the WRIG output was connected directly to the electrical utility grid.

The base speeds that are referred to in this thesis are speed levels that are relative to each of the generators under test. For the WRIG the base speed refers to 1462.5 rev/min and for the PMSG the base speed is 2062.5 rev/min. These numbers were decided upon by using a combination of factors. The first of the factors considered, was the synchronous speeds of each of the generators. To adequately generate electricity, the machines must run at a speed greater than their synchronous speeds. The other factor in consideration was the MSRF dynamometer acceleration limitation of 300 rev/min/s. This meant that the dynamometer could only reach a change in speed of 262.5 rev/min in .875s. The combination of the synchronous speed as the minimum value of the sine and the maximum value at the synchronous speed plus 525 rev/min,

i.e. 262.5 * 2 for the trough to peak operation. The combined effects result in an average median base speed equal to the synchronous plus 262.5rev/min, or 1200 + 262.5 = 1462.5 rev/min for the WRIG and 1800 + 262.5 = 2062.5 rev/min for the PMSG.

2.1 Permanent Magnet Synchronous Generator

2.1.1 Per-Phase Equivalent Circuit

To begin generator testing on the permanent magnet synchronous generator the per phase equivalent circuit parameters were found. The following tests were conducted to solve for the per-phase equivalent circuit parameters.

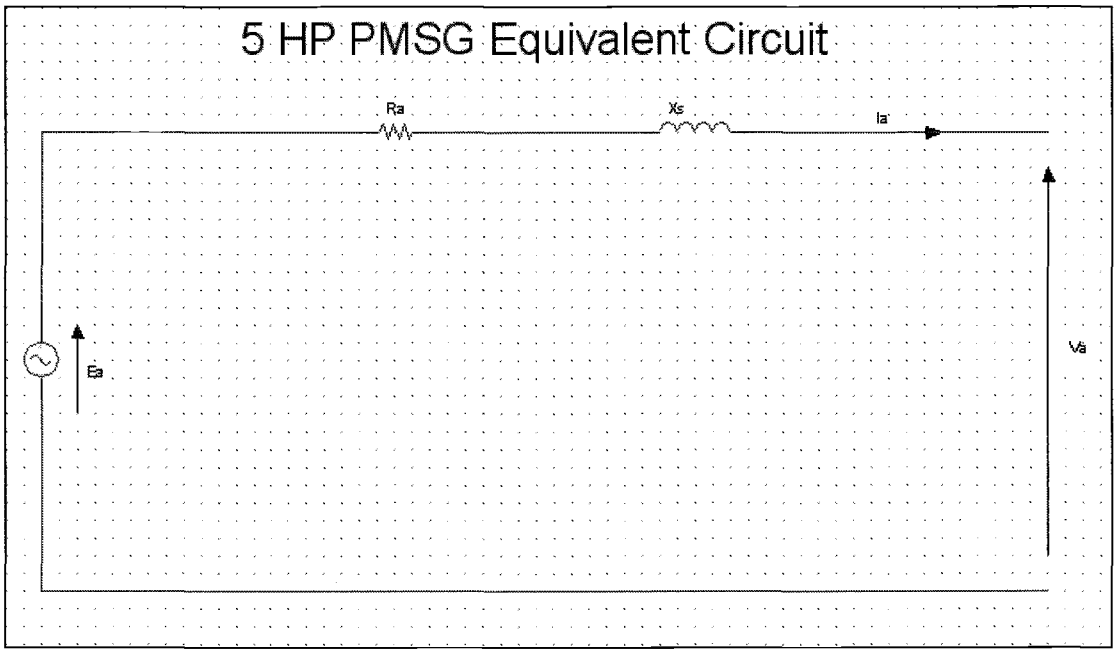

Fig. 2.2: Basic Per-Phase Equivalent Circuit for the PMSG

1. DC resistance test

   The dc resistance test is used to find the value of the motors phase resistance. The resistance determined from this testing is equal to twice the resistance Ra in Fig. 2.2 due to the fact that the generator is wye connected.

2. No Load Test

   The no-load test is used to get a baseline curve for the generator output voltage that is proportional to the speed. To get a useable output the speed

of the generator was ramped up in 100 rev/min increments and the resulting Emf from the generator was recorded, then the values were plotted on a volt vs. speed chart, see Fig. 2.3.

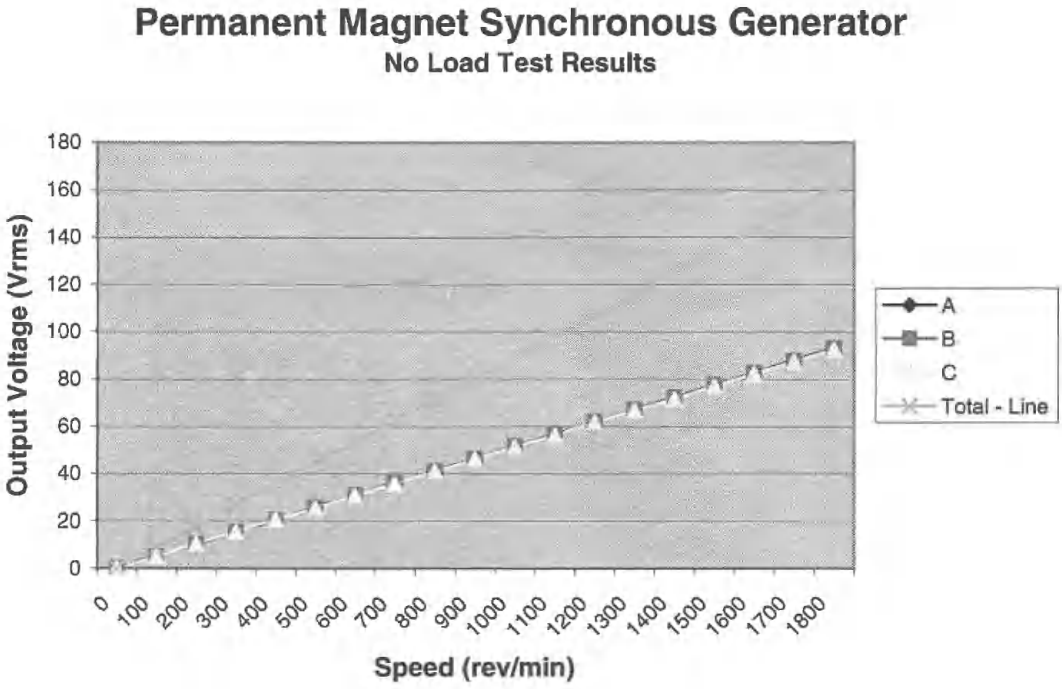

Fig. 2.3: Volt Vs. Speed Output from the No-Load Test

3. Short Circuit Test

The short circuit test is used to find the value of the speed that creates a rated current through the armature of the permanent magnet synchronous generator.

4. Calculations

Once the speed that renders the rated current to flow though the armature has been realized from the short circuit test, the corresponding voltage from the no-load test can be found.

From this combination the overall impedance of the system can be found.

$$Z = \frac{E_a}{I_{rated}} = \sqrt{R_a^2 + X_s^2} \tag{2.1}$$

E_a = Generator Electromotive Force
I_{rated} = Rated Current
R_a = Stator Phase Resistance
X_s = Stator Phase Reactance

Once the complete impedance is found the reactance can be solved for by using the following equation.

$$\therefore X_s = \sqrt{Z^2 - R_a^2} \tag{2.2}$$

The short circuit test rendered a rated current at 78 rev/min therefore the value could be found based on the known linear speed-voltage profile in Fig.2.3.

The calculations for the equivalent parameters are as follows;

$$Z_{p.u} = \frac{V_{base}}{I_{base}} = \frac{160}{11} = 14.55$$

$$Ea \cong \frac{Measured\_Speed}{Rated\_Speed} \times V_{base} = \frac{78}{1800} \times 160 = 6.93V \tag{2.3}$$

$$Z = \frac{Measured\_Speed}{Rated\_Speed} \times Z_{p.u.} = \frac{78}{1800} \times 14.55 = .63\Omega \tag{2.4}$$

$$X_s = \sqrt{Z^2 - R_a^2} = \sqrt{.63^2 - .42^2} = .47\Omega$$

At a frequency of $\frac{78}{1800} \times 60 = 2.6Hz$

The resulting equivalent circuit parameters are:

Ea = 6.93V

Ra = .42Ω

Ls = 29mH

A quick sanity check using ohms law confirms these values are correct.

$$I = \frac{Ea}{Z} = \frac{6.93}{.42 + j.47} = 10.99\angle -.841 rad$$

Which has a magnitude of $10.99A \approx 11A$, the expected rated current.

The final equivalent circuit model can be seen in Fig. 2.4.

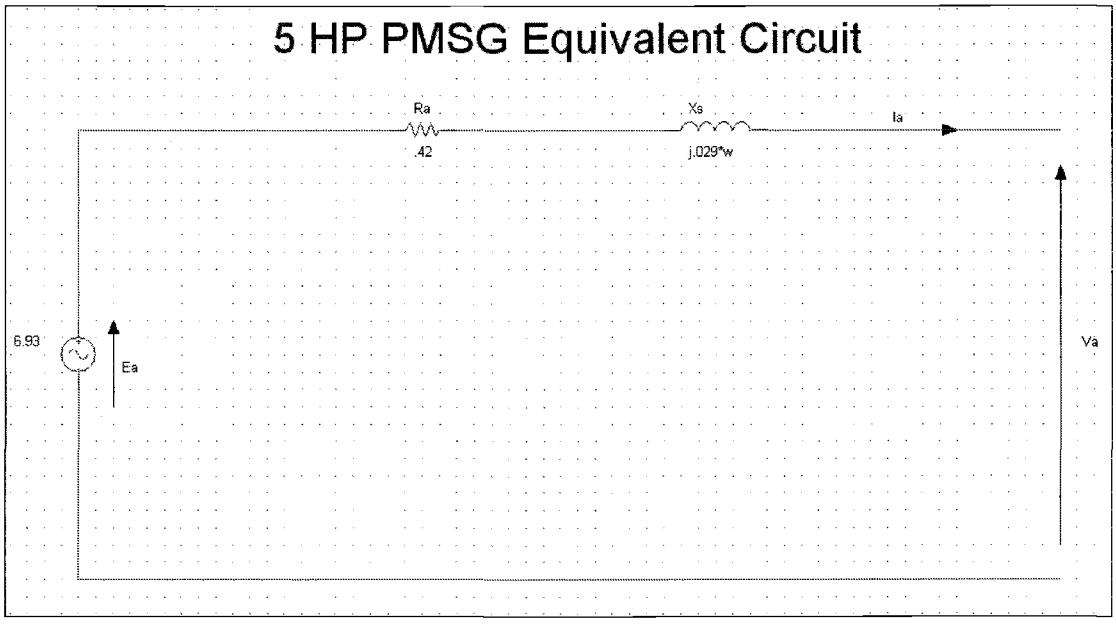

Fig. 2.4: Final PMSG Per-Phase Equivalent Circuit

2.1.2 Baseline Steady State Testing

The steady state experiment created a baseline characterization for standard generator operation. This experimentation acted as the control output for comparison purposes.

The metrics measured were the output current, voltage, real, and reactive power, the power factor, and the torque in steady state operation. These gave the necessary baseline output.

The tests were run at both full speed and at 262.5 rev/min, the maximum attainable speed that is possible for ¼ period, due to the dynamometer acceleration limits stated previously.

2.1.3 Directly Connected Reciprocating Investigation

The PMSG was run through an experiment that simulated a directly driven buoy. The test was composed of a direct connection to the dynamometer, then taking the resulting measurements of the output voltage, current, power, power factor, and torque as the generator is run from 262.5 rev/min clockwise to 262.5 rev/min counterclockwise. The experiments were conducted with the same load characteristics as the steady state testing so that the results were suitable for direct comparison.

The directly connected reciprocating test were centered around the 0 rev/min speed axis and the dynamometer was programmed with a sinusoid using the characteristics seen in Fig. 2.5.

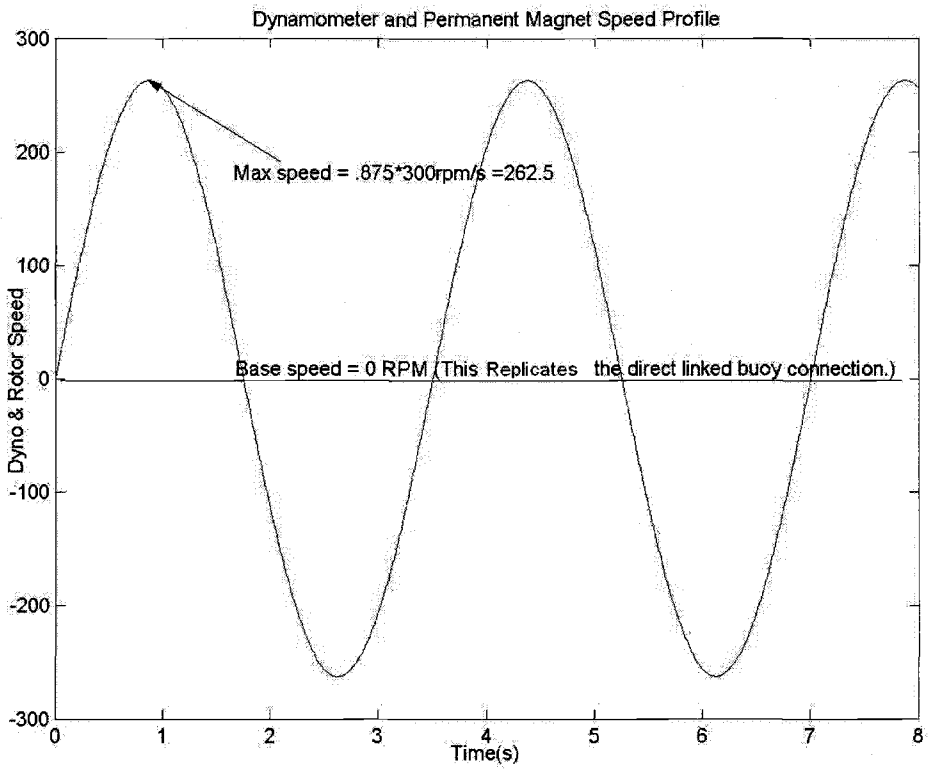

Fig. 2.5: Dynamometer Speed Profile for Reciprocating Investigation

The purpose of the direct connection testing was to mimic the buoy/generator reaction to a continuous single frequency wave cycle in a wave flume. The input to the generator replicates that produced by an actual buoy floating in the ocean with the PMSG directly connected to the drive screw.

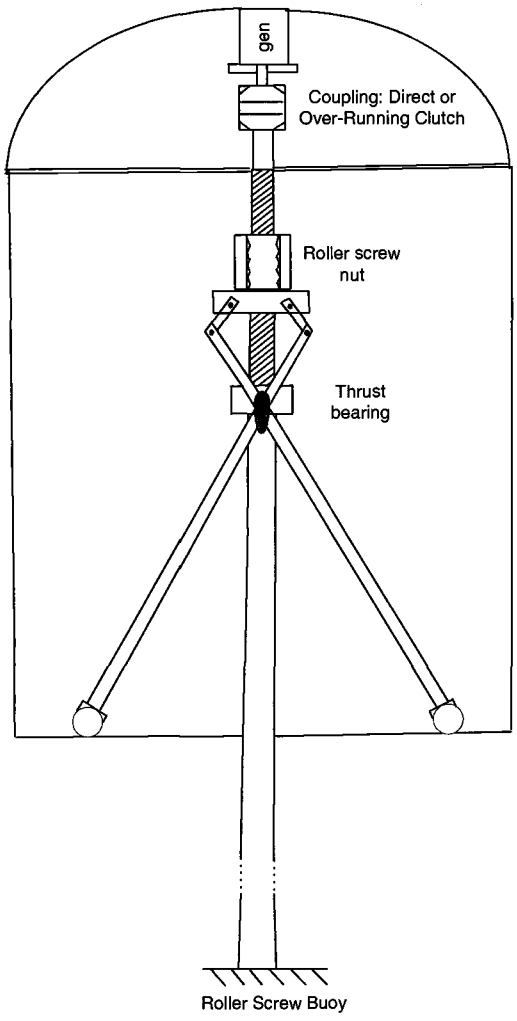

Fig. 2.6: Conceptual Drawing of the Direct Drive Buoy Generator

2.1.4 Investigation of Reciprocating Drive via Over-Running Clutch

To simulate the action that a wave would have on a unidirectional driven directly connected buoy generator, an over-running clutch was attached to the coupling between the PMSG and the Dynamometer. The purpose of the over-running clutch was to allow the generator to remain spinning in the same direction throughout the entire stroke as the buoy travels along the wave profile. This design, when applied in conjunction with a return spring, allows for a smoother voltage and current output.

By running the dynamometer sinusoidally from 262.5 rev/min through 0 rev/min and down to -262.5 rev/min an accurate interpretation of the effects an over-running clutch connection had on the PMSG could be obtained. The results of the investigation were then compared with the directly connected approach.

2.1.5 Directly Connected Base Speed with an Added Sine Component

The PMSG was also tested using a ramp up and mean value sine wave based on the previously mentioned wave profile in Fig. 2.1. The dynamometer profile for the directly connected synchronous speed with added sine testing being discussed is shown in Fig. 2.7.

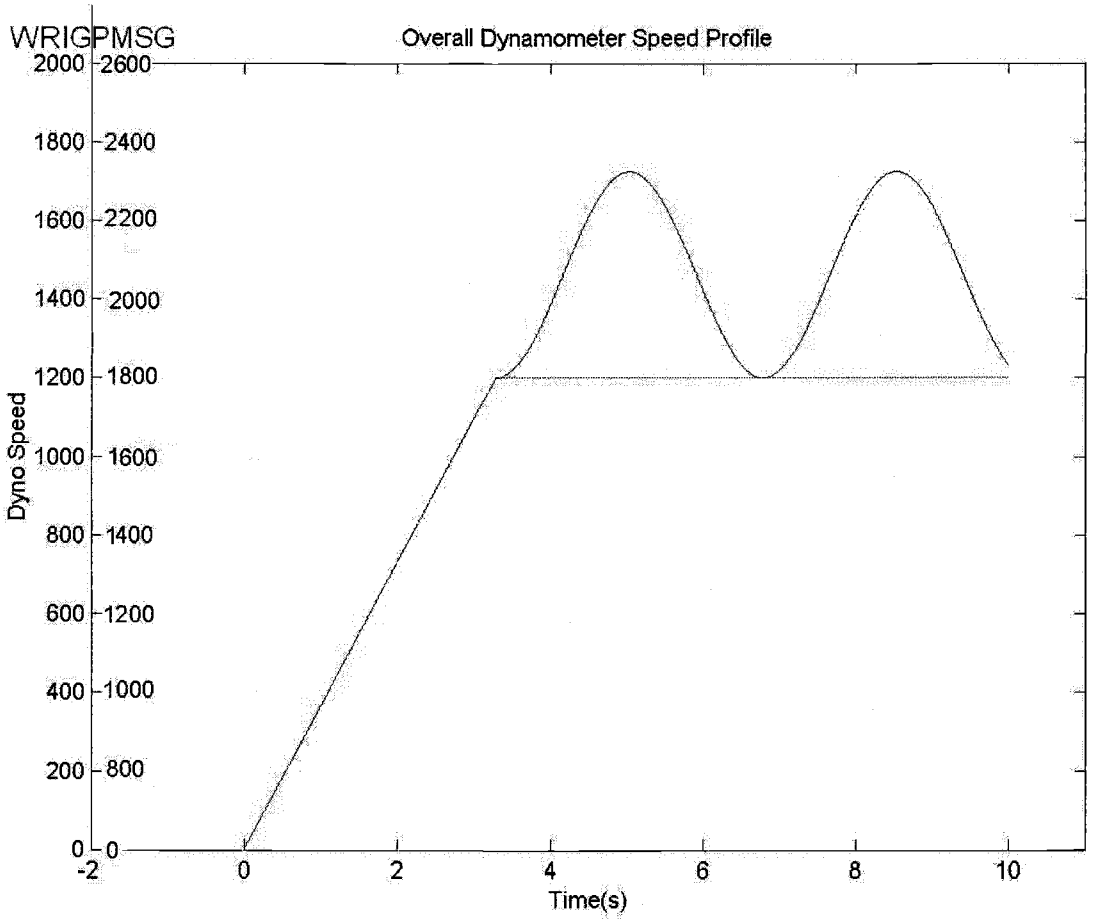

Fig. 2.7: Dynamometer Speed Profiles for the Directly Connected Base Speed with Added Sine Component

The testing was conducted to correlate with the testing that was done on the WRIG and discussed later. Both outputs were compared to see the effects of the different generator types to the same form of inputs.

The goal of the directly connected synchronous speed with an added sine component testing was to determine the performance of the generators under this unusual operating regime. The design was intended to replicate an overrunning clutch connection to the drive screw. It would ramp the unloaded generator speed up slowly until the system reached a critical speed (preferably the synchronous generator speed

plus the offset) and then slightly oscillate with each subsequent wave period about that critical speed.

The capability of the MSRF allows the researchers to accurately produce the necessary prime mover stimulus that would simulate this type of wave to generator system interaction.

2.1.6 Over-Running Clutch Connected Base Speed with Added Sine Component

The over-running clutch was added into the PMSG profile for the base speed with added sine component experiment to investigate the usability of the PMSG when it was ramped up to a base generating speed and then allowed to fluctuate with the wave profile. The output of the experiment was then compared to the output of the WRIG base speed with added sine component experiment to see how the two generators compared. The results of the test on the PMSG and the WRIG can be found in sections 3.1.5 and 3.2.3, respectively.

2.2 Wound Rotor Induction Generator

The most popular and widely used type of electric machine operational in industry today is the induction machine. [3] WRIG's are also the state-of-the-art in wind turbine generator systems. As a result of this popularity additional experimentation was conducted on a WRIG that is readily available on the open industrial market. The goal of the investigation was to show the output of an induction generator applied to a prime mover directly connected to a reciprocating roller screw or ball screw. The resulting output shows the viability of the continuing use of a WRIG in this and any other application of similar nature.

The WRIG was configured to include an external parallel resistance and inductance added into the rotor circuit. [8,9] The testing conducted included: baseline testing, directly connected base speed with added sine component, and over-running clutch connected base speed with added sine component.

2.2.1 Per-Phase Equivalent Circuit

Before any of the previously mentioned investigations were conducted, a per-phase equivalent model for the wound rotor induction motor had to be found. To do this, a number of tests were conducted to find the parameter values for the per-phase stator and rotor circuit, as shown in Fig. 2.8.

The tests include the no load test, blocked rotor test, and a windings ratio test. Each test gave the values of a different set of parameters.

The no-load test gave information about excitation current and rotational losses. The rotor was kept uncoupled from a mechanical load. The loss in the machine at no

load was due to the core loss and the friction and windage loss and these losses were considered to remain constant at full load. [3]

The blocked rotor test gave information about the leakage impedances. To correctly run these tests the rotor was completely blocked so that the generator was unable to rotate. [3]

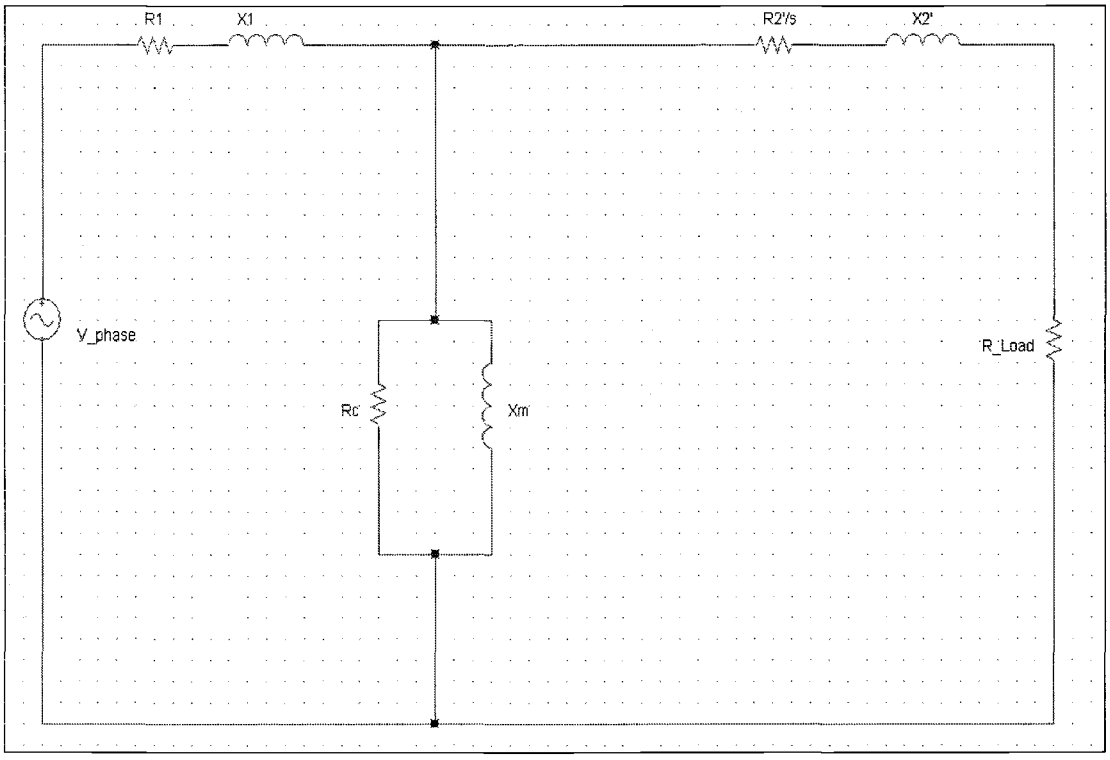

Fig. 2.8: Basic WRIG Per-Phase Equivalent Circuit

The following equations were used to find the per-phase equivalent circuit parameters.

Winding Ratio Test

The winding ration test specifies the rotor to stator winding ratio. To do this test a known ac voltage was applied to the three phases in the stator. The voltage induced in the rotor phases are then individually measured. This measured rotor voltage was then

divided by the stator applied voltage to get the ratio. All of line-to-line ratios were then averaged and the corresponding ratio was used as the rotor to stator winding ratio.

No-Load Test

1. Measured Values

   R_1; Stator resistance

   R_2; Rotor Resistance

   P_{NL}; No-Load Power

   I_{NL}; No-Load Current

2. No-Load Rotational Loss

$$P_{Rot} = P_{NL} - 3I_{NL}^2 R_1$$

3. Phase Voltage

$$V_\phi = \frac{V_{LL}}{\sqrt{3}}$$

4. No-Load Impedance

$$Z_{NL} = \frac{V_\phi}{I_{NL}}$$

5. No-Load Resistance

$$R_{NL} = \frac{P_{NL}}{3I_{NL}^2}$$

6. No-Load Reactance

$$X_{NL} = \sqrt{Z_{NL}^2 - R_{NL}^2}$$

Blocked Rotor Test

7. Measured Values

   P_{BR}; Blocked Rotor Power

I_{BR}; Blocked Rotor Current

8. Blocked Rotor Resistance

$$R_{BR} = \frac{P_{BR}}{3I_{BR}^2}$$

9. Blocked Rotor Impedance

$$Z_{BR} = \frac{V_{\phi}}{I_{BR}}$$

10. Blocked Rotor Reactance

$$X_{BR} = \sqrt{Z_{BR}^2 - R_{BR}^2}$$

11. Rotor and Stator Reactance

$$X_{BR} \approx X_1 + X_2^{'}$$
$$\therefore X_1 = X_2^{'} = \frac{X_{BR}}{2}$$

12. Rotor Resistance

$$R_2^{'} = R_{BR} - R_1$$

13. Magnetizing Reactance

$$X_m = X_{NL} - X_1$$

14. Magnetizing Voltage

$$V_m = V_1 - I_{NL}(R_{NL} + X_1)$$

15. Core Power Loss

$$P_c = P_{NL} - I_{NL}^2 R_{NL}$$

16. Core-loss Resistance

$$R_c = \frac{V_m^2}{P_c}$$

By using these equations the per-phase equivalent circuit model can be completed. The basic model is seen in Figure 2.8.

2.2.2 WRIG with Rotor Connected External Impedance (External R & L)

A WRIG provides the ability to change its torque-speed characteristic by adding additional external impedance into the rotor circuit. This addition effectively extends the useful range of the torque speed characteristic, making it more appropriate for an unregulated energy source. A resistor alone will make a significant change in this characteristic, but at the expense of reduced efficiency. If in addition to an external resistor an inductor is added in parallel, a resulting efficiency increase will be seen, which is explainable by analyzing the frequency dependent inductive impedance. At low rotor speeds, the resulting impedance is low and the resistor is effectively shorted by the inductor, which results in efficiency similar to that of the generator alone. At higher speeds and higher slips, the inductor has a high impedance value and the rotor current is diverted into the resistor.

To adequately test this scenario, the external component values had to be determined. In the past, these values have been found through an iterative, repetitive process, which is both tedious and time consuming. [8,9] To improve on that approach, an analytical approach to establish the component values has been developed. To accomplish this, a set of corresponding simultaneous equations had to be set up using the known variables of rated torque, rated slip, maximum torque, and the slip at maximum torque. The equations for the latter two components can be found in [3].

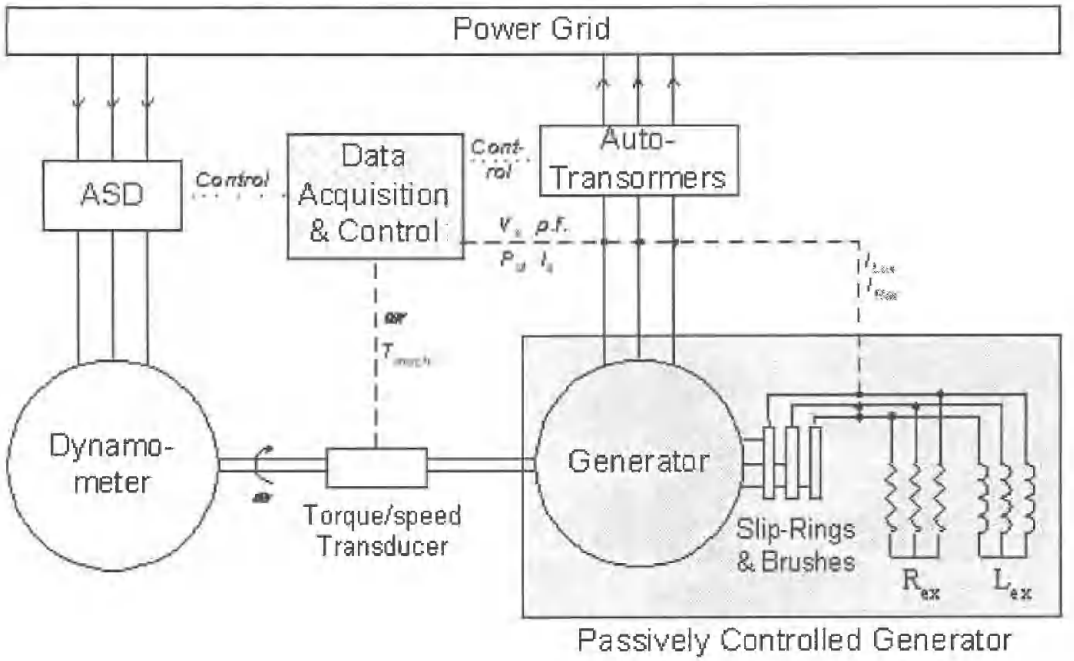

Fig. 2.9: Set-up for the Directly Connected WRIG with Added External Impedance. [8]

To solve for the necessary total external resistance required for the simulation the following procedure was used. The component values are based on the values of the WRIG equivalent circuit from section 2.2.1.

Equivalent External Resistance Calculations

1. Initially start with the per phase torque equation [3]

$$Torque = \frac{1}{\varpi_{syn}} \frac{V_{th}^2}{(R_{th} + \frac{R_2'}{s})^2 + (X_{th} + X_2')^2} \frac{R_2'}{s} \tag{2.5}$$

2. Solve for R2'

   Set equation equal to 0

$$\frac{s}{R_2'}\left[(R_{th} + \frac{R_2'}{s})^2 + (X_{th} + X_2')^2\right] - \frac{1}{\varpi_{syn}} \frac{V_{th}^2}{Torque} = 0$$

3. Multiply through the R2' squared terms

$$\frac{s}{R_2^{'}}\left[R_{th}{}^2+2\frac{R_2{}'R_{th}}{s}+\frac{R_2{}'^2}{s^2}+(X_{th}+X_2^{'})^2\right]-\frac{V_{th}^2}{\varpi_{syn}*Torque}=0$$

4. Multiply the equation by $\frac{s}{R_2^{'}}$

$$\frac{s}{R_2^{'}}R_{th}{}^2+2R_{th}+\frac{R_2{}'}{s}+\frac{s(X_{th}+X_2^{'})^2}{R_2{}'}-\frac{V_{th}^2}{Torque*\varpi_{syn}}=0$$

5. Multiply by R2' to simplify

$$sR_{th}{}^2+2R_2{}'R_{th}+\frac{R_2{}'^2}{s}+s(X_{th}+X_2^{'})^2-\frac{V_{th}^2\times R_2{}'}{\varpi_{syn}\times Torque}=0$$

6. Multiply by s to simplify further

$$s^2R_{th}{}^2+2sR_2{}'R_{th}+R_2{}'^2+s^2(X_{th}+X_2^{'})^2-\frac{V_{th}^2\times R_2{}'}{\varpi_{syn}\times Torque}s=0$$

7. Next add the R_{eq} Value into the equation by substituting $R_2^{'}=R_2^{'}+R_{eq}$

$$s^2R_{th}{}^2+2s\left(R_2{}'+R_{eq}\right)R_{th}+\left(R_2{}'+R_{eq}\right)^2+s^2(X_{th}+X_2^{'})^2-\frac{V_{th}^2\times\left(R_2{}'+R_{eq}\right)}{\varpi_{syn}\times Torque}s=0$$

8. Solve for R_{eq}

9. Multiply the R_{eq} Terms

$$s^2R_{th}{}^2+2sR_{th}R_2{}'+2sR_{th}R_{eq}+R_2{}'^2+2R_{eq}R_2{}'+R_{eq}{}^2+s^2(X_{th}+X_2^{'})^2-\frac{V_{th}^2R_2{}'}{\varpi_{syn}\times Torque}s-\frac{V_{th}^2R_{eq}}{\varpi_{syn}\times Torque}s=0$$

10. Set up the quadratic form of R_{ext}

$$R_{eq}^2+R_{eq}\left(2sR_{th}+2R_2^{'}-\frac{V_{th}^2}{\omega_{syn}\times Torque}s\right)+s^2R_{th}^2+2sR_{th}R_2^{'}+R_2^{'2}+2R_2^{'}+s^2\left(X_{th}+X_2^{'}\right)^2-\frac{V_{th}^2R_2^{'}}{\omega_{syn}\times Torque}s$$

11. Set up the quadratic formula variables

$$A = 1$$

$$B = \left(2sR_{th} + 2R_2 - \frac{V_{th}^2}{\varpi_{syn} \times Torque} s \right)$$

$$C = \left(s^2 R_{th}{}^2 + 2sR_{th}R_2' + R_2'^2 + 2R_2' + s^2 (X_{th} + X_2')^2 - \frac{V_{th}^2 R_2'}{\varpi_{syn} \times Torque} s \right)$$

$$R_{eq1} = \frac{-B + \sqrt{B^2 - 4AC}}{2A} = .84$$

$$R_{eq2} = \frac{-B - \sqrt{B^2 - 4AC}}{2A} = -.3$$

The resulting R_{eq} is the equivalent total external resistance that will be necessary to create the required output of the machine once it is at full steady state operation.

Equivalent External Inductance Calculations

The external inductance that will be added onto the rotor circuit has to be allotted by using a set value for the allowable amount of current to be leached through the inductor at full steady-state operating conditions. Ideally the resistance from the rotor-connected circuit would only have an effect on the system once the generator had reached its full operating speed, this is why the external resistance has been connected mechanically in the past. [9]

The purpose of adding a parallel inductor is two-fold, first the inductor will act like a short at the initial start up, due to the low rotor frequency this will in turn draw most of the current through the inductor as it will act as the low impedance path, resulting in an efficiency and generator operation approximately the same as the generator itself without any external impedance. Secondly once the generator is at its operating frequency the inductor can be sized such that its impedance is so high compared to

that of the external resistor and the majority of the current is diverted through the resistor, resulting in the torque-speed curve becoming extended.

To solve for the necessary value of the inductor to be used, a rating scenario was needed. Ideally there would be a parallel inductor that would act as a perfect short at start-up and an open circuit at full speed. Getting an inductor to act, as a near perfect short is possible at low frequencies. At synchronism the rotor frequency is at 0Hz; consequently the inductive reactance is zero. Therefore the problem reduces to choosing an inductance suitable for the generator at its rated speed of operation. There was no way to, practically, make the inductance large enough that its reactance would be even approximately infinite at the operating speed, however by allowing a certain small percentage of rated current through the inductor at full operating speed is an acceptable approximation.

The approximation is based on the current divider that is formed by the parallel external impedance. If the rated stator current is referred to the rotor and the rated rotor current can be found through the relationship $I_r = \frac{N_s}{N_R} I_s$, then by setting an allowable amount of current through the inductor an acceptable inductor size can be derived.

The research was conducted at an operating slip of 0.22. The resulting rotor frequency was $f_{rot} = f_{syn} \times s = 60Hz \times .22 = 13.2Hz$ and $\omega_{rot} = 2\pi f_{rot} = 26.4\pi$. The acceptable limit for current through the inductor was set at 1% of the rated rotor current ($.01I_r$) and the overall resistance is known from the previous calculations the inductance value can then be determined.

Analytically the solution can be found by using the following calculations.

$$Z_{Lex} = R_{Lex} + jX_{Lex}$$

Set up the current divider based on the current through the inductive branch.

$$.01I_r = \left(\frac{R_{ext}}{R_{Lex} + R_{ext} + X_{Lex}} \right) I_r$$

Cancel I_r from both sides of the equation

$$.01 = \left(\frac{R_{ext}}{R_{Lex} + R_{ext} + X_{Lex}} \right)$$

$$R_{Lex} + R_{ext} + X_{Lex} = \frac{R_{ext}}{.01}$$

$$X_{Lex} = \frac{R_{ext}}{.01} - R_{ext} - R_{Lex}$$

$$X_{Lex} = 99R_{ext} - R_{Lex}$$

At operating speeds the R_{Lex} term will be sufficiently small that it can be neglected, therefore the external reactance of the external impedance is

$$X_{Lex} \cong 99R_{ext}$$

$$X_{Lex} = \omega_{rot} L_{ext}$$

$$\therefore L_{ext} = \frac{X_{Lex}}{\omega_{rot}} \tag{2.6}$$

Recall that there is a parallel combination of the external resistance and the intrinsic resistance of the inductor coil.

$$\frac{R_{Lex} R_{ext}}{R_{Lex} + R_{ext}} = R_{eq} \cong .84\Omega$$

$$R_{ext} = \frac{R_{Lex} R_{eq}}{R_{Lex} - R_{eq}} \tag{2.7}$$

Both equations 2.6 and 2.7 above must be approximately satisfied to produce the desired output. Based on these equations and the 15 hp WRIG that was tested, the

result was that an additional amount of resistance in series with the inductor was necessary. After the calculations had been run, it was figured that an additional 1.04Ω would be necessary for use with the MSRF three-phase inductor.

The per-phase equivalent circuit of the generator with the external components is shown in the Fig. 2.10. The overall external equivalent impedance of the parallel components is shown in the following equation.

$$Z_{ext} = \frac{R_{ext}(R_{Lex} + jX_{Lex}s)}{s(R_{ext} + R_{Lex} + jX_{Lex}s)}$$

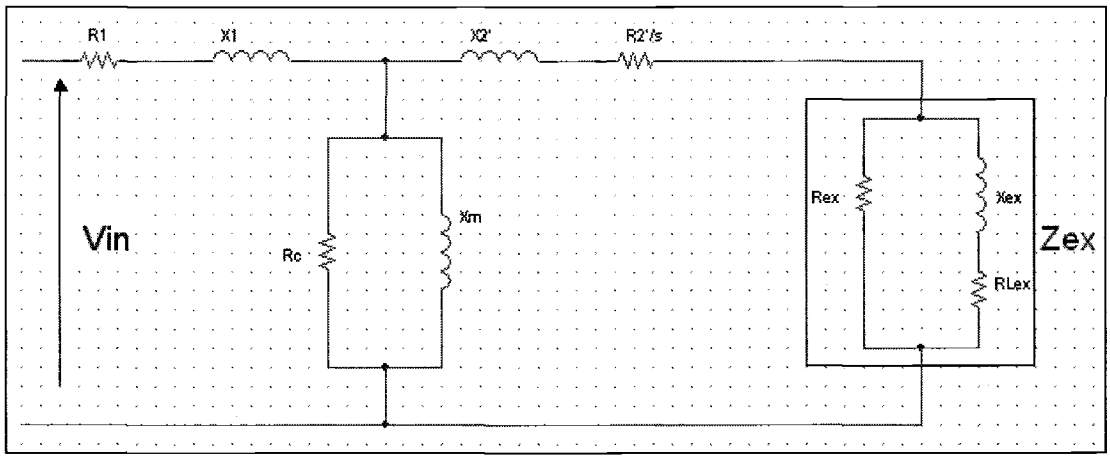

Fig. 2.10: Per phase Equivalent Circuit with External Rotor Components

2.2.2.1 *Baseline Steady State Testing*

The WRIG was tested in a standard operating mode that would allow for a baseline characterization of the generator's operating condition. Once the generator output had been verified, the data from the following additional investigations could be compared to the baseline test results and conclusions could be made toward the viability of the use of the WRIG in applications similar to those that the tests are geared toward.

2.2.2.2 *Over-Running Clutch Base Speed with an Added Sine Component*

An overrunning clutch was added into the WRIG test setup shown in Fig. 2.9 to test the idea of a unidirectional directly driven buoy generator. The theory behind the addition of the over-running clutch is, as the buoy heaves up and down along the wave front only one half of the oscillation will be used to directly drive the generator. On the other half of the stroke the energy will be stored into a return spring and the generator is allowed to spin freely due to the inertial mass of the rotor itself. Ideally this would allow the generator to spin up to its full operating speed and then there would only be a slight deviation as the drive screw rotational speed and the generator speed coincide. The result is that the drive screw can have a significantly different velocity relative to the generator, but when the direction and speed of the drive screw are equal to the speed of the generator the two would engage and the generator would then be fully driven by the dynamometer.

Fig.2.11 depicts the rig setup with the over-running clutch and dynamometer combination.

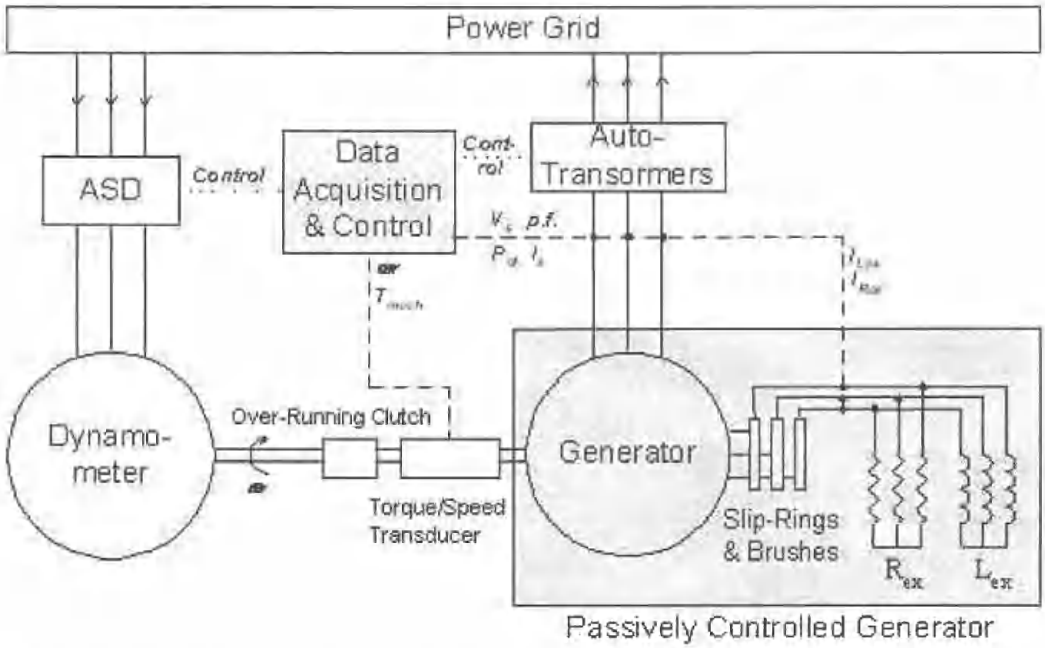

Fig. 2.11: Set-Up for the Over-Running Clutch Connected WRIG with Added External Impedance

To simulate the expected output of the system in a computer program prior to physical testing, an equivalent electrical circuit model was used. The model consisted of a simple ac circuit using passive components including a diode, a capacitor, and a resistor. The equivalent resistance and capacitive circuit model, seen in Fig. 2.12, displays a charge and discharge cycle of a capacitor. The electrical components are a very suitable approximation of how the mechanical system works, as each of the mechanical components has an electrical equivalent. The dynamometer drive corresponds to the ac source, the over-running clutch requires the same physical unidirectionality that the diode provides electrically, the residual inertia of the generator, is easily simulated by the resistor and capacitor charge and discharge cycles. The equivalent circuit and output, as given by the Pspice model, are shown in figures 2.12 and 2.13, respectively.

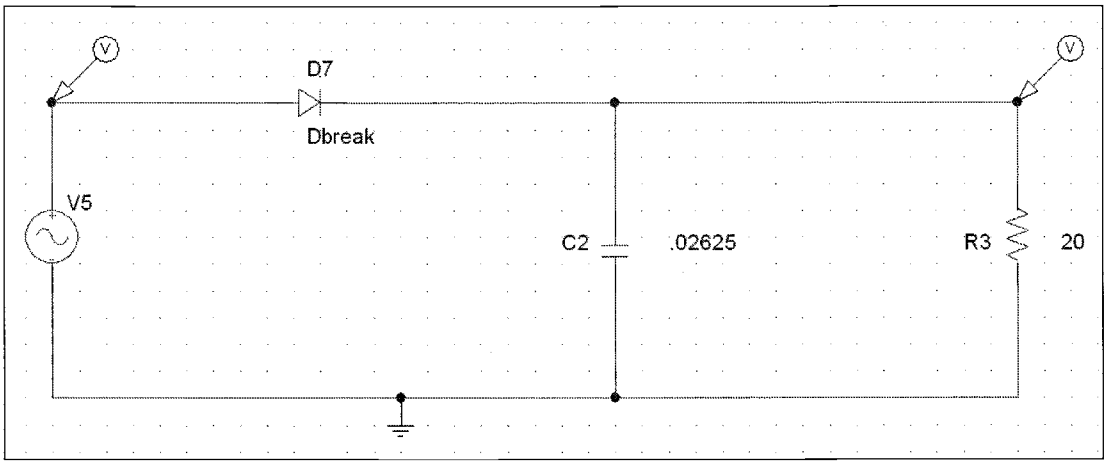

Fig. 2.12: The Electrical Equivalent Circuit of the Physical Speed Relationship of the Generator with Respect to the Dynamometer Drive

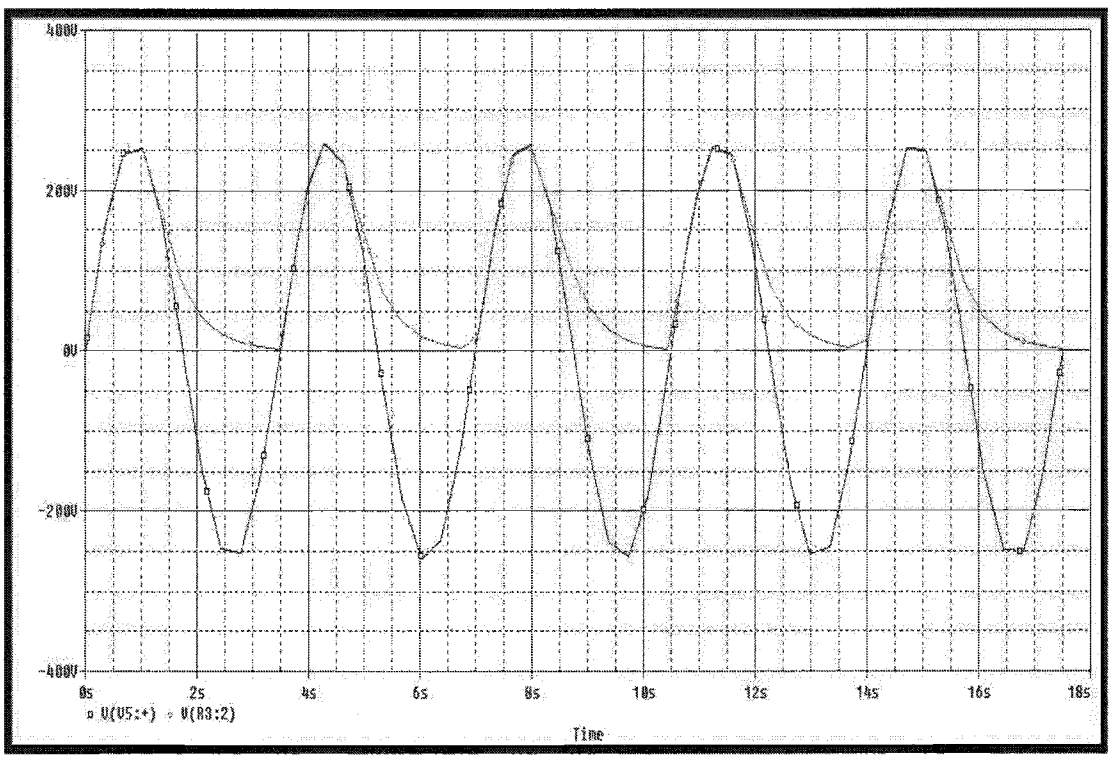

Fig. 2.13: Output of the Electrical Equivalent Circuit for the

In Fig. 2.13 the completely sinusoidal trace, denoted by the square's, corresponds to the input ac voltage, which is the electrical equivalent of the dynamometer speed.

The other trace with the exponential decay is the capacitor voltage, or the analog to the generator speed.

As can be seen in the output, the speed of the generator is expected to stay equal to or greater than the speed of the dynamometer. This was possible due to the connection of the generator to the dynamometer through the overrunning clutch, which would produce a unidirectional rotary output to the generator.

3 RESULTS

3.1 Permanent Magnet Synchronous Generator

3.1.1 Baseline Steady-State Testing

The baseline testing was performed as per the description given in section 2.1.1, and the results of the testing are shown in the following figures and tables.

Full Speed

The outputs were obtained from the PMSG under standard steady-state operation. The values were taken at different load levels to act as a control with which to compare with the results of subsequent tests.

The first such experiment was the no-load baseline test.

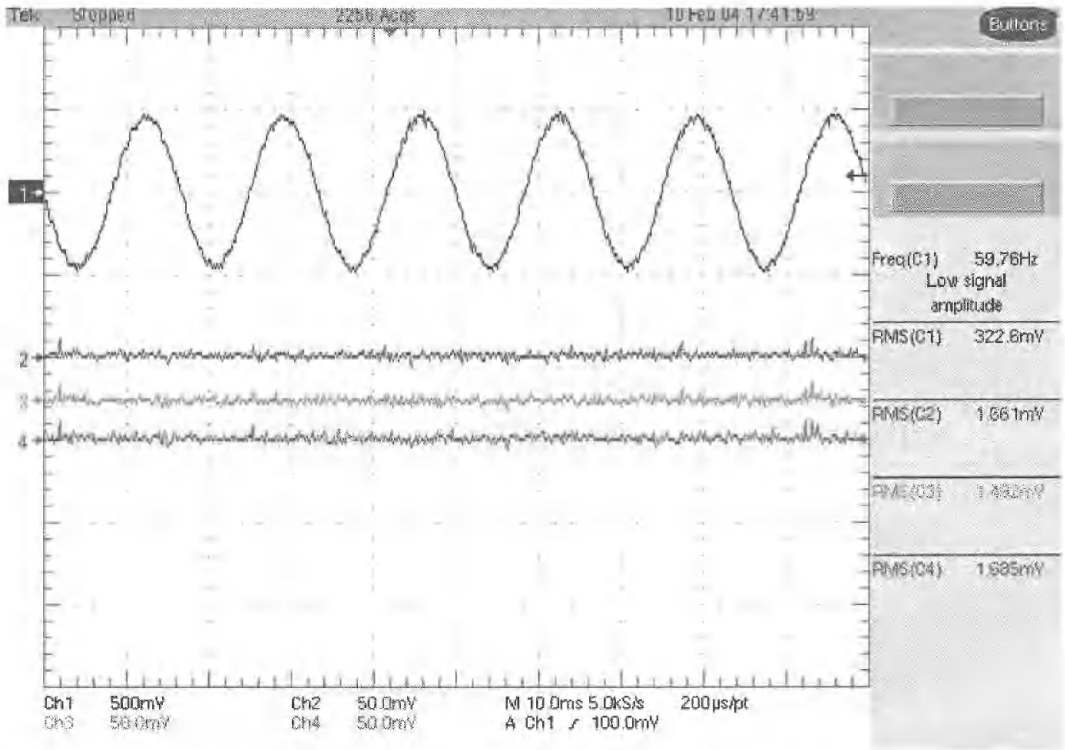

Fig. 3.1: Baseline Testing, No Load 1800 Rev/Min – Rated Speed

Fig. 3.1 shows the output of the PMSG on the oscilloscope. Channel 1 shows a single phase of the ac output voltage. Channels 2 through 4 show the three-phase currents and are seen below the voltage waveform in the screen capture. In the case for no load operation the three phases have zero current.

As can be seen on the right hand side of the screen capture, Freq(C1), the frequency of the output is approximately 60 Hz as expected in normal generator operation at 1800 rev/min for a 4 pole machine. For a breakdown of the quantitative output the rms current and voltage values are shown in Table 3.1: which indicates that the PMSG has well balanced phases.

Table 3.1: Tabular Results for Baseline Testing, No Load 1800 Rev/Min – Rated Speed

No Load (0Nm)	Phase Quantities			
	A	B	C	Total – Line
Irms (A)	0	0	0	0
Vrms (V)	93.84	92.89	92.49	161.22

The next baseline test shown is the fully loaded generator steady state test. This allows for a full overall analysis of the generator output. The resulting output shows the sinusoidal voltage and the three-phase currents. Again channel 1 is the single phase ac output voltage and channels 2, 3, and 4 are the three-phase currents. At full load the maximum output voltage was approximately 160 Vrms, at 20 Arms. This data verifies a suspicion that the permanent magnets in the PMSG may have been slightly demagnetized since the PMSG was new. The nameplate rated voltage is 230 Vrms. The comparison of these output voltage levels reflected the level of magnetic degradation. The amount of demagnetization, however, does not significantly detract from the proof of concept for this simulation. The output of this investigation is shown pictorially in Fig. 3.2, and in a raw data form in Table 3.2. Both voltages and currents show good balance between the phases.

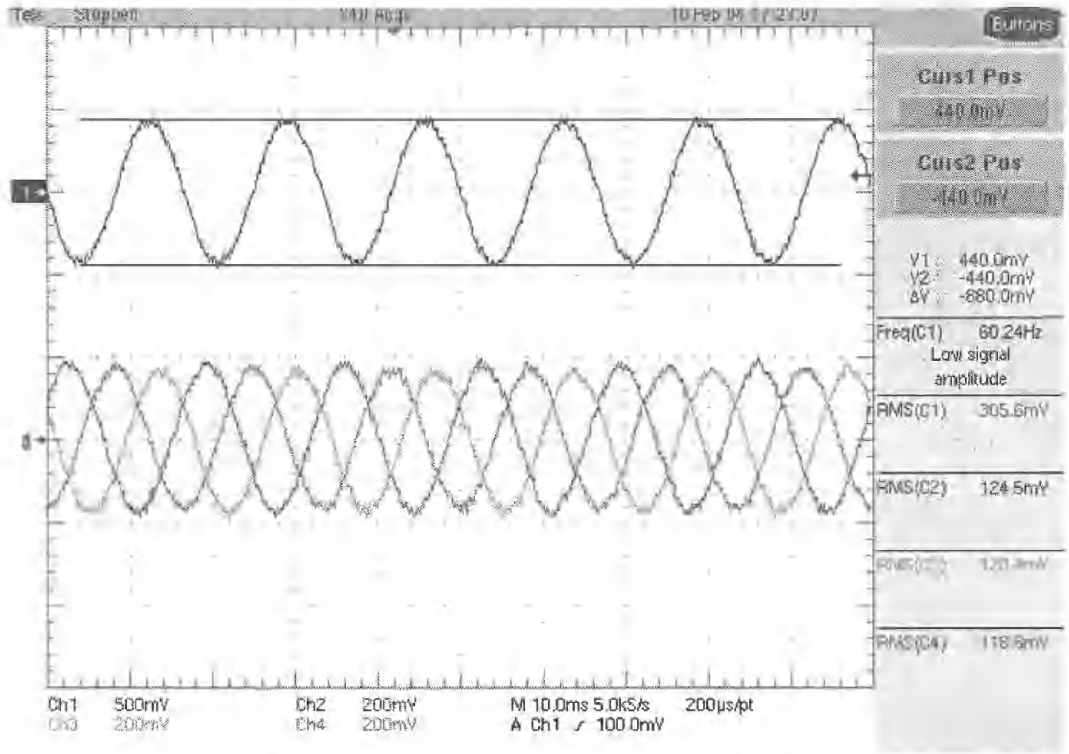

Fig. 3.2: Baseline Testing, Full Load 1800 Rev/Min – Full Speed

Table 3.2: Tabular Results for Baseline Testing, Full Load 1800 Rev/Min - Rated Speed

Full Load (18.3Nm)	Phase Quantities			
	A	B	C	Total – Line
Irms (A)	11.77	11.17	11.35	11.41
Vrms (V)	87.91	94.07	88.01	155.96
P (kW)	-1.03	-1.05	-1.00	-3.079
Q (kVar)	.103	.031	.027	.248
S (kVA)	1.04	1.05	1.0	3.089

Reduced Speed – 262.5 rev/min

As was discussed earlier in this thesis, the dynamometer in the MSRF has boundaries that it must stay within to function properly. One of those is its ability to accelerate. The peak acceleration that the dynamometer can reach is 300 rev/min/s, therefore in ¼ of a 3.5s wave period the dynamometer can only reach a maximum angular velocity of 262.5 rev/min. As a result, a baseline steady state test was

conducted at this speed level. Similar to the full speed testing done prior, the steady state reduced speed testing will provide a control with which to compare later values.

Fig. 3.3 shows the no-load case for the PMSG. As in the case for full speed, the figure shows that there is an output voltage, on channel 1, but no output current, channels 2, 3, and 4. The primary difference between the two is at the decreased shaft speed the overall output voltage is considerably less.

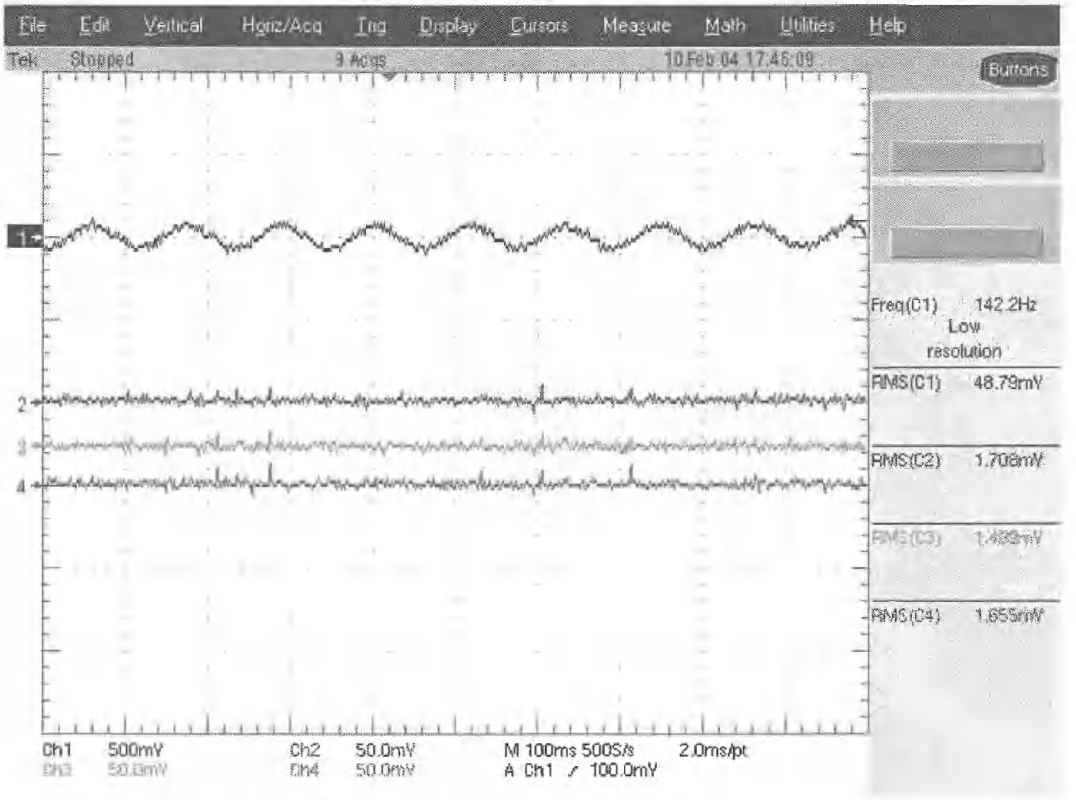

Fig. 3.3: Baseline Testing, No Load 262.5 Rev/Min

Table 3.3: Tabular Results for Baseline Testing, No Load - 262.5 Rev/Min

No Load (0Nm)	Phase Quantities			
	A	B	C	Total - Line
Irms (A)	0.00	0.00	0.00	0.00
Vrms (V)	13.44	13.70	13.35	23.38

The relationship between the full speed voltage and the reduced speed voltage is based on the ratio of the speeds.

$$\frac{Adjusted\_Speed}{Rated\_Speed} \times Tested\_Voltage = Output\_Voltage \qquad (3.1)$$

$$\frac{262.5}{1800} \times 161.22 = 23.51 \approx 23.38$$

The output that was seen at the terminals of the PMSG is within a few percentage points of what was expected.

Additional investigation with the system under load was conducted, and again the outputs of the system were as expected, to within a percentage or so. Fig. 3.4 shows the output for the system when the load was brought up to the saturation point in the PMSG, and the subsequent table displays the actual recorded values of the output.

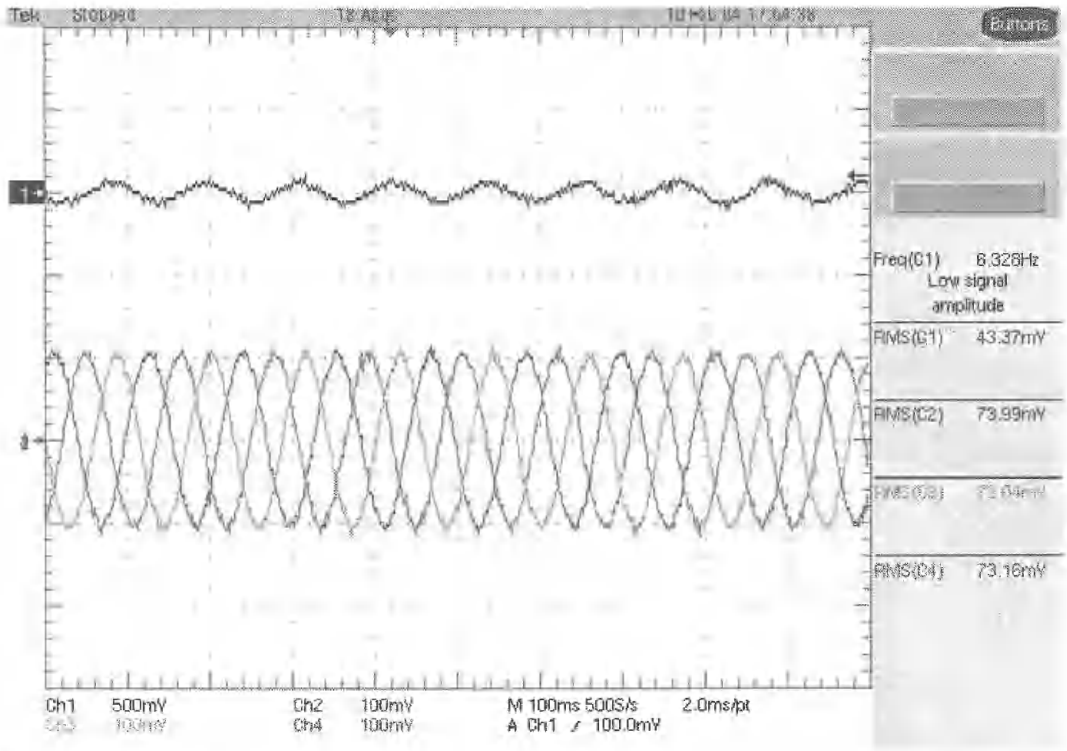

Fig. 3.4: Baseline Testing, Full Load 262.5 Rev/Min

Table 3.4: Tabular Data for Baseline Testing, Full Load - 262.5 Rev/Min

Full Load (14Nm)	Phase Quantities			
	A	B	C	Total – Line
Irms (A)	6.93	6.92	7.00	6.95
Vrms (V)	13.543	14.06	13.87	23.95
P (kW)	-.09	-.10	-.10	-.29
Q (kVar)	.01	.002	.01	.03
S (kVA)	0.09	.10	.10	.29

3.1.2 Directly Connected Reciprocating Investigation

For the directly connected reciprocating investigation the generator was applied to a somewhat unusual prime mover scenario. Unlike regular motor/generator operation the generator was driven in a reciprocating fashion from 262.5 rev/min to -262.5 rev/min in a sinusoidal pattern based on the velocities derived from the wave profile in Fig. 3.5.

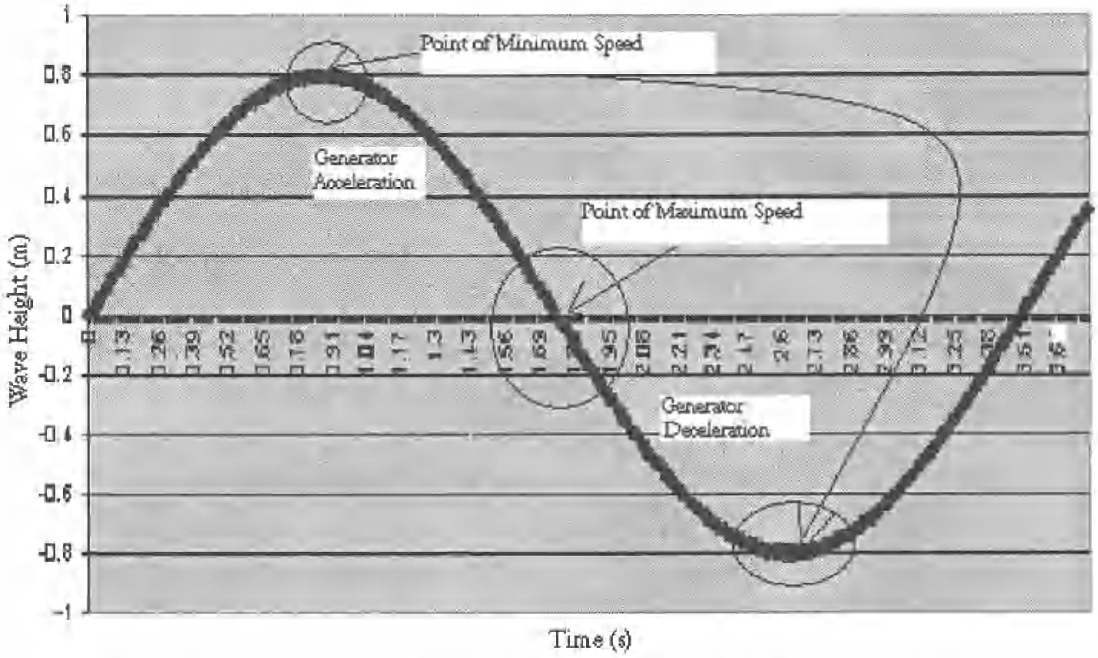

Fig. 3.5: The Basic Wave Profile and the Associated Points of Minimum and Maximum Generator Speed

Starting at the peak of the wave profile, where the generator is at 0 rev/min the buoy slides down the surface of the wave and the generator gradually accelerates. As the buoy reaches the median point associated with the wave height zero crossing the generator will reach its maximum speed and then begin to decelerate until it reaches the trough of the wave, at which point the generator would again stop, reverse direction, and begin the cycle all over.

This can be seen as the regions on Figs. 3.6 and 3.7 where the output voltage, and in Fig. 3.7 output currents are approximately zero.

This cycle will continue as a periodic function, which is shown in both Figs. 3.6 and 3.7.

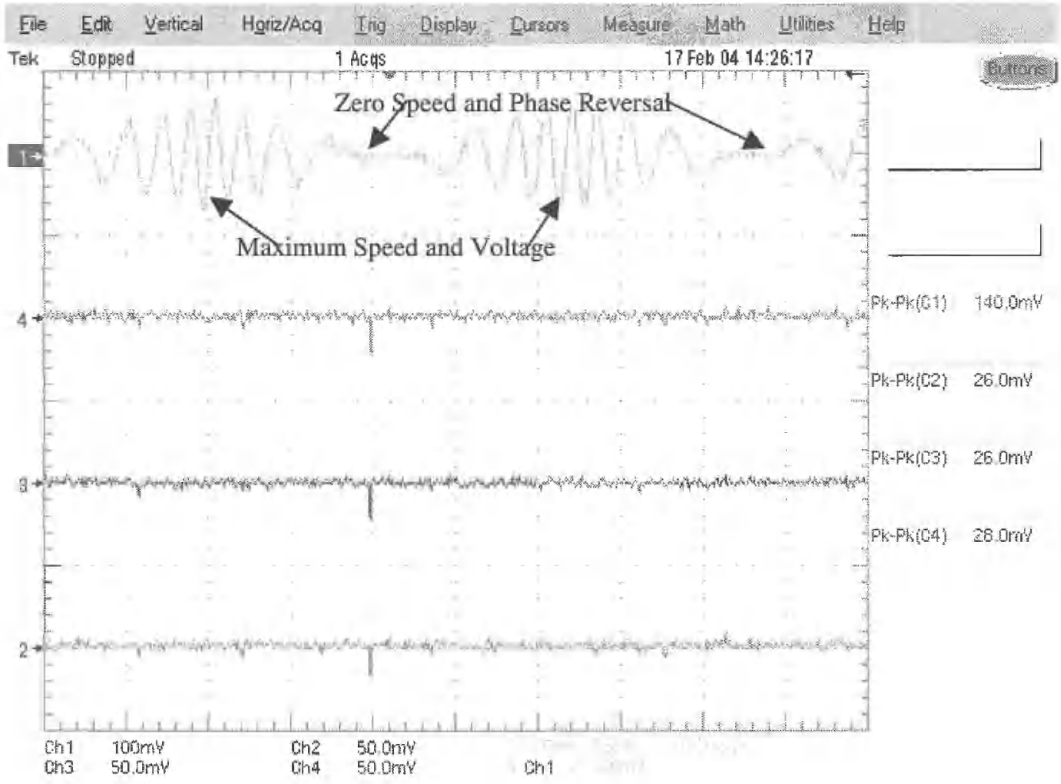

Fig. 3.6: Directly Connected Reciprocating Test, No Load

Table 3.5: Tabular Data for Directly Connected Reciprocating Test, No Load

No Load (0Nm)	Phase Quantities			
	A	B	C	Total -Line
Irms (A)	0.00	0.00	0.00	0.00
Vrms (V)	11.41	11.81	11.70	20.18

In Fig. 3.6 channel 1 shows an output voltage from the system. Again, with the no load profile there is a voltage but no current. Table 3.6 shows the rms values of the outputs from the directly connected reciprocating test while the PMSG was under load.

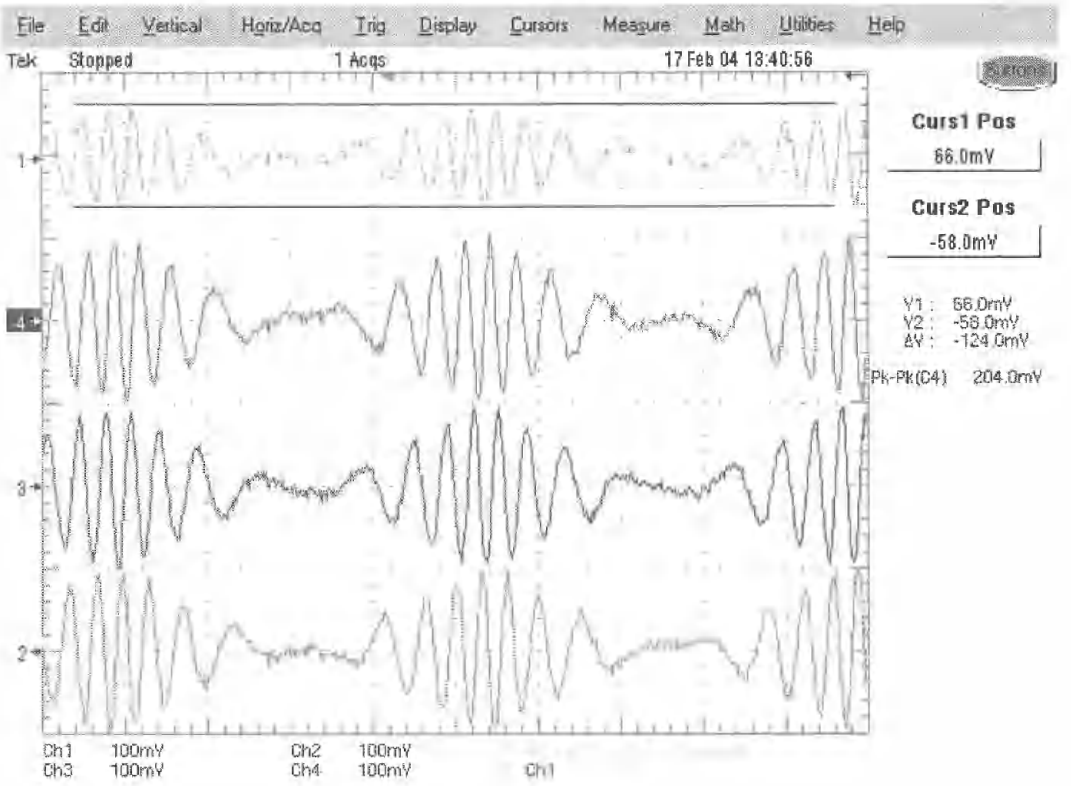

Fig. 3.7: Directly Connected Reciprocating Test, Full load

Table 3.6: Tabular Data for Directly Connected Reciprocating Test, Under Load

Full Load (14Nm)	Phase Quantities			
	A	B	C	Total - Line
Irms (A)	5.71	5.69	5.89	5.76
Vrms (V)	9.76	9.87	9.89	17.05
P (kW)	-0.05	-0.05	-0.05	-0.17
Q (kVar)	0.01	0.05	0.05	0.13
S (kVA)	0.06	0.06	0.06	0.17

The primary difference of Fig. 3.7 when compared to Fig. 3.6 is that since a full load has been applied to the system there will now also be a set of three-phase output currents, channels 2, 3, and 4. As expected, the currents follow the same cyclical pattern of output as the voltage because the system load was purely resistive. In Table

3.6 the output values have been tabulated, the minimum outputs are all approximately zero. When compared to the values of the baseline testing discussed in the section 3.1.1, it can be seen that even under full load with the reciprocating profile the generator line currents are still kept down around half of the associated baseline full load values. This phenomenon may be significant when specifying particular generators for buoy designs where this type of prime mover scenario is to be utilized.

3.1.3 Investigation of Reciprocating Drive via Over-Running Clutch

3.1.3.1 Investigation of Reciprocating Drive via Over-Running Clutch, Speed Profiles

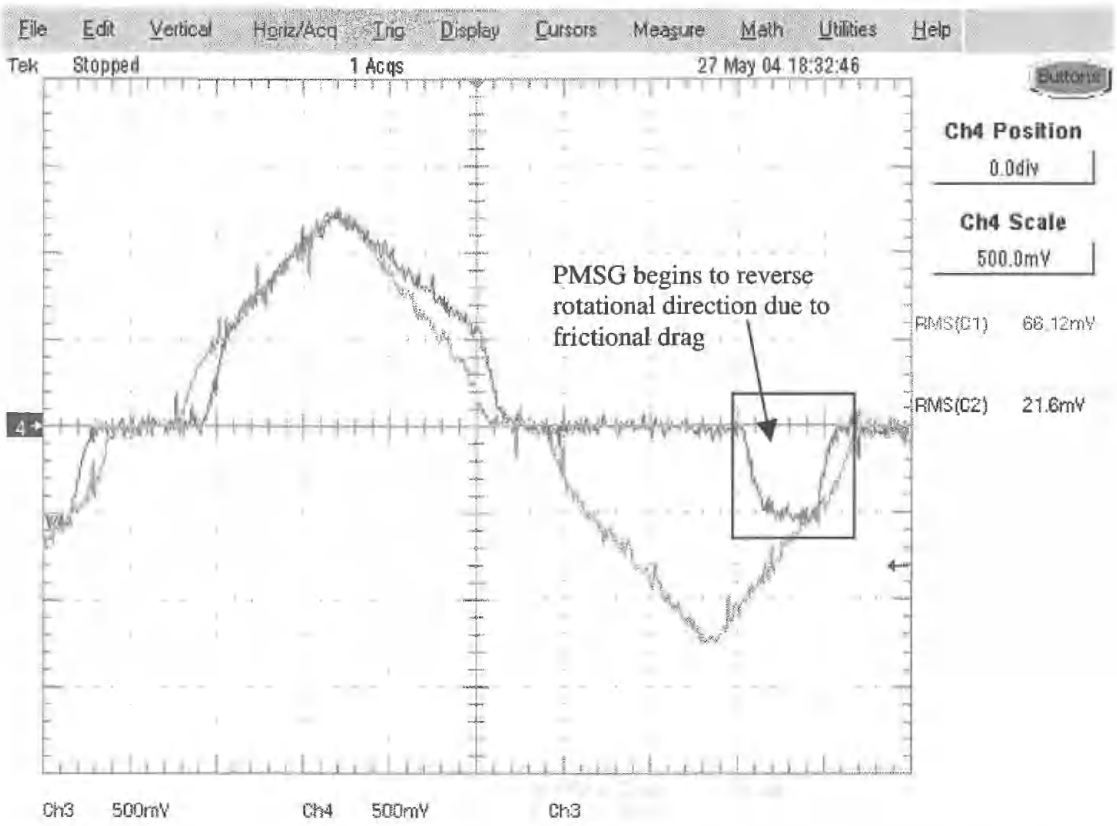

Fig. 3.8: Investigation of Reciprocating Drive via Over-Running Clutch, No-Load, Speed Output

The speed profiles shown in Figs. 3.8 and 3.9 show the relationship between the PMSG speed and the dynamometer speed. Ch4 correlates to the speed of the dynamometer and Ch3 is the speed of the generator. The speed profiles show short time frames where the output from the speed indicator reads 0 rev/min, these regions were due to the capabilities of the Lebow torque/speed meters, transforming the signals from the speed transducers into a dc level output. At very low speeds the meter was unable to decipher the rotational speed and, consequently, outputs a value of 0 rev/min, hence the "haystack" shape rather than a symmetric triangular waveform. In practice the threshold value is around ± 25-30 rev/min.

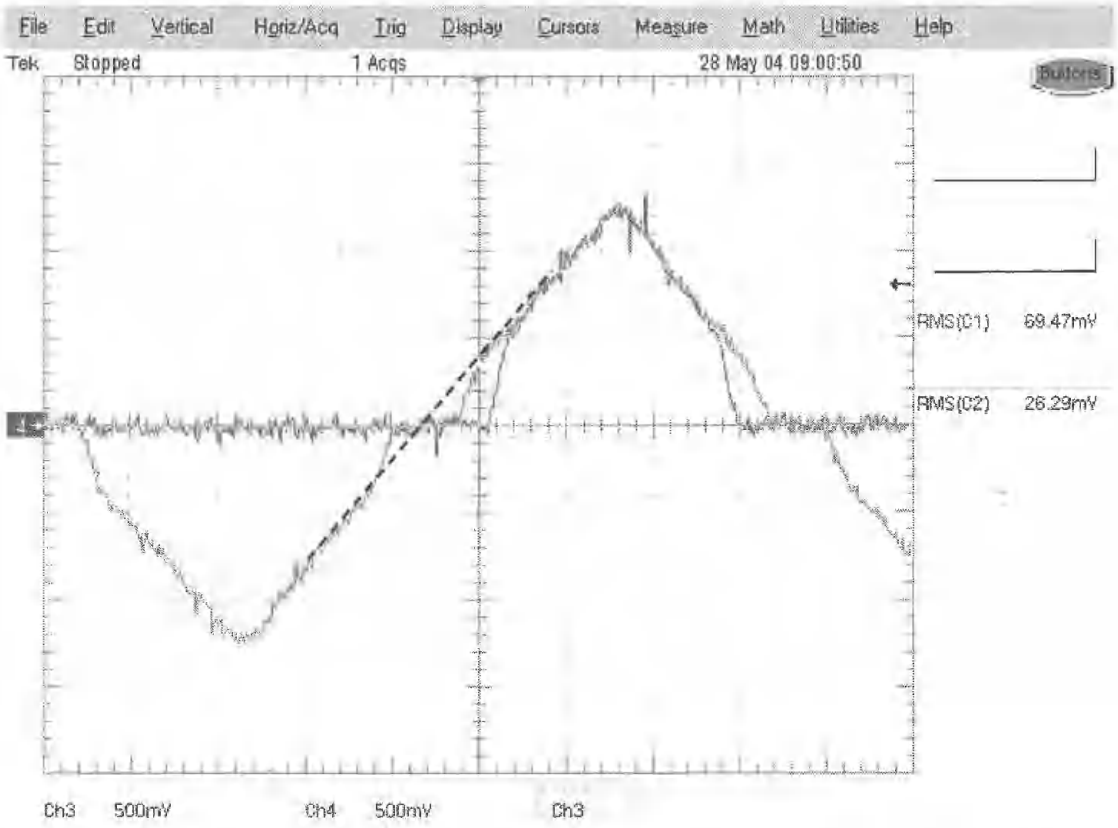

Fig. 3.9: Investigation of Reciprocating Drive via Over-Running Clutch, Full Load, Speed Output

Figs. 3.8 and 3.9 indicate that the PMSG speed follows a different trend when loaded. In Fig. 3.8 the effect of the unloaded PMSG is shown. Under no load the speed of the generator stayed above the speed of the dynamometer immediately after reaching the maximum speed. However, when the dynamometer had nearly completed the negative direction of the sinusoid the generator slowly began to rotate in the negative direction producing a small amount of voltage, as is shown in Fig. 3.10 in the comparison between the main voltage output signals in the no load output.

Fig. 3.9 shows that once a load has been applied to the PMSG the speed of the generator more closely follows the speed of the dynamometer in the positive direction. However once the dynamometer reaches 0 rev/min and begins to go in the negative direction the force from the load is greater than the frictional force of the over-running clutch and the speed remains at 0 rev/min until the dynamometer again reaches the 0 rev/min axis, after which the over-running clutch reengages and drives the generator.

3.1.3.2 Investigation of Reciprocating Drive via Over-Running Clutch, Unrectified Output

Figs. 3.10 and 3.11 show the output waveforms for the Investigation of Reciprocating Drive via Over-Running Clutch with an unrectified output. Both figures show the voltage on Ch1 and the current on Ch2.

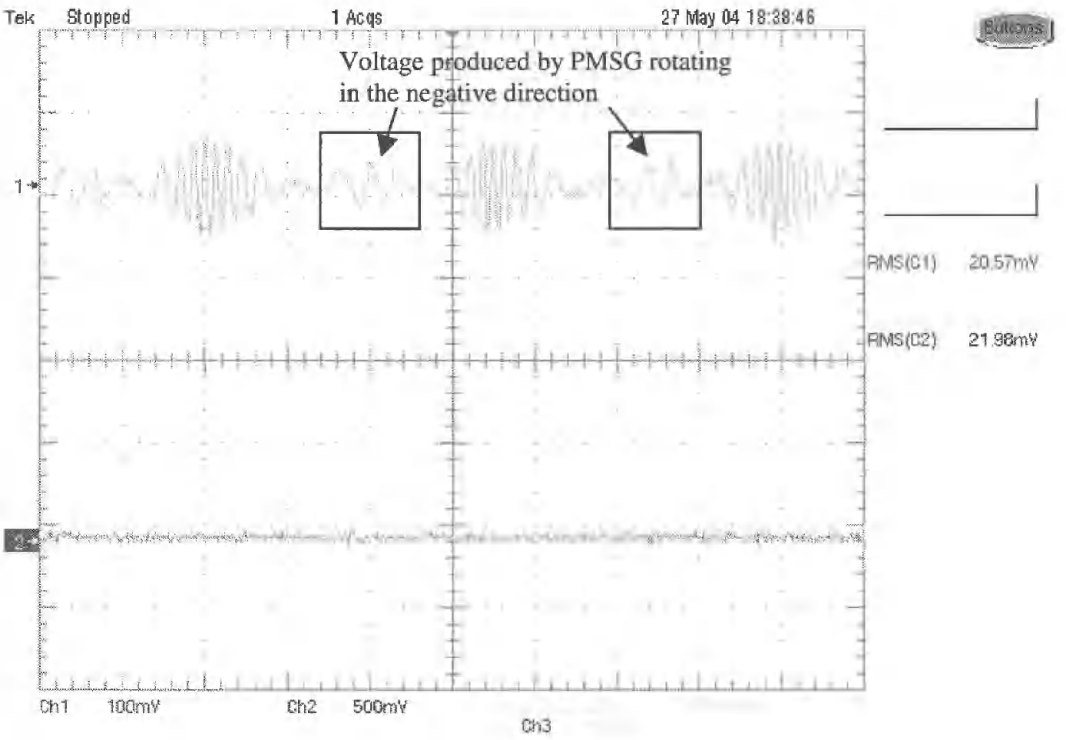

Fig. 3.10: Investigation of Reciprocating Drive via Over-Running Clutch, No-Load, Unrectified

Fig. 3.10 shows the output from the no load test. The additional components of generated voltage resulting from the momentary reverse direction of the PMSG in the periodic cycle is shown between the primary components of the voltage signal, see inset of Fig. 3.10. This additional voltage is at a very low frequency and had a considerably smaller magnitude than the driven voltage. With increased loads this phenomenon disappears, as is seen in Fig. 3.11 where there are no additional components in the voltage waveforms. For the tabular output of the no load Investigation of Reciprocating Drive via Over-Running Clutch refer to Table 3.7.

Table 3.7: Quantitative Output for Over-Running Clutch Connected Reciprocating Test, No-Load, Unrectified

No Load (0Nm)	Phase Quantities			
Peak	A	B	C	Total - Line
Irms (A)	0.00	0.00	0.00	0.00
Vrms (V)	10.53	10.59	10.60	18.53

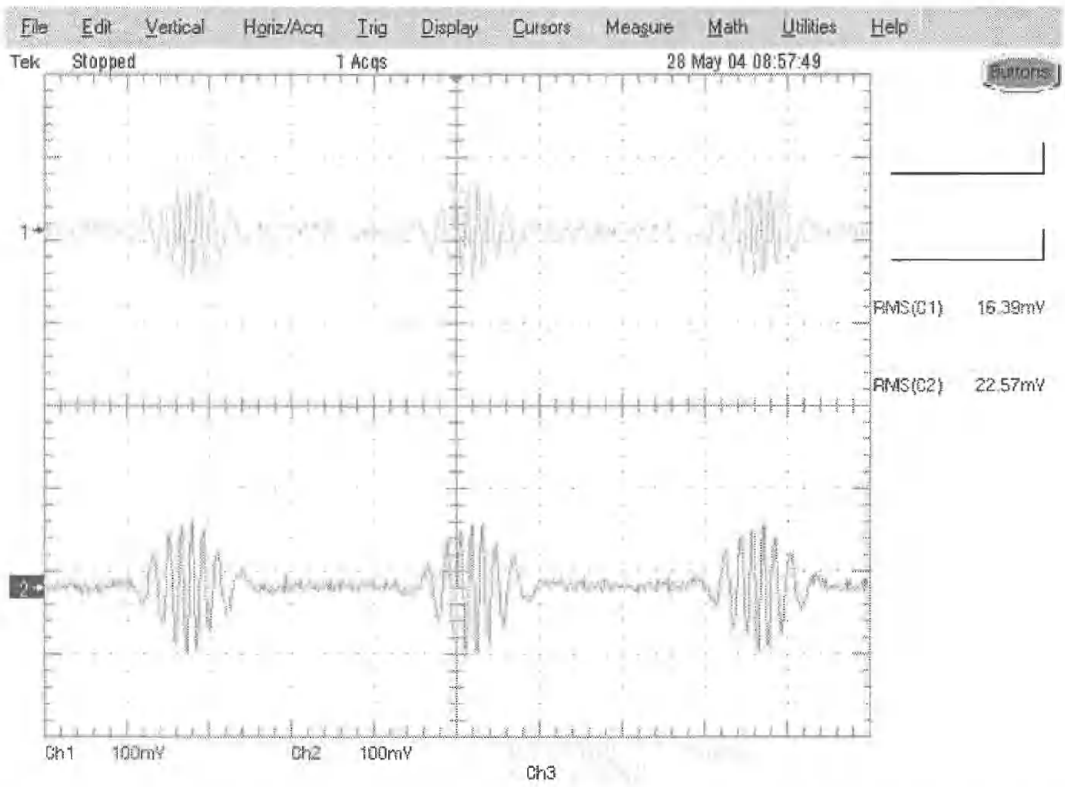

Fig. 3.11: Investigation of Reciprocating Drive via Over-Running Clutch, Full Load, Unrectified

Fig. 3.11 shows the voltage and current output of the PMSG when a full load is applied. Unlike with the directly connected reciprocating investigation the output from the over-running clutch connected investigation only yields approximately half of the voltage output, due to the PMSG stall and hold at 0 rev/min, while the dynamometer is in the reverse direction.

Table 3.8 summarizes the output from the full loaded experimentation of the Investigation of Reciprocating Drive via Over-Running Clutch.

Table 3.8: Quantitative Output for Over-Running Clutch Connected Reciprocating Test, Full Load, Unrectified

Full Load (14Nm)	Phase Quantities			
Peak	A	B	C	Total - Line
Irms (A)	5.03	4.99	4.85	4.96
Vrms (V)	9.83	10.10	9.72	17.12
P (kW)	-.05	-.05	-.05	-.15
Q (kVar)	.01	.01	.01	.02
S (kVA)	.05	.05	.05	.15

3.1.3.3 Investigation of Reciprocating Drive via Over-Running Clutch, Rectified Output

Figs. 3.12 and 3.13 show the output waveforms for the Investigation of Reciprocating Drive via Over-Running Clutch with a rectified output. Both figures show the ac voltage from the generator on Ch1 and the ac current on Ch2 prior to rectification. The rectified output is shown as the rectified voltage in Ch3 and the rectified current in Ch4.

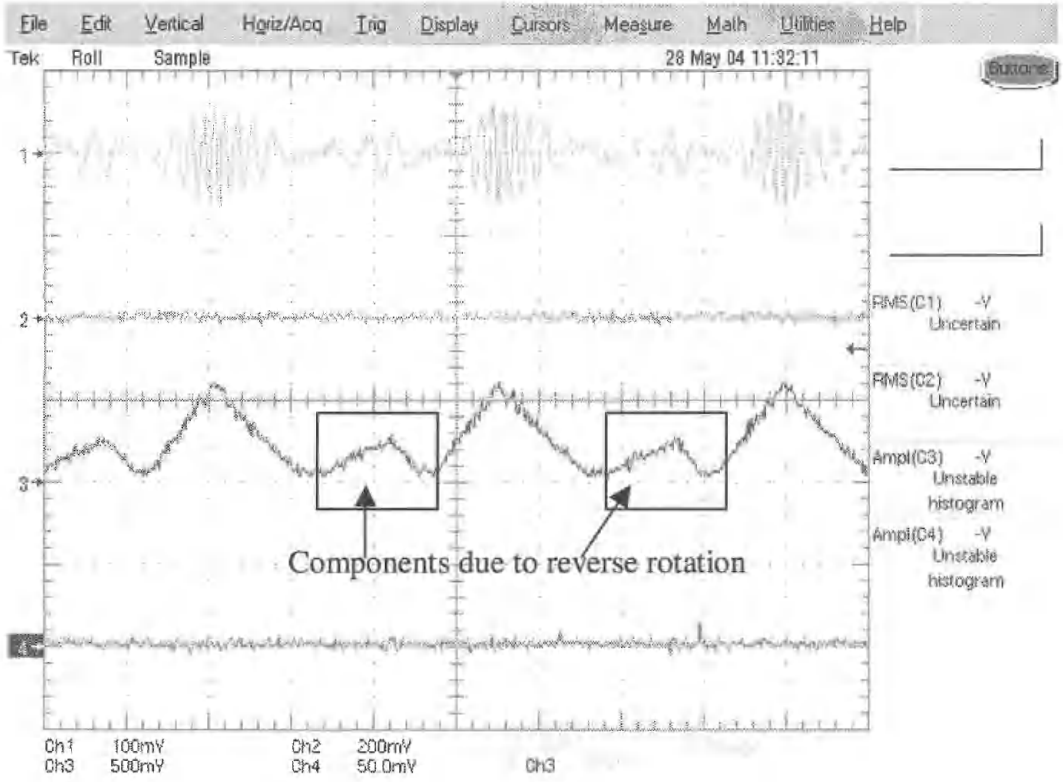

Fig. 3.12: Investigation of Reciprocating Drive via Over-Running Clutch, No Load, Rectified Output

Fig. 3.12 shows the output from the PMSG when the no load reciprocating investigation was rectified. Ch3 shows the voltage output from the rectifier into the load rheostat. The additional component is a result of the momentary reverse in generator direction discussed in section 3.1.3.3. This additional component in the voltage is only seen when the PMSG is at a no load condition. Once a load has been applied the pulse disappears. Therefore it will have no ill effects on the PMSG output once the system is under load.

For a quantitative view of the output refer to Table 3.9.

Table 3.9: Tabular Data for Investigation of Reciprocating Drive via Over-Running Clutch, No-Load, Rectified Output

Full Load (18.3Nm) Phase Quantities

Peak	A	B	C	Total – Line	Rectified Values
Irms (A)	0.00	0.00	0.00	0.00	0.00
Vrms (V)	11.33	11.08	11.15	19.38	24.3

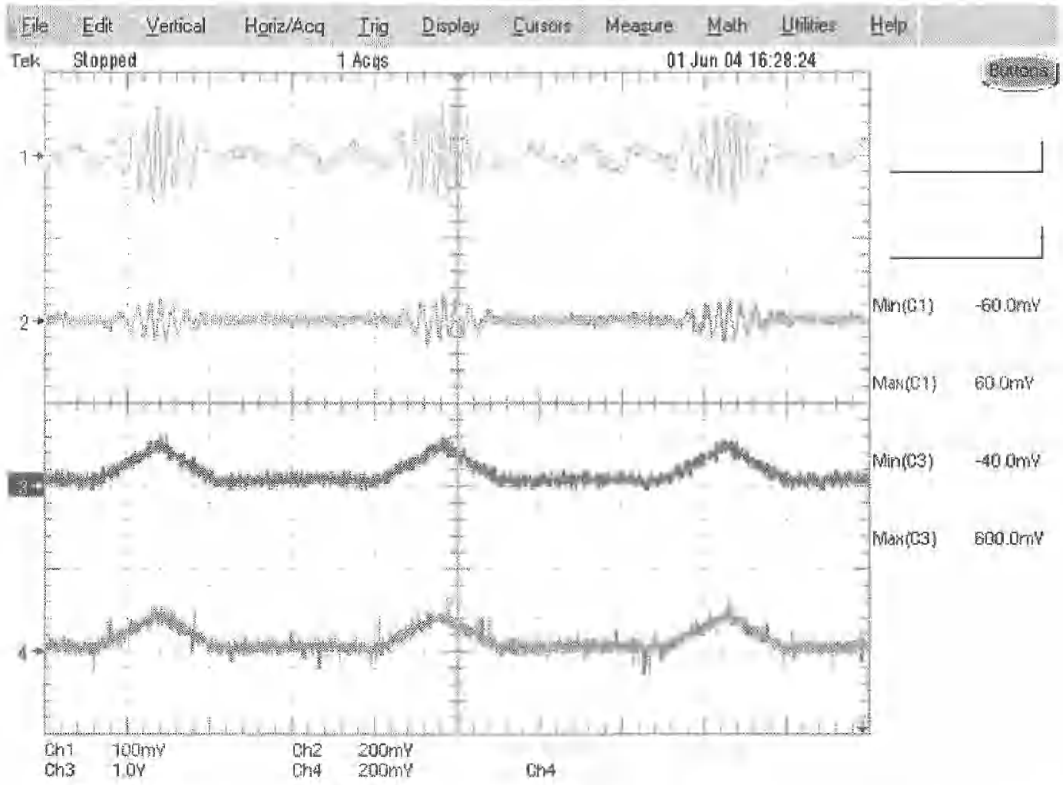

Fig. 3.13: Investigation of Reciprocating Drive via Over-Running Clutch, Full Load, Rectified Output

The output voltage and current waveforms for the Investigation of Reciprocating Drive via Over-Running Clutch in Fig. 3.13 shows both the direct ac and rectified output: Ch1 shows the ac voltage and Ch2 the ac current; and the rectified output, Ch3 and Ch4 are the voltage and current waveforms, respectively. The output shows that, similar to the no load outputs the rectifier essentially linearizes the voltage into an

approximately triangular voltage profile that is only evident for the PMSG when it is being directly driven by the dynamometer. When the over-running clutch disengages the output of the PMSG and, consequently, the rectifier is at 0V. The current follows the same linearization pattern as the voltage.

Table 3.10: Tabular Data for Investigation of Reciprocating Drive via Over-Running Clutch, Full Load, Rectified Output

Full Load (18.3Nm)	Phase Quantities				
Peak	A	B	C	Total – Line	Rectified Values
	High	High	High	High	High
Irms (A)	3.35	3.23	3.31	3.30	4.67
Vrms (V)	9.00	8.90	8.97	15.53	16.34
P (kW)	-.03	-.03	-.03	-.08	.08
Q (kVar)	.01	.01	.01	.03	-
S (kVA)	.03	.03	.03	.09	-

3.1.4 Directly Connected Base Speed with an Added Sine Component

For a complete description for the directly connected base speed with an added sine component refer back to section 2.1.4. The directly connected synchronous speed with an added sine component investigation for the PMSG was conducted to act as comparison values for the WRIG research with the same general characteristics. The following output for no-load and full load are presented below, all additional outputs are available in Appendix C. For the graphical outputs see Figs. 3.14 and 3.15 and the actual high and low values are shown in Tables 3.11 and 3.12.

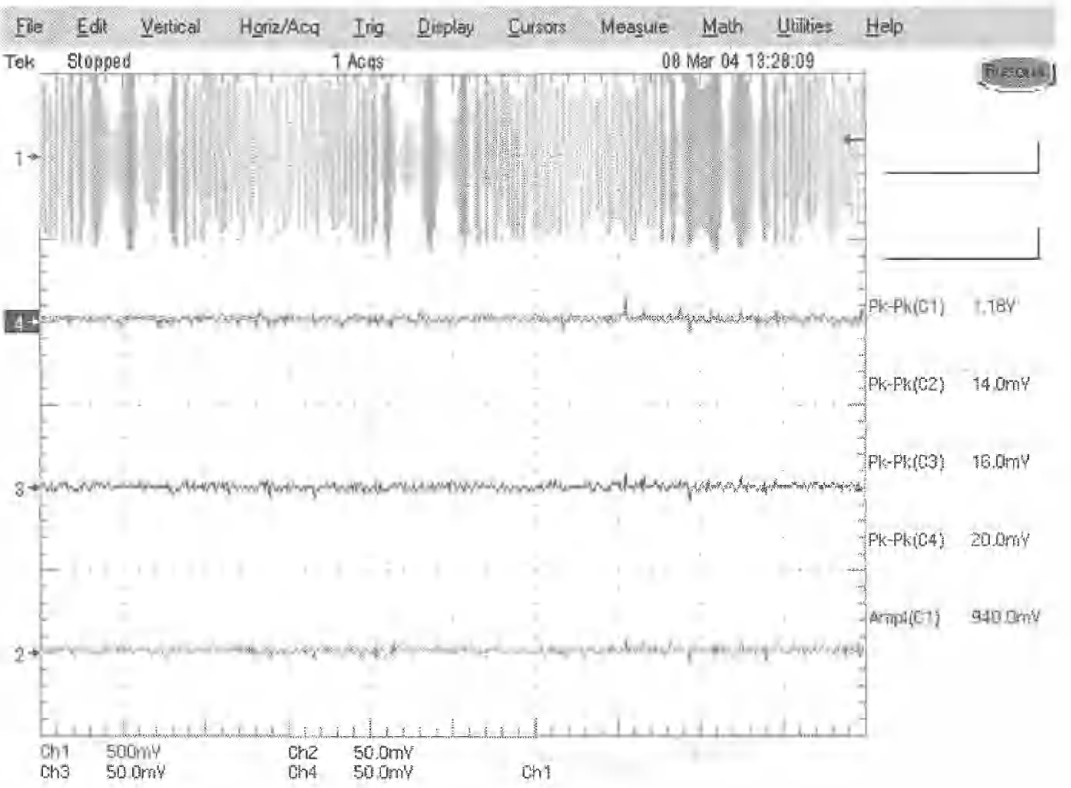

Fig. 3.14: Output for the PMSG with the Directly Connected Synchronous Speed with an Added Sine Component, No Load

Table 3.11: Tabular Output for the PMSG with the Directly Connected Synchronous Speed with an Added Sine Component, No Load

No Load (0Nm)	Phase Quantities							
Peak	A		B		C		Total – Line	
	High	Low	High	Low	High	Low	High	Low
Irms (A)	0.00	0.00	0.00	0.00	0.00	0.00	0.00	0.00
Vrms (V)	112.21	95.77	111.07	94.75	111.11	94.5	193.06	164.56

For Fig. 3.14 the channel 1 trace is the voltage and the additional 3 channels show the phase current values, as before the output values of the currents are zero for the no load condition. Fig. 3.15 shows that the voltage is similar to the no load condition except there is a periodic output current in each of the phases.

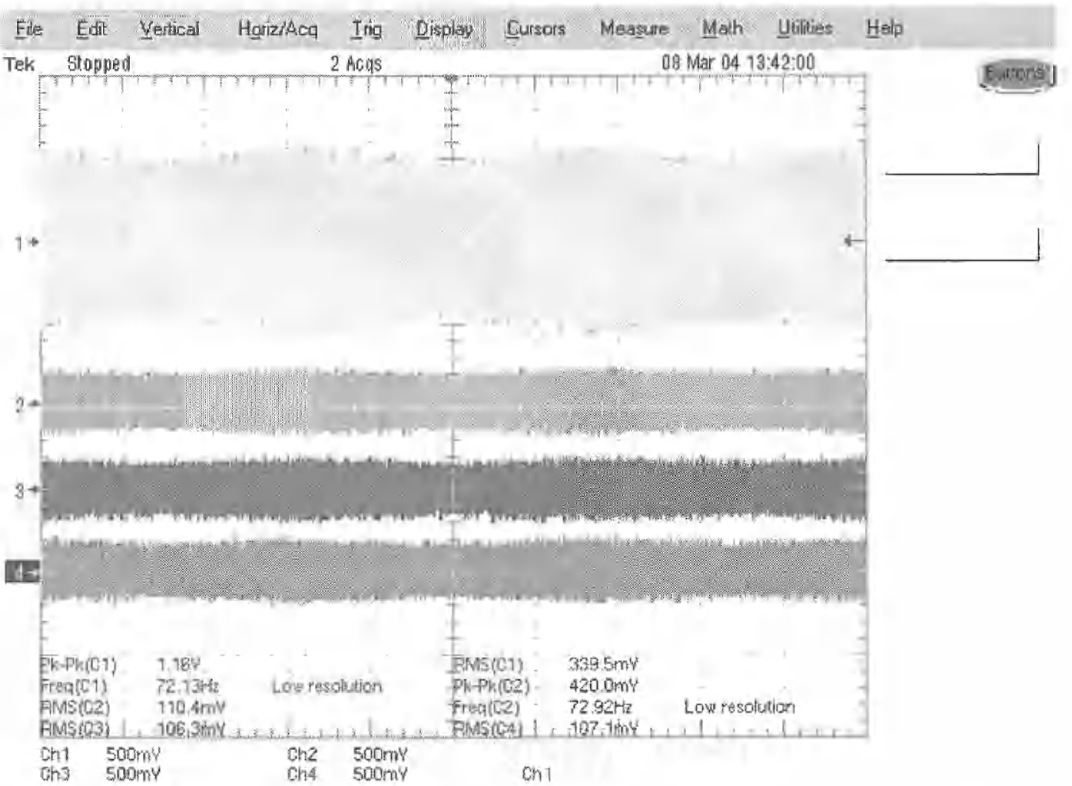

Fig. 3.15: Output for the PMSG with the Directly Connected Synchronous Speed with an Added Sine Component, Full Load

Table 3.12: Tabular Output for the PMSG with the Directly Connected Synchronous Speed with an Added Sine Component, Full Load

Full Load (18.3Nm) Phase Quantities

Peak	A		B		C		Total – Line	
	High	Low	High	Low	High	Low	High	Low
Irms (A)	12.18	10.28	12.84	10.88	12.43	10.56	12.48	10.57
Vrms (V)	116.82	101.26	107.95	94.68	107.52	94.56	191.99	167.8
P (kW)	-1.41	-1.03	-1.41	-0.94	-1.40	-0.98	-4.22	-2.146
Q (kVar)	0.162	0.129	1.166	0.874	1.089	0.82	2.935	2.2
S (kVA)	1.422	1.041	1.386	1.03	1.336	0.998	4.151	3.073

In both Figs., 3.14 and 3.15, the 3.5s period is evident in the voltage trace, Ch1. The fully loaded output has the most relevance for a comparison between the two generator types.

3.1.5 Over-Running Clutch Connected Base Speed with Added Sine Investigation

3.1.5.1 Over-Running Clutch Connected Base Speed with Added Sine Investigation, Speed Profile

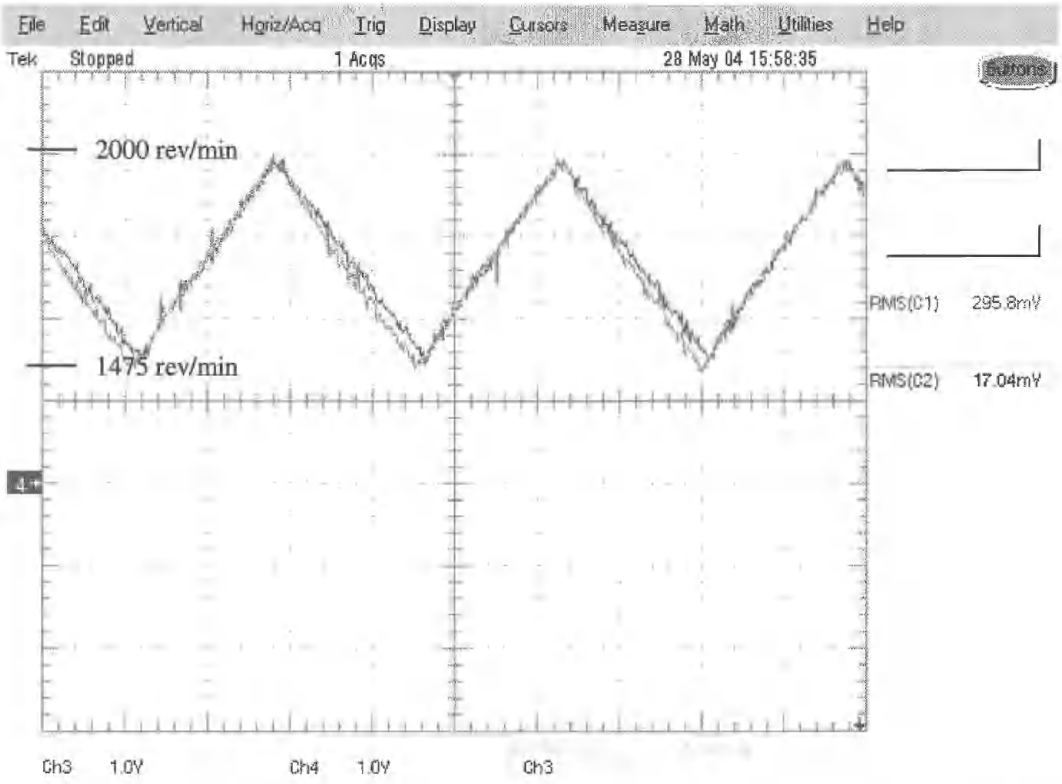

Fig. 3.16: Over-Running Clutch Connected Base Speed investigation, Speed Profile - No Load

The profiles in Figs. 3.16 and 3.17 show the speed of the PMSG and dynamometer when operated at no load and full load, respectively. What is seen in the two figures is similar to the effects shown in the reciprocating investigation, section 3.1.3.1, and later in the WRIG experiments, section 3.2.3. At the no load condition the inertia of the generator is sufficient to maintain its speed, which is greater than that of the dynamometer as it slows. When comparing Fig. 3.16 with Fig. 3.17 it is shown that the generator profile changes. In Fig. 3.16 the PMSG speed actually remains at a

higher speed than the dynamometer for the portion of the time relative to when the dynamometer speed is decreasing.

Fig. 3.17 shows that when the PMSG is under load the speed profile of the dynamometer and the PMSG are effectively identical. This again helps to reinforce the hypothesis that when the inertial force of the generator is greater than the load force the generator speed would be more constant resulting in a more constant output.

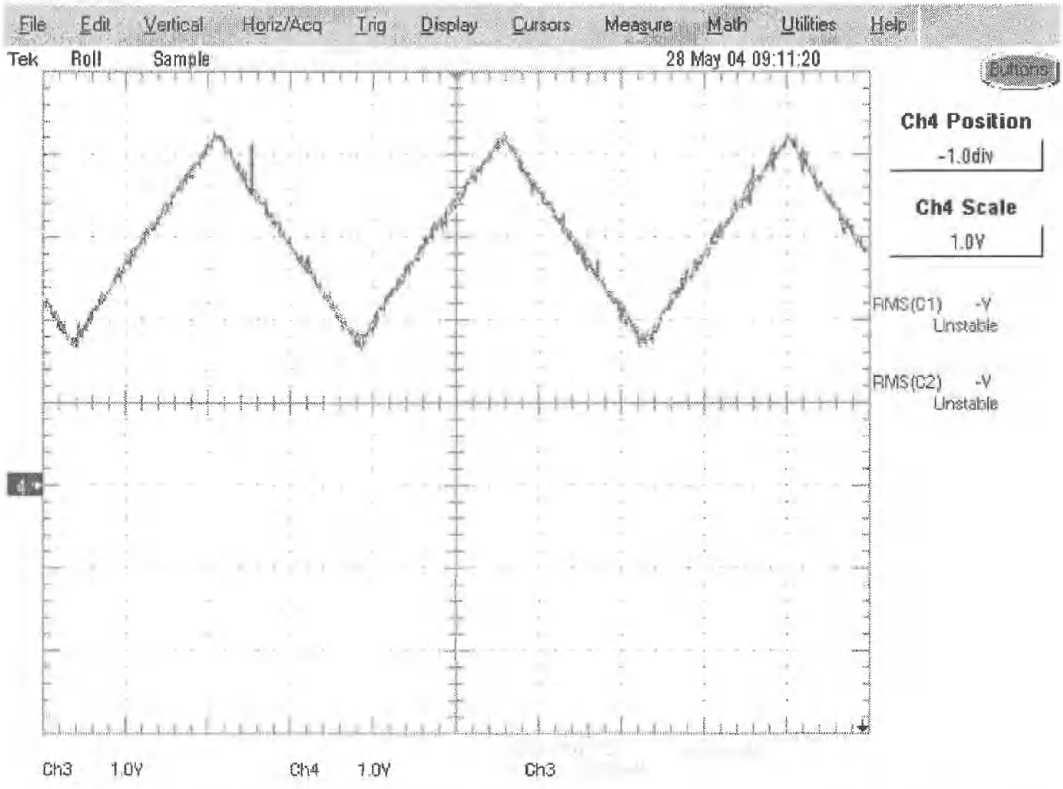

Fig. 3.17: Over-Running Clutch Connected Base Speed investigation, Speed Profile – Full Load

3.1.5.2 *Over-Running Clutch Connected Base Speed with Added Sine Investigation, Unrectified Output*

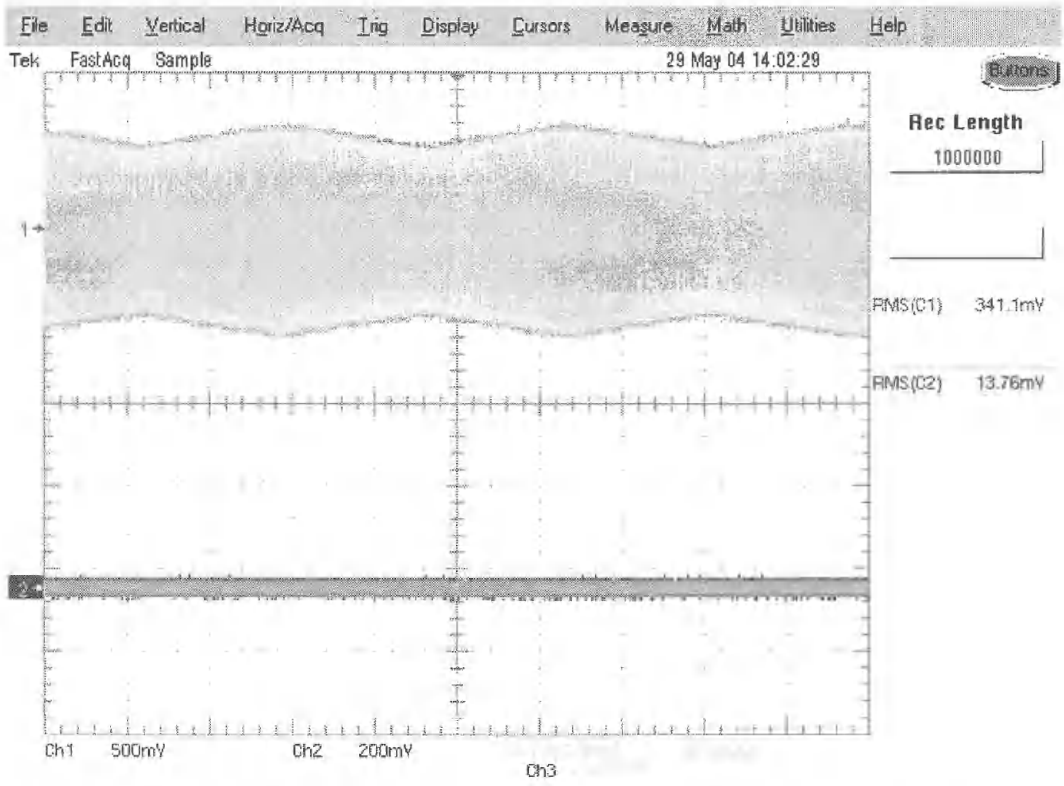

Fig. 3.18: Over-Running Clutch Connected Base Speed with Added Sine Investigation, Unrectified, No Load

Fig 3.18 shows the PMSG output when the generator is applied to a sinusoidal oscillation after it has reached a base speed. For this investigation that base speed was 2062.5 rev/min. The 3.5s overall oscillation period is evident in the Ch1, ac voltage, output. The quantitative results taken at the extremes of the output have also been added to this discussion those results can be seen in Table 3.13.

Table 3.13: Tabular Data for Over-Running Clutch Connected Base Speed with Added Sine Investigation, Unrectified, No Load

No Load
(0 Nm)

Peak	Phase Quantities							
	A		B		C		Total – Line	
	High	Low	High	Low	High	Low	High	Low
Irms (A)	0.00	0.00	0.00	0.00	0.00	0.00	0.00	0.00
Vrms (V)	116.42	94.55	116.2	64.69	115.98	94.78	201.6	163.98

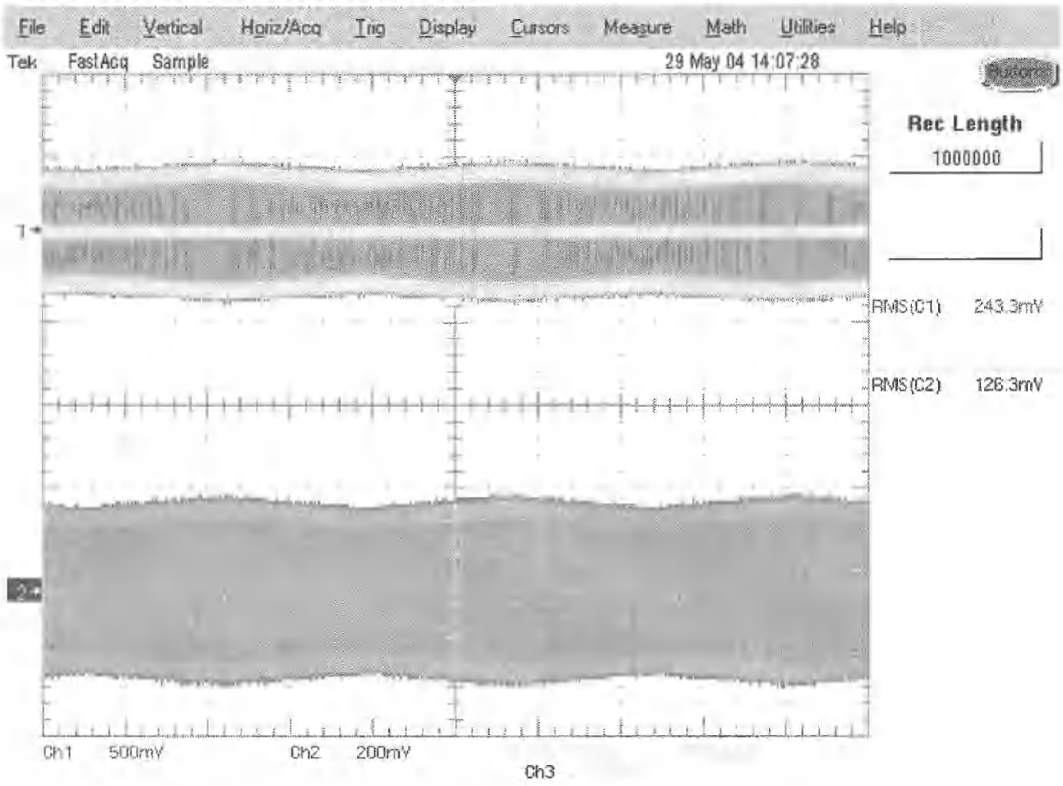

Fig. 3.19: Over-Running Clutch Connected Base Speed with Added Sine Investigation, Unrectified, Full Load

The results for the over-running clutch connected base speed with added sine investigation at full load are shown in Fig. 3.19 and Table 3.14. This output shows that there is some difference in the high and low extremes of such a modulated signal. Based on the investigations conducted, and experience with the PMSG the output

follows a relatively linear change as the speed changes. This is substantiated by the values in Table 3.14 and the PMSG no load test conducted in section 2.1.1.

Table 3.14: Over-Running Clutch Connected Base Speed with Added Sine Investigation, Unrectified, Full Load

Full Load (18.3Nm)	Phase Quantities							
Peak	A		B		C		Total – Line	
	High	Low	High	Low	High	Low	High	Low
Irms (A)	10.64	9.53	9.83	8.77	10.00	8.93	10.16	9.08
Vrms (V)	116.04	98.83	124.92	104.44	117.98	99.71	207.34	174.97
P (kW)	-1.23	-.94	-1.23	-.91	-1.18	-.89	-3.63	-2.74
Q (kVar)	.10	.08	.08	.07	.06	.55	.34	.26
S (kVA)	1.24	.94	1.23	.92	1.18	.89	3.65	2.75

3.1.5.3 Over-Running Clutch Connected Base Speed with Added Sine Investigation, Rectified Output

The outputs from the rectified over-running clutch connected base speed with added sine investigation are shown in Figs. 3.20, 3.21, 3.22, and 3.23. For these figures Ch1 shows the ac voltage, Ch2, the ac current, Ch3, the rectified voltage, and Ch4, the rectified current.

This indicated that when the output from the PMSG was rectified, and the base speed with added sine was implemented as the prime mover, it had some voltage ripple. Adding some form of dc bus filtration, possibly as simple as a capacitor bank, will sufficiently negate the probable disturbances that this can cause in the power system.

Due to the relative difficulty extracting direct values from the oscilloscope captures in Figs. 3.20 and 3.22, Tables 3.15 and 3.16 have been included, these tables include the values of the voltage, current, power, etc., enabling easy verification of the

investigation. Additionally, Figs. 3.21 and 3.23 show the same output metrics as Figs. 3.20 and 3.22 with the time scale considerably tightened.

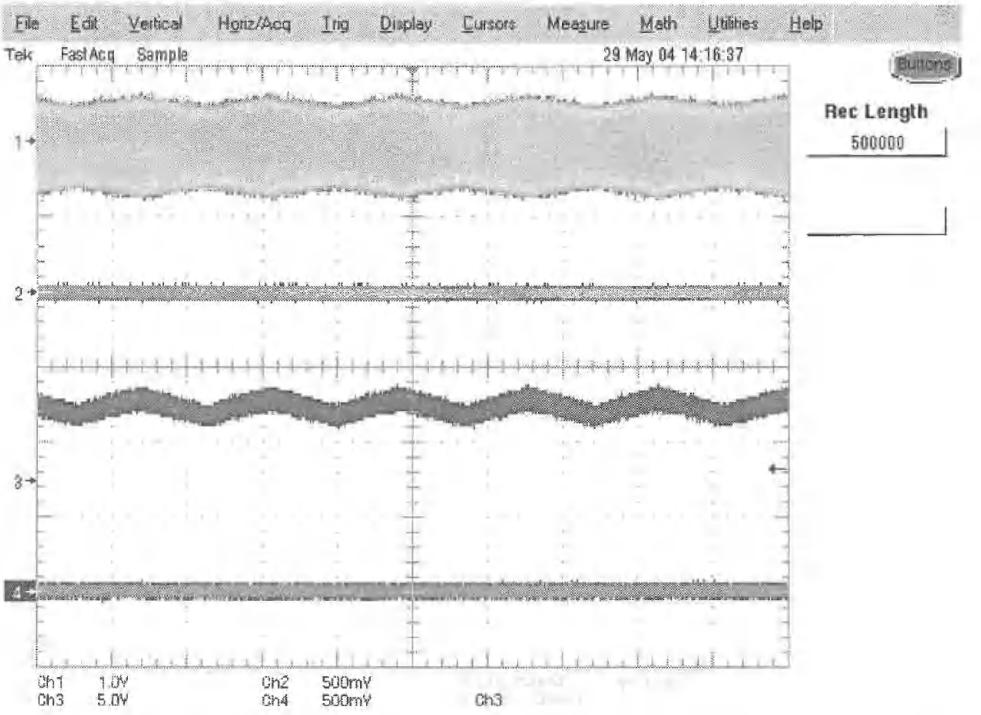

Fig. 3.20: Over-Running Clutch Connected Base Speed with Added Sine Investigation, Rectified, No Load

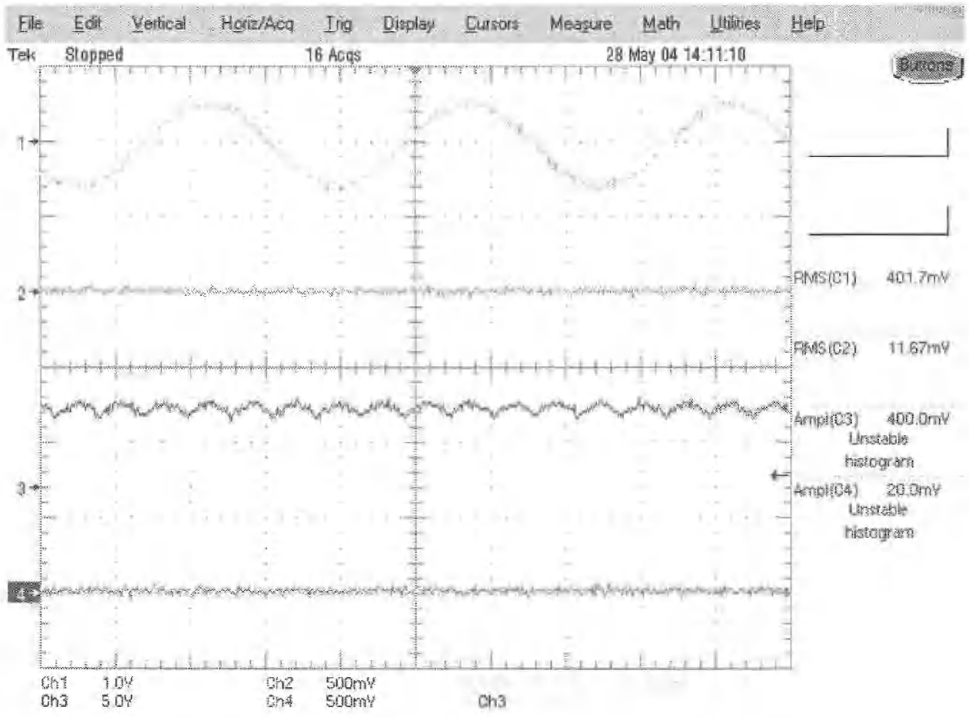

Fig. 3.21: Close up of Over-Running Clutch Connected Base Speed with Added Sine Investigation, Rectified, No Load

Table 3.15: Tabular Data for Over-Running Clutch Connected Base Speed with Added Sine Investigation, Rectified, No Load

Full Load (18.3Nm) Phase Quantities

Peak	A		B		C		Total – Line		Rectified Values	
	High	Low	High	Low	High	Low	High	Low	High	Low
Irms (A)	0.00	0.00	0.00	0.00	0.00	0.00	0.00	0.00	0.00	0.00
Vrms (V)	117.11	96.50	116.83	96.03	116.66	96.22	202.42	166.71	268.65	222.01

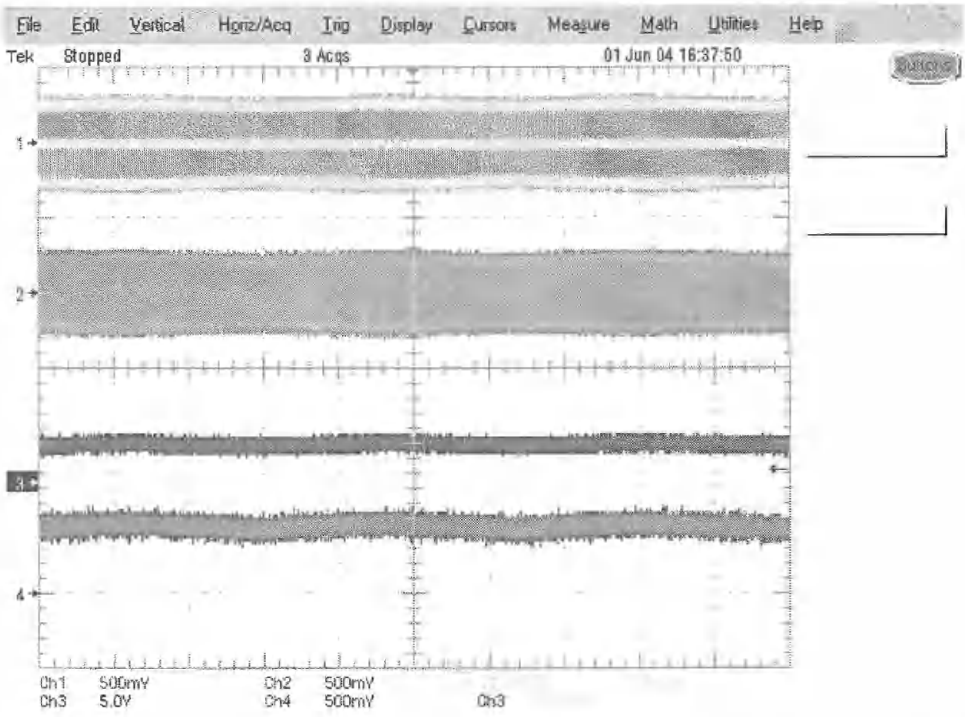

Fig. 3.22: Over-Running Clutch Connected Base Speed with Added Sine Investigation, Rectified, Full Load

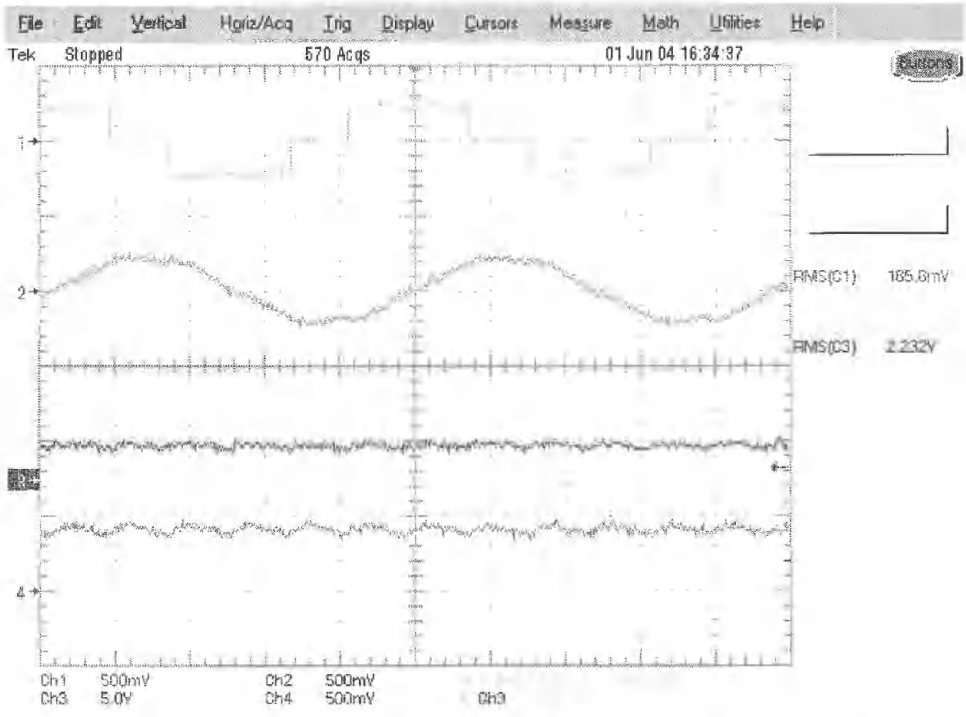

Fig. 3.23: Close up of Over-Running Clutch Connected Base Speed with Added Sine Investigation, Rectified, Full Load

When the time scale was decreased to the point where the 60 Hz frequency could be seen, as in Ch1 of both Figs. 3.21 and 3.23, an interesting output was noticed. Under no load conditions, Fig. 3.21, the voltage was smooth as expected, however when the generator was loaded the output voltage became "stair stepped", see Fig. 3.23, Ch1. This stair step is believed to be due to the reflection of the three phases on each other by mutual inductance. Each of the steps for the single phase of the PMSG shows a length of approximately 120° electrical, which correlates well with the three phases of the PMSG. It is hypothesized that the stair step comes from the reflection of the voltage off the forward biasing of the rectifier for each phase. This effect is likely to be amplified by the relationship between the accompanied torque ripple and the permanent magnets. As the torque increases or decreases the permanent magnet will have an equal and opposite reaction.

Table 3.16: Tabular Data for Over-Running Clutch Connected Base Speed with Added Sine Investigation, Rectified, Full Load

Full Load (18.3Nm) Phase Quantities

Peak	A		B		C		Total – Line		Rectified Values	
	High	Low	High	Low	High	Low	High	Low	High	Low
Irms (A)	14.48	12.32	14.37	12.23	14.38	12.25	14.41	12.27	19.3	17.1
Vrms (V)	84.87	76.71	84.68	76.5	84.83	76.51	146.87	132.63	176.55	160.10
P (kW)	-1.15	-.88	-1.14	-.87	-1.14	-.87	-3.42	-2.62	-3.41	-2.74
Q (kVar)	.44	.35	.44	.34	.44	.34	1.32	1.03	-	-
S (kVA)	1.23	.95	1.22	.94	1.22	.94	3.67	2.82	-	-

3.2 Wound Rotor Induction Generator

3.2.1 Per-Phase Equivalent Circuit

Before the performance investigation of the WRIG it is necessary to determine the per-phase equivalent circuit model so that the parameters can be used to solve for additional requirements. To complete this testing a series of machine tests were conducted to obtain the required parameters. The following is a list of tests that were conducted.

1. Winding Ratio Test

   The winding ratio test is used to solve for the ratio between the rotor and stator windings. The relevance of the information is that without knowing the winding turns ratio between the rotor and stator windings a referred equivalent circuit model cannot be found. The winding turns ratio is required to refer any rotor components to the stator circuit to build a stator referred per-phase equivalent circuit.

2. No-Load Test

   The no-load test is used to find the core losses and the windage and friction losses. This relates to the parameters of the core.

3. Blocked Rotor Test

   The blocked rotor test is used to find the necessary information regarding leakage impedances and there relationships to the rest of the circuit.

The combination of the three previously mentioned tests with the equations in section 2.2.1 yields all of the necessary primary referred per-phase equivalent parameters at 60 Hz. supply frequency, shown in Fig. 3.24.

a = 1.1061 (rotor:stator winding turns ratio

R_c = 93.63Ω (core loss resistance)

X_m = 4.65Ω (magnetizing reactance)

R_1 = .18Ω (stator winding resistance)

R_2' = .33Ω (primary referred rotor winding resistance)

X_1 = .40Ω (stator winding reactance)

X_2' = .40Ω (rotor winding reactance)

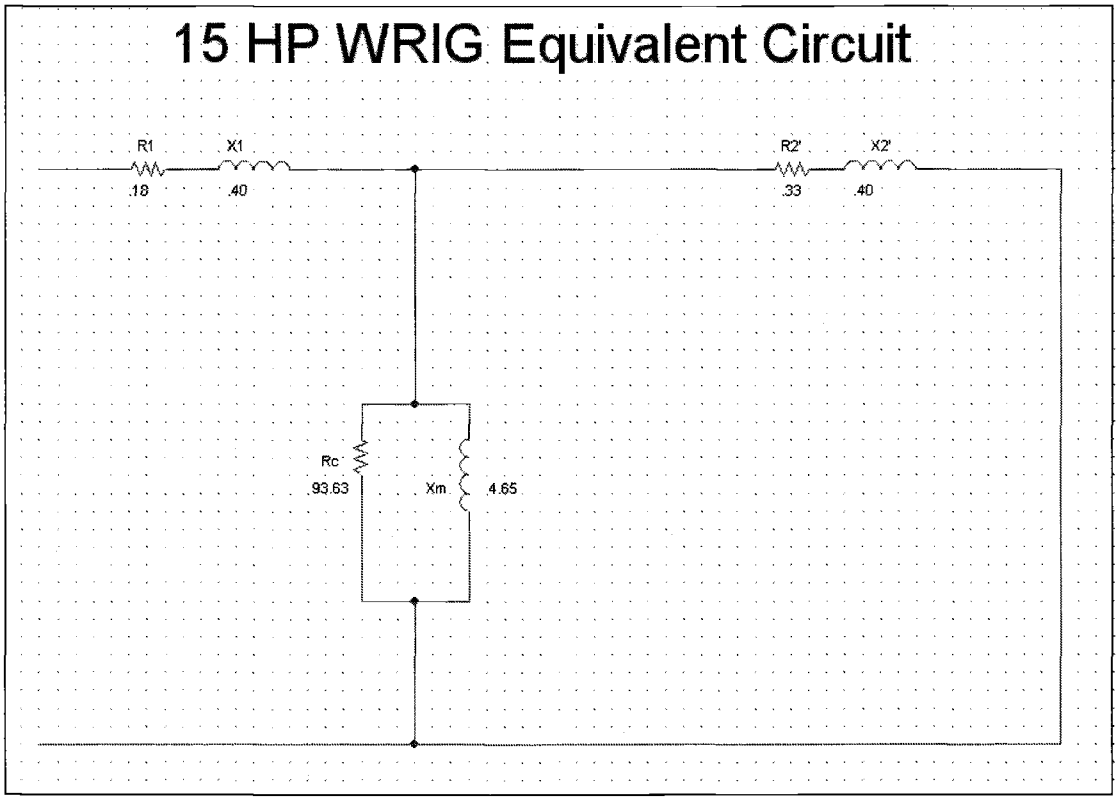

Fig. 3.24: Final 15 HP Wound Rotor Induction Generator Per-Phase Equivalent Circuit

3.2.2 Baseline Steady State Testing

The baseline steady state test for the WRIG was used to act as a characterization of the generator under standard operating procedure. The generator was brought up to

synchronous speed and then the utility connection to the stator circuit was energized and generator was initiated.

Fig 3.25 shows the output of the WRIG running under steady state conditions at its synchronous speed of 1200rev/min.

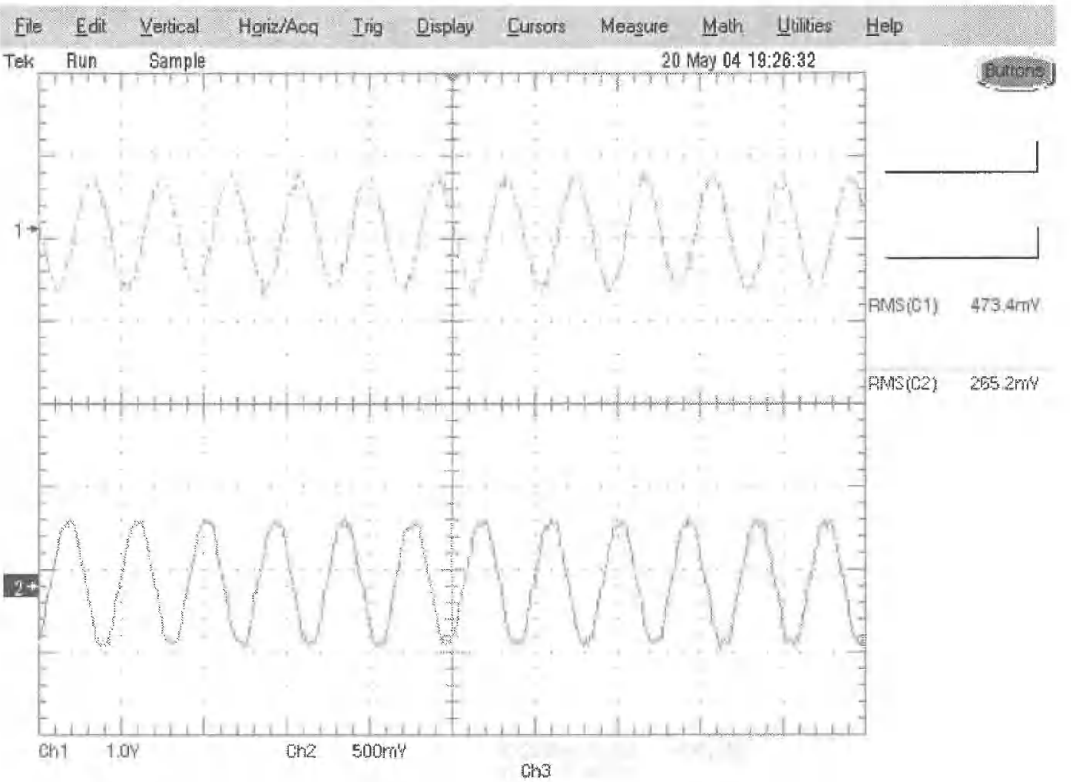

Fig. 3.25: Baseline Test for the WRIG at 1200 Rev/Min

The upper trace, CH1, is the trace corresponding to the output voltage of a single phase and the lower trace, Ch2, corresponds to a single phase of the generator current. Table 3.17 shows the quantitative values for the WRIG.

Table 3.17: Quantitative Output for the Baseline Test for the WRIG at 1200 Rev/Min

Speed: 1200	Phase Quantities			Torque:3.3Nm
Peak	A	B	C	Total-Line
Irms (A)	26.96	26.37	25.49	26.27
Vrms (V)	233.6	231.6	233.5	232.9
P (kW)	0.38	0.379	0.365	0.926
Q (kVar)	3.66	3.51	3.39	10.56
S (kVA)	3.6	3.53	3.41	10.53

As the table shows the generator is actually in a motoring condition. This can be seen by the polarity of the power metrics, when the generator is generating the power will show negative values. This helps to illustrate a 4 pole WRIG will only generate power at speeds greater than their synchronous speed of 1200 rev/min.

With the added external rotor impedance, the useable generator speed was effectively increased, the impedance values used on the rotor circuit enabled the rated generating speed to be changed from 1260 rev/min to approximately 1462.5 rev/min. The resulting output at steady state is shown in Fig. 3.26. The oscilloscope capture, Fig. 3.26 shows the same two outputs with the phase voltage on CH1 and the phase current on CH2.

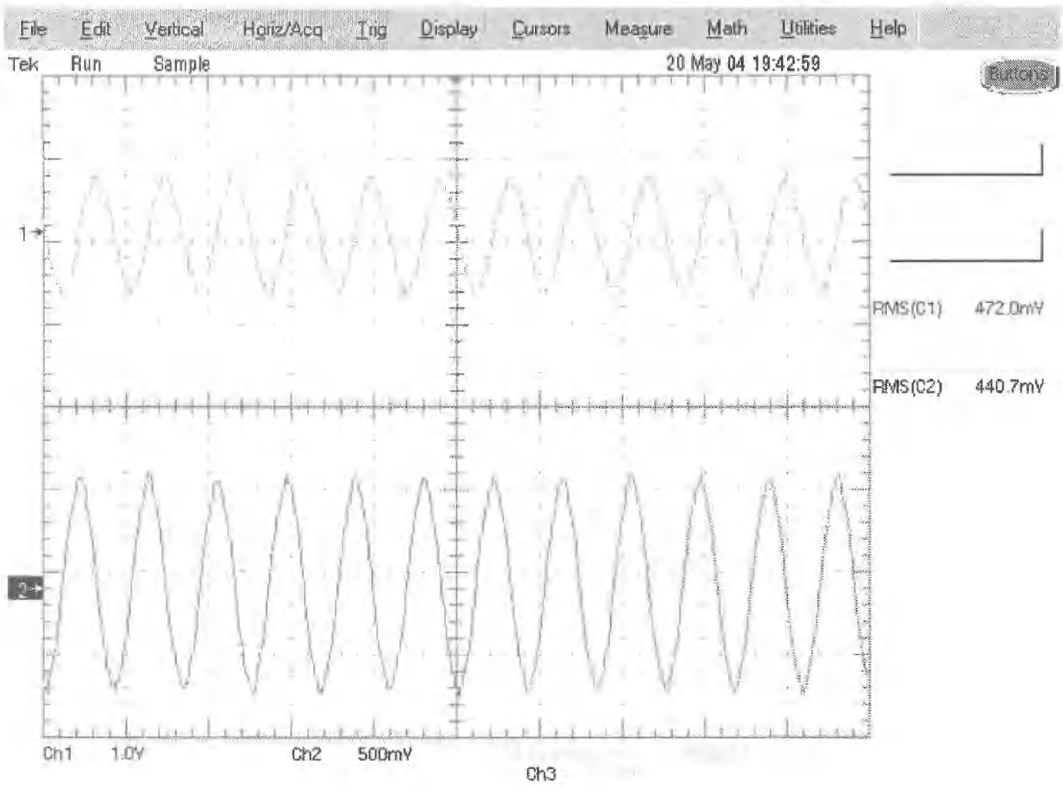

Fig. 3.26: Baseline Test for the WRIG at 1462.5 Rev/Min

Table 3.18 shows the output for the WRIG at steady state, 1462.5 rev/min.

Table 3.18: Quantitative Output for the Baseline Test for the WRIG at 1462.5 Rev/Min

Speed: 1462.5	Phase Quantities			Torque:94.4Nm
Peak	A	B	C	Total-Line
Irms (A)	44.97	44.85	43.07	44.29
Vrms (V)	234	232.2	234.01	232.2
P (kW)	-3.21	-3.36	-3.09	-9.68
Q (kVar)	5.25	4.95	4.877	15.073
S (kVA)	5.99	5.97	5.81	17.75

As the Table 3.18 shows, at 1462.5 rev/min the generator was generating near its expected full output. The variation between the expected output and the actual measured output is most likely due to the high tolerances of the impedances that were added into the rotor circuit.

The last steady state output that will be shown is for 1550 rev/min. This output is significant because it stretches the limits of the generators ratings. Fig. 3.27 shows that even at higher speeds the WRIG was able to withstand the increased load.

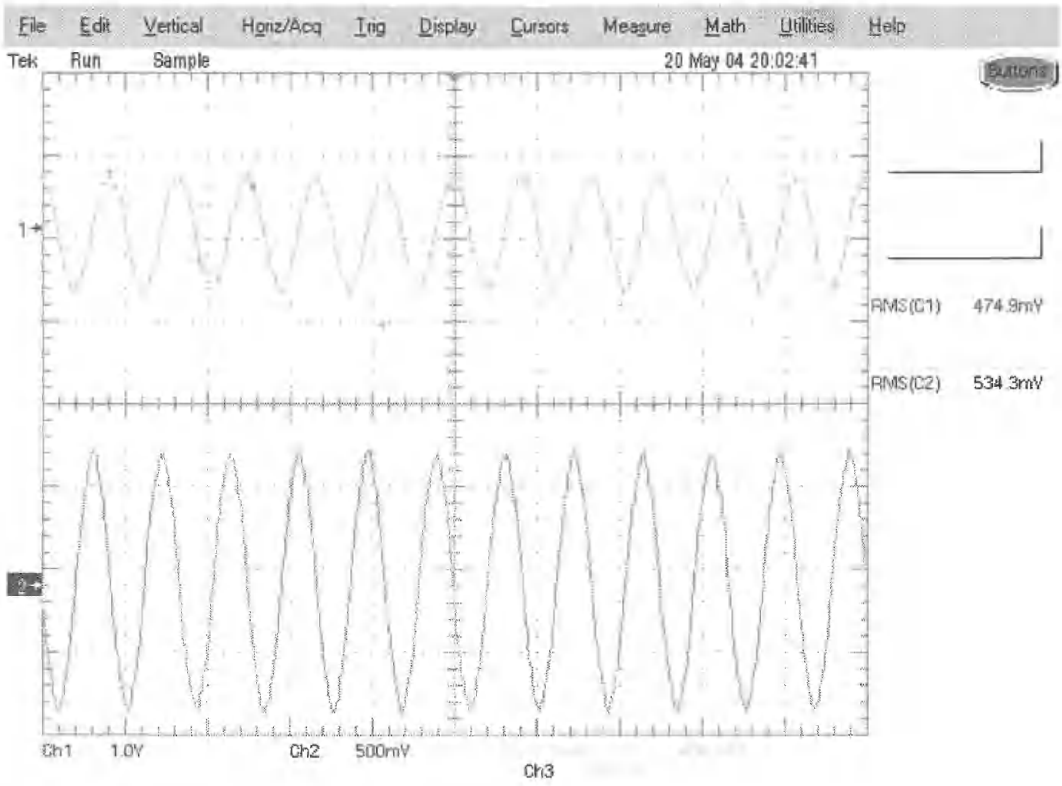

Fig. 3.27: Baseline Test of WRIG - 1550 Rev/Min

Table 3.19: Tabular Data for Baseline Test of WRIG - 1550 Rev/Min

Speed: 1550	Phase Quantities			Torque:126Nm
	A	B	C	Total-Line
Irms (A)	53.14	54.06	52.19	53.13
Vrms (V)	234.4	231.8	233.8	233.3
P (kW)	-4.29	-4.47	-4.22	-12.99
Q (kVar)	5.84	5.65	5.56	17.048
S (kVA)	6.91	6.23	6.77	19.89

Table 3.19 shows the values of the currents, voltages, real and reactive power and the apparent power all of which are well over the 1.15 service factor of the generator.

The overall percent efficiency of the generator at 1550 rev/min is $\frac{P_{out}}{P_{in}} \times 100 = \frac{12.99kW}{T \times \omega_{rot}} \times 100 = \frac{12990W}{126Nm \times (1550 \frac{rev}{\min} \times \frac{2\pi rad}{60s})} \times 100 = 63.5\%$, when this is compared to the efficiency at 1462.5rev/min of 67% it shows that as the speed is increased above the rating the efficiencies will decrease. The ability to investigate the higher speed operation is due to the change in the impedance of the rotor circuit as a function of the frequency.

3.2.3 Over-Running Clutch Base Speed with an Added Sine Component

The over-running clutch base speed with an added sine experiment was conducted to show the output of the WRIG when it is applied to a wave profile. The assumption behind this mode of operation was that the unloaded generator would spin up to a baseline speed and then, once it had reached the base speed, it would reciprocate above and below that speed in a periodic fashion. The over-running clutch would allow the generator inertia to keep the output more constant than if it were directly connected.

Due to the maximum ratings of the WRIG the magnitude of the oscillation was reduced from 262.5 rev/min to 150 rev/min. The output from the generator under these conditions was sufficient enough to draw the necessary conclusions for verifying the usefulness of the WRIG in this mode of operation.

Fig. 3.28 shows the output voltage on CH1 and the current on CH2. The reciprocating type of prime mover using a WRIG with external rotor impedance produces an approximately constant voltage output and a reciprocating current output. The current waveform distinctly shows the 3.5s period modulating the generated

16.6ms period of 60 Hz. Fig 3.29 is the spectral analysis (FFT) of the output current shown in Fig. 3.28. Fig. 3.29 shows the main spectral component in the generation at the line frequency of 60 Hz. A second component is shown at around 0.25 Hz, this component is from the mechanical 3.5s oscillation, which should be at a maximum at a frequency of .29 Hz. $f = \frac{1}{Period} = \frac{1}{3.5s} = .29Hz$

The values for the frequencies can be seen in the upper right corner of the oscilloscope capture, Fig. 3.29.

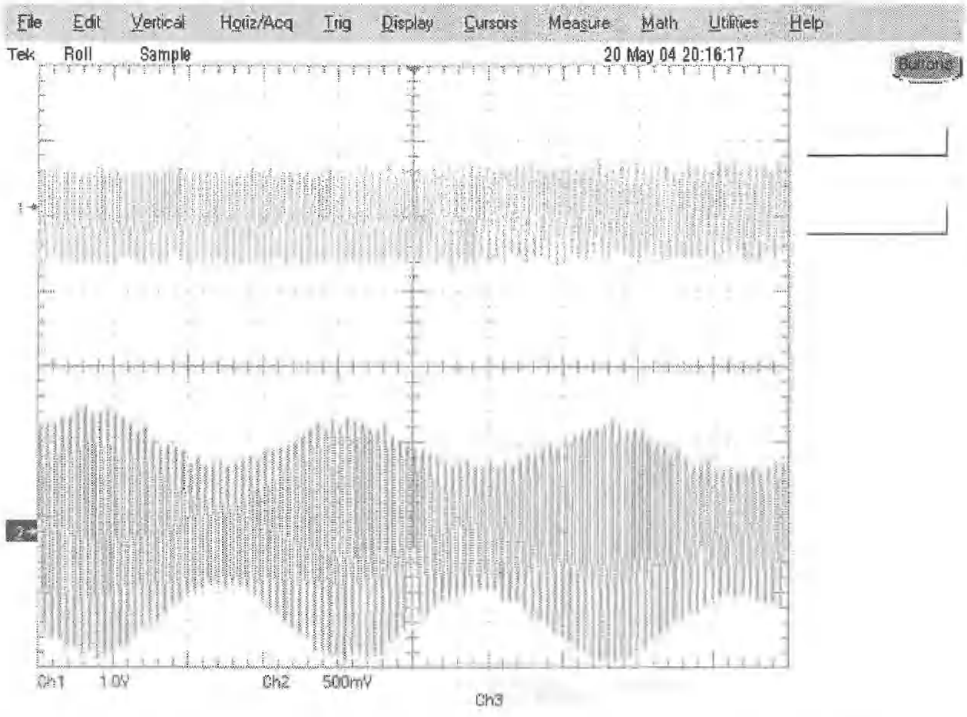

Fig. 3.28: Base Speed with an Added Sine Experiment for the WRIG

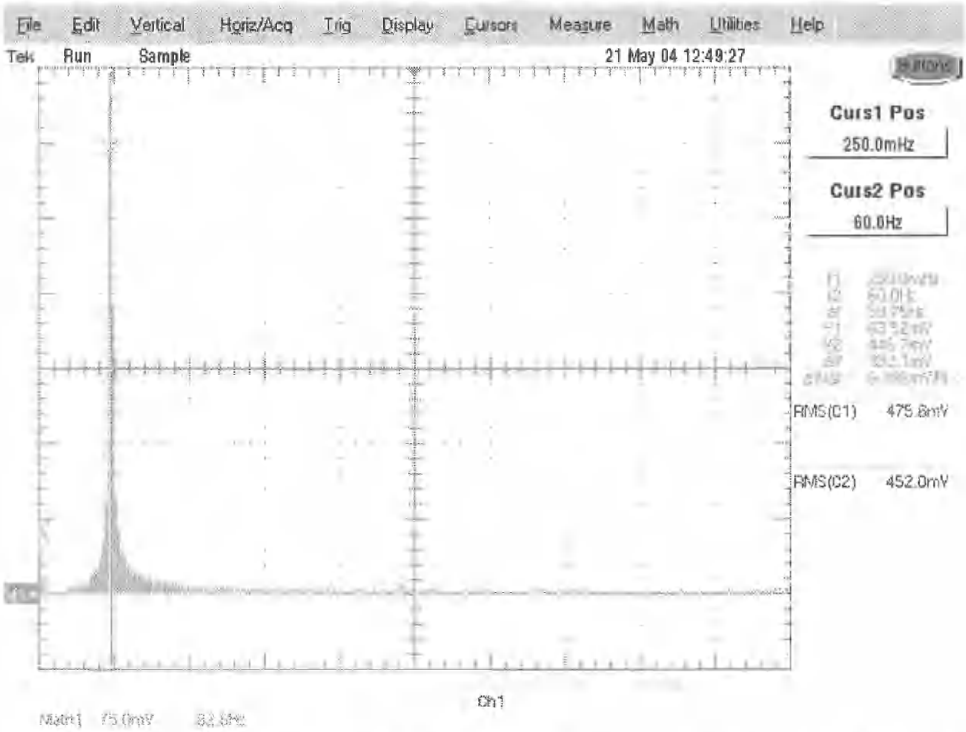

Fig. 3.29: Spectral Analysis (FFT) of the Base Speed with an Added Sine Experiment Current output.

Table 3.20 shows the quantitative data for the base speed with added sine experiment, the data was taken at the extremes of the speed range. High is at 1612.5 rev/min and the low is at 1312.5 rev/min. The values from this test match the expected values at these levels from the baseline testing.

Table 3.20: Tabular Data for Base Speed with Added Sine Experiment for the WRIG

Speed: Recip.	Phase Quantities - Grid Connected							
Torque: Recip.	A		B		C		Total-Line	
Peak	High	Low	High	Low	High	Low	High	Low
Irms (A)	57.84	32.29	59.09	32.4	57.24	31.33	58.05	32
Vrms (V)	235	234.5	231.9	232.3	234	233.9	233.6	233.6
P (kW)	-4.85	-1.24	-5.014	-1.37	-4.77	-1.23	-14.63	-3.85
Q (kVar)	6.23	4.23	6.07	4.1	5.99	4.01	18.29	12.35
S (kVA)	7.89	4.41	7.87	4.32	7.65	4.2	23.4	12.93

During the investigation it was discovered that without a flywheel or some other form of added physical inertia onto the rotor of the WRIG it would not be able to maintain a speed greater than that of the driving dynamometer. However, when the dynamometer drives the generator while completely disconnected from the electrical utility grid, the inertia is enough to prove that with an added inertia under load the generator would spin as discussed in section 2.2.2.3. To find the speed of both the generator when the clutch was engaged and disengaged an additional speed transducer was mounted on the rear shaft of the WRIG.

The disconnected speed profile is shown in Fig. 3.30, and the loaded speed profile of the reciprocating scheme is shown in Fig. 3.31. Fig 3.31 shows that the generator and the dynamometer speeds are equivalent. However with the information shown in Fig 3.30 it can be seen that with an inertial load greater than the load of the generator the over-running clutch will function as the model in section 2.2.2.3 with the electrical equivalent model predicted. This is the same phenomenon that was seen in the PMSG investigation. At no load the generator had a slightly greater inertial force than load force, therefore the generator speed would remain at higher speeds than the dynamometer through the reciprocating cycle.

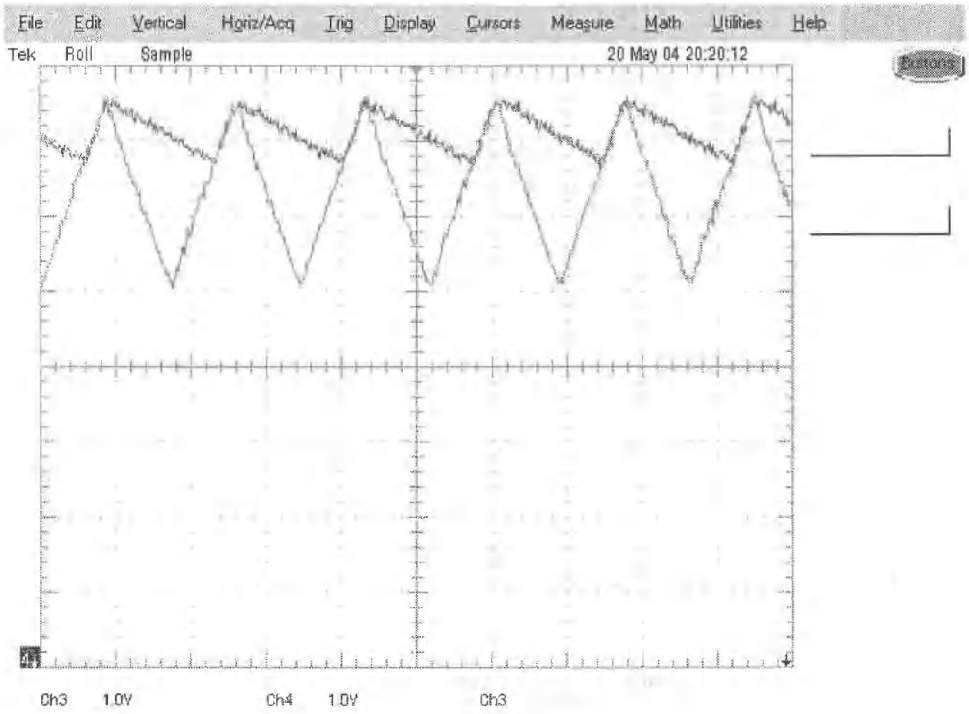

Fig. 3.30: Dynamometer and Generator Reciprocating Speed Profiles when the Generator was Disconnected from the Utility

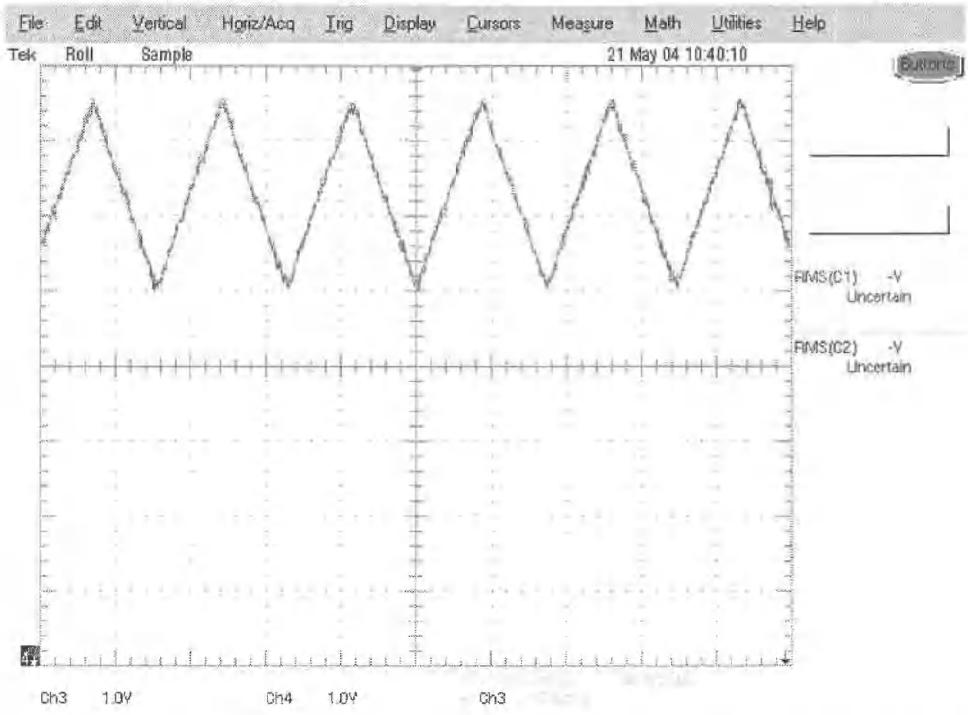

Fig. 3.31: Dynamometer and Generator Reciprocating Speed Profiles when the Generator was Connected to the Utility

Figs. 3.32, 3.33, and 3.34 show pictures of the actual experimental setup that was used in the MSRF lab to conduct the baseline and reciprocating experiments. Fig. 3.32 shows an overview of the rig with the additional components, the over-running clutch and the additional speed transducer. Fig 3.33 shows the configuration of the external impedance that was added into each phase of the rotor. Finally Fig. 3.34 is a close up view of the overrunning clutch and its connection between the dynamometer and the WRIG.

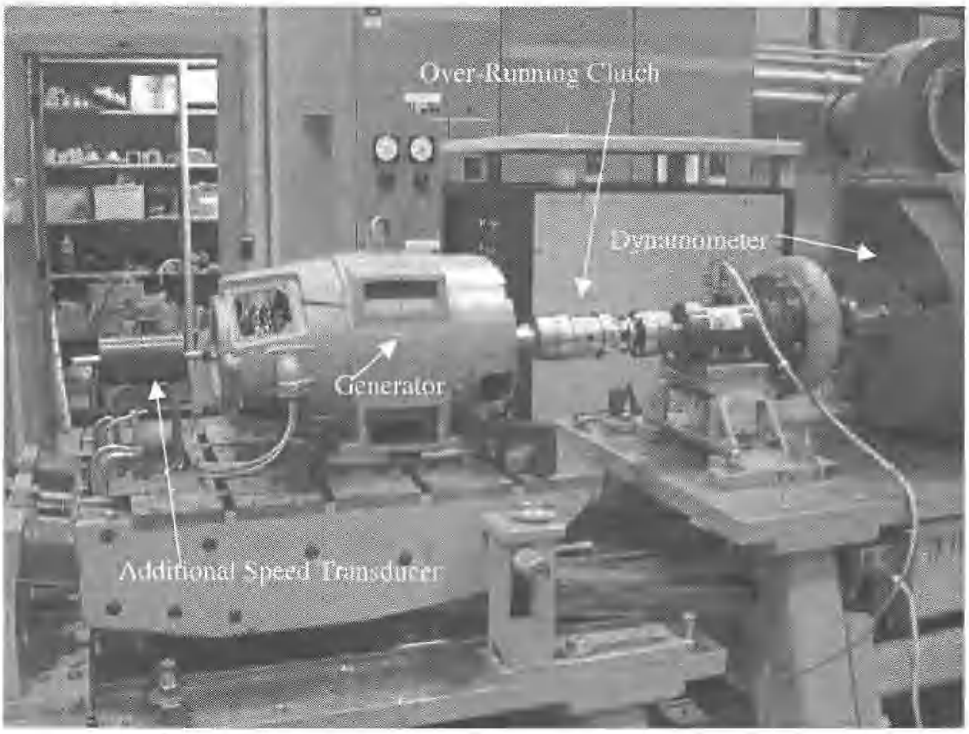

Fig. 3.32: WRIG Experimental Setup in the MSRF

Fig. 3.33: Configuration of External Impedance into the Rotor Circuit

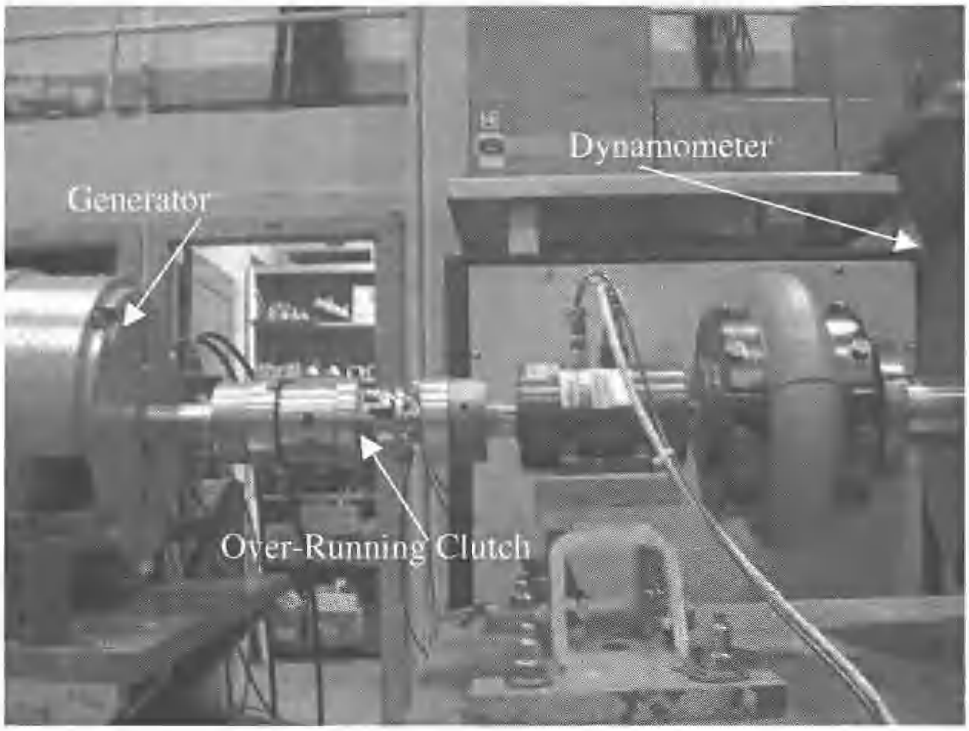

Fig. 3.34: Close Up View of Over-running Clutch Between WRIG and Dynamometer

In the interest of brevity, the results section displays the outputs of the research conducted, graphically and in tabular form. A complete listing of all of the results is available in Appendix C.

4 CONCLUSIONS AND RECOMMENDATIONS FOR FUTURE WORK

4.1 Conclusions

In this thesis the basis of Ocean Energy Extraction using two types of directly driven generators were explained. By directly connecting the generator to a rotating drive screw, a ball screw or a roller screw, the need for a complicated and maintenance intensive hydraulic system used in several prototypical ocean energy extraction devices can be completely omitted.

This thesis brings together many techniques that have been researched previously in the MSRF. These include external impedance in the rotor circuit of the WRIG to sinusoidal control of an ac dynamometer, and this thesis applies them to the idea of streamlining directly driven generation for ocean energy extraction.

One interesting finding from the research in this thesis was the validity of inertial loading of generators. The testing done using the over-running clutch helps to shed some light on the concept, that with a substantial inertia, the output of a generator can be significantly smoothed out mechanically. This allows the generator to "free wheel" for part of the buoy 's flotation cycle. The result is, the generator speed remains more constant, and consequently, the generated output power is better regulated.

The results from investigating the two generator types, PMSG and WRIG, both yielded outputs that will help designers when choosing which type of generators will be best suited for a specific buoy generator design.

Both the PMSG and the WRIG can be made to work in an electrical generation buoy. The question that needs to be answered is which would work better for a given situation.

The question itself is multi-faceted and has two major components; what type of power take-off (PTO), and what type of physical drive-screw to generator connection will be used. The answer to these questions will lead the designer to choose which generator will work best for their specific application.

If the PTO design called for the output power to be rectified, tied together, transmitted to shore, and then inverted back to ac, the PMSG would be preferable. The PMSG has the ability to maintain an output regardless of the rotor speed and load. This is due to the constant field that is supplied by the permanent magnets in the rotor of the PMSG.

On the other hand if the PTO used the generator output with minimal preprocessing, the WRIG's constant voltage profile is more likely to be preferred.

The proposed buoy matrix layout, involving multiple generators in one ocean area equally spaced apart on all sides should theoretically help to supply a more constant current and voltage output, when appropriately summated. Essentially, one generator would fill any gaps in the output from any other single generator. The more generators added into the matrix, the smoother the output power profile.

The two main types of transmission to generator direct connections that were discussed in this thesis were directly connected and over-running clutch connected. This physical connection is where the whole selection process will begin.

Fig. 4.1 shows a rundown of which generators would be best suited for which application based on the results of this thesis.

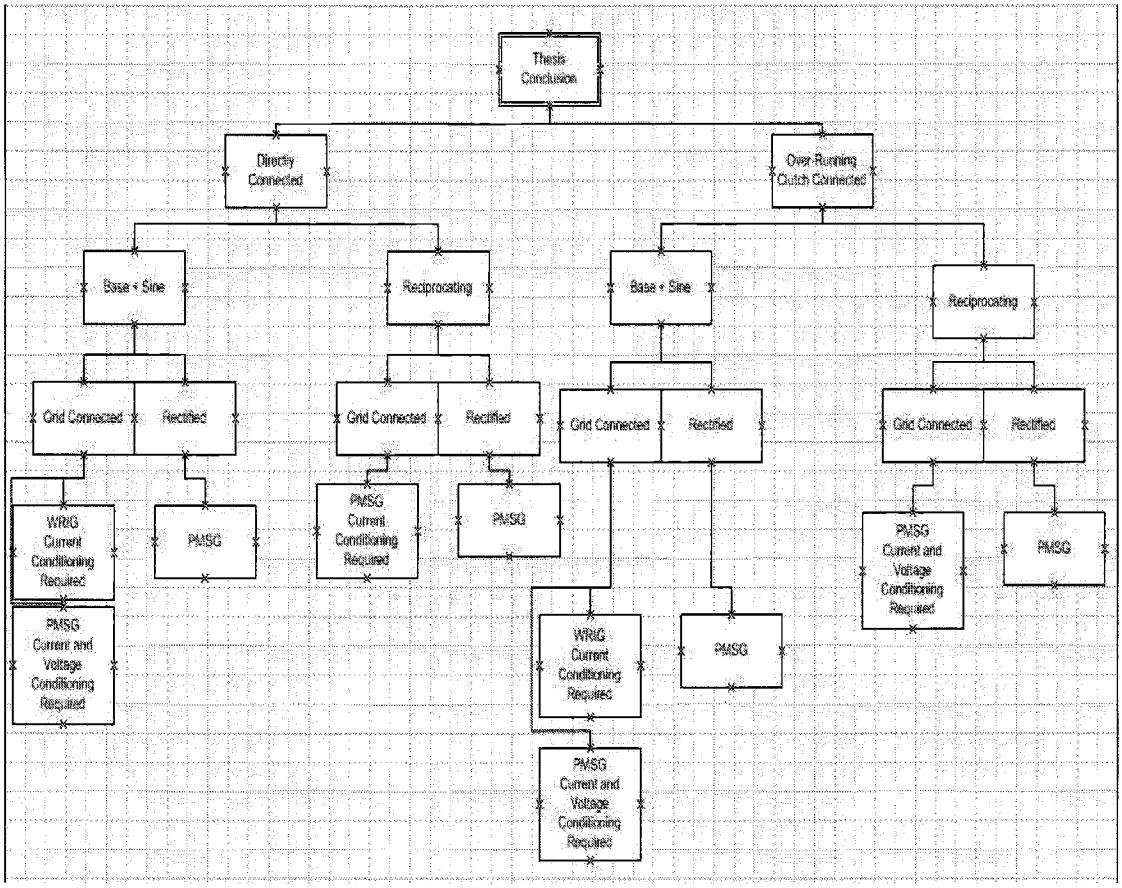

Fig. 4.1: Flowchart for Generator Selection

4.2 Recommendations for Future Work

The concept of ocean energy extraction involving a drive screw directly connected to a generator, with an ocean buoy as the prime mover, lends itself to many ideas that will need to be investigated before they can be implemented. The testing in this thesis rendered outputs for known sinusoidal inputs. The ocean provides a less than perfect sinusoidal driver. Additional investigation would produce useful results if the inserted wave profile were based on a random wave height and period that would more closely mimic the actual wave to buoy system interaction in an open ocean setting.

The experiments that were conducted on the WRIG brought some inherent questions that should be the subject of future investigations. The predominant questioning is how to control the output current when the generator is in an oscillating drive scheme. Three options were voiced as possible solutions.

The first is to add a controlled inverter into the rotor circuit of the WRIG that, through a feedback circuit monitoring output levels, could inject power into the rotor circuit that will, in effect, fill in the low spots and level out the current. It seems that from a comparison of electrical and mechanical frequencies and injection of the necessary power via the rotor, that the relative frequency of the machine would remain constant. This would potentially accomplish the desired leveling effect by means of electronic energy storage.

An alternative solution is to add inertia onto the rotor of the generator so that when it is operating at full speed the inertial force would be greater than the load force thereby allowing the generator speed variations to be much less than the prime mover input. This option is appropriate for both the WRIG and the PMSG.

The final option suggested will be to create a model of multiple buoy generators in a matrix and examine if the stratification of the buoy generators would provide enough of a time shift in the peak waveforms to effectively provide the aggregate power output as constant.

The next step is to take the data and apply it to a physical design of a buoy device that can be tested in a more real life ocean related environment.

The resulting device can then be tested for effectiveness at the O. H. Hinsdale Wave Research Lab on the Oregon State University campus. By running the physical tests of the generator in an actual buoy to screw to generator configuration it can then be decided if the direct drive buoy generator is a feasible option to be used as a utility connected electrical generator in the ocean. The last step before actual full service implementation of a buoy generator is to run a suite of tests at a specified site along the Oregon coast.

5 BIBLIOGRAPHY

[1].National Renewable Energy Laboratory. Washington D.C. http://www.nrel.gov

[2].Wavegen. Invernes, United Kingdom. http://www.wavegen.co.uk

[3].Sen, P.C. "Principles of Electric Machines and Power Electronics". 2nd Edition John Wiley and Sons. New York. 1997

[4].IEEE Standards Collection. "Electric Machinery". IEEE Press. New York. 1993

[5].Zhang, Heng. "Oregon Sea Grant proposal". Oregon State University. 2003

[6].Stewart, James. "Calculaus Early Transcendentals" 3rd Edition. Brooks/Cole Publishing Company. New York.1995

[7].Rodrigues, T.K. " Computerized Dynamic Control of an AC Dynamometer", M.S. Thesis, Oregon State University, 1998

[8].Bathon, Tobias Siegfried, "Passively Controlled Variable Speed Generator System", M.S. Thesis, Oregon State University, 1999

[9].Kinjo Fuminao, "Maximization of Energy Capture of Passive, Variable Speed Wind-Turbine Generator", M.S. Thesis, Oregon State University, 2003

[10]. Gourishankar, Vembu & Kelly, Donald H. "Electromechanical Energy Conversion". 2nd Edition. Intext Educational Publishers. New York 1973

[11]. Ocean Power Delivery Limited. Edinburgh, United Kingdom. http://www.oceanpd.com/

[12]. AquaEnergy Group. Mercer Island, Wash. USA. http://www.aquaenergygroup.com/home.htm

[13]. Simoes, M. Godoy and Felix A. Farret. "Renewable Energy Systems: Design and Analysis with Induction Generators". CRC Press. New York. 2004

APPENDICES

6 APPENDICES

A. APPENDIX A: Motor System Resource Facility (MSRF)

The manufacturer data of the dynamometer system and the measurement devices used during the practical tests in the MSRF are listed below. Furthermore, a calibration example of the torque/speed measurement system is given.

Dynamometer System

Converter

Manufacturer:	Kenetech Windpower, Livemore, CA
Model:	MD-300
Volts:	480 V
Full load current:	350 A
Horsepower:	300 hp
Frequency range:	0 to 135 Hz
Phases:	3
Duty:	Cont
Serial No.:	001

Dynamometer

Manufacturer:	Marathon Electric Co., Wausau, WI
Model:	1K 447THDN4038 AA-W
Type:	Wound rotor induction machine
Volts:	460 V
Full load current:	332 A
Horsepower:	300 hp
rev/min:	0 to 4,000
Poles:	4
Duty:	Cont
Serial No.:	41890480-9/16

Measurement Devices

Torque Calibration Example

Table A shows a calibration example, which was actually adjusted for an 80 kW generator investigation. It includes the actual calibrated torque, the ideal torque and the error in percent. The non-linearity of the torque/speed transducer is evident.

Table C.1: Torque Calibration Example

Calibrated Torque (Nm)	Ideal Torque (Nm)	Error in %
59.8	59.78	+ 0.03
119.7	119.56	+ 0.12
179.6	179.34	+ 0.14
239.5	239.13	+ 0.15
359.2	358.69	+ 0.14
477.9	478.25	- 0.07
598.8	597.81	+ 0.17
717.4	717.38	- 0.00
955.8	956.6	- 0.08

Torque and Speed Measurement System

Manufacturer:	Eaton Corp. - Lebow Products
Model:	1804-1K transducers, 7530-115 signal conditioner
Torque Rating:	1,000 lb-in
Nonlinearity:	± 0.05 % of full scale
Nonrepeatablity:	± 0.025 % of full scales
Hysteresis:	0.05 % of full scale
Temp. Compensated:	70 ° F to 170 ° F
Speed Range:	0-27,000 r/min

Definition:	60 pulses per rev
Error:	< 1 count per second

Power Analyzer

Manufacturer:	Voltech
Model:	PM 3300 Power Analyser
Serial No.:	9463
Specified Accuracy at dc and 45 to 450 Hz:	
Voltage and Current:	0.05 % reading
	+ 0.05 % range
Power, VA, and VAR:	0.1 % reading
	+ 0.1 % range

Oscilloscope

Manufacturer:	Tektronix
Model:	TDS 460 A
Serial No.:	B020686
Frequency:	0 to 400 MHz
Accuracy:	± 1.5%
Channels:	4

AC Current Probe

Manufacturer:	Fluke
Model:	80i-1000s
Serial No.:	67963900
Frequency:	5 to 100 kHz
Inputs:	0.1 to 1000 A
Isolation from Earth:	600 V

High Voltage Differential Probe

Manufacturer:	Tektronix
Model:	P5200
Serial No.:	B013746

B. APPENDIX B: Generator Nameplate Data

Permanent Magnet Generator

Nameplate Data:

Reliance Electric Corporation Cleveland OH, 44117

Duty Master AC Motor Permanent Magnet Synchronous Motor

Frame: L184 TCZ

Type: P

Insulation Class: F

Identification Number: P18G1119D QL

Horse Power: 5

Volts: 115/230

Amperage: 22/11

Frequency: 60 Hz.

RPM: 1800

SF: 1.0

Code: J

Phase: 3

Drive End Bearing: 30BC02XPP30A26

Opposite Drive End Bearing: 30BC02XPP30A26

Ambient: 40°C

Duty: Continuous

Induction Generator

Nameplate Data:

Westinghouse Life – Line Wound Rotor Motor/Generator

Serial Number: 7309

Frame: 284T

Insulation Class: B

Motor Style: 73Y64108

Horse Power: 15

Volts: 230/460

Amperage: 42/21

Secondary Volts: 240

Secondary Amps: 352.5

Frequency: 60 Hz.

RPM: 1140

Ser. Fac.: 1.15

Phase: 3

Drive or Lower Bearing: 55BC03JPP3

Opposite Drive or Upper Bearing: 45BC02JPP3

Model: TWDP

C. APPENDIX C: Complete Test Results from Generator Testing

C.1. Permanent Magnet Motor

C.1.1. Baseline Steady-State Testing

Full Speed

No Load – 0 Nm

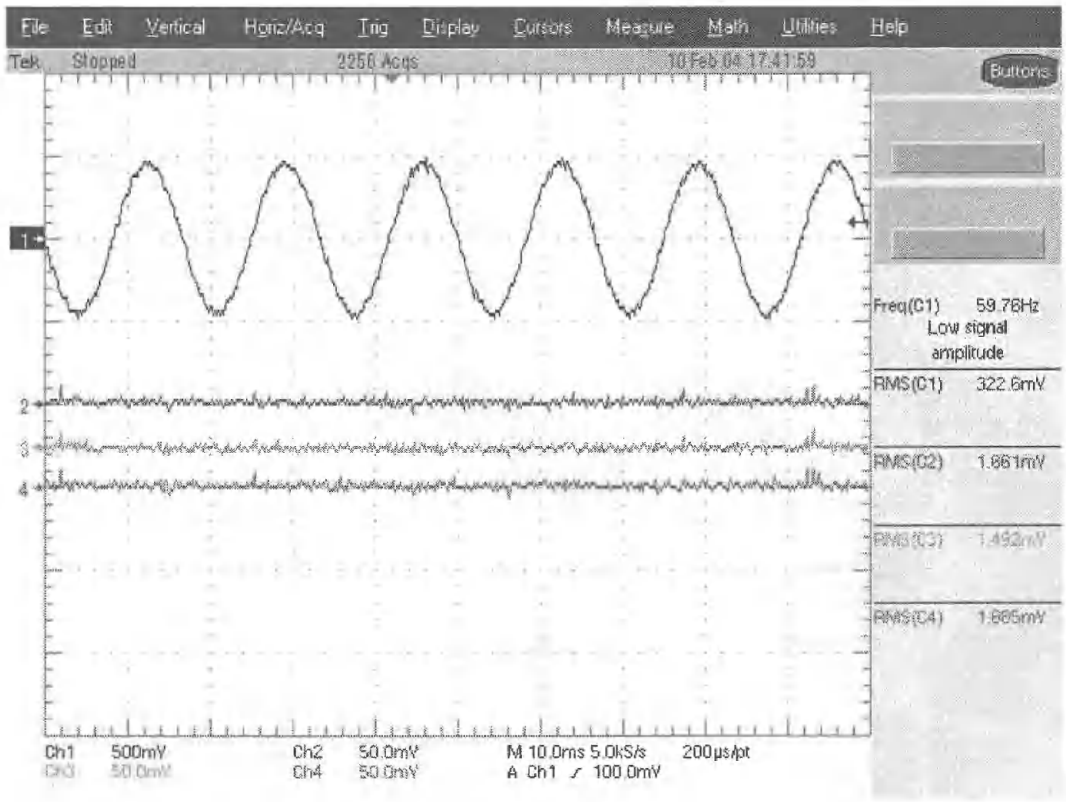

Fig. C.1: PMSG Baseline, No Load, Full Speed

Table C.2: PMSG Baseline, No Load, Full Speed

No Load (0Nm)	Phase Quantities			
	A	B	C	Total-Line
Irms (A)	0	0	0	0
Vrms (V)	93.84	92.89	92.49	161.22

1/4 Load – 4.6 Nm

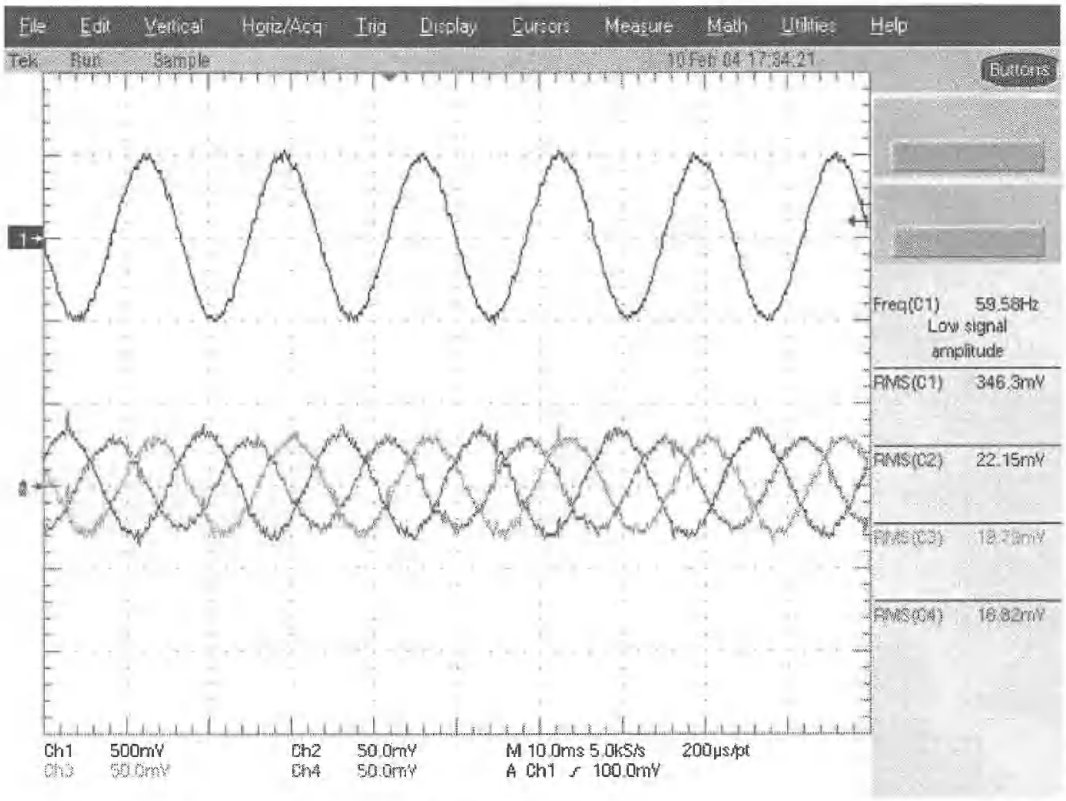

Fig. C.2: PMSG Baseline, 1/4 Load, Full Speed

Table C.3: PMSG Baseline, 1/4 Load, Full Speed

¼ Load (4.6Nm)	Phase Quantities			
	A	B	C	Total-Line
Irms (A)	2.40	2.37	3.23	2.67
Vrms (V)	101.68	97.62	97.58	171.44
P (kW)	0.21	0.12	0.13	0.46
Q (kVar)	0.14	0.20	0.29	0.66
S (kVA)	245.00	0.23	0.32	0.80

1/2 Load – 9.2 Nm

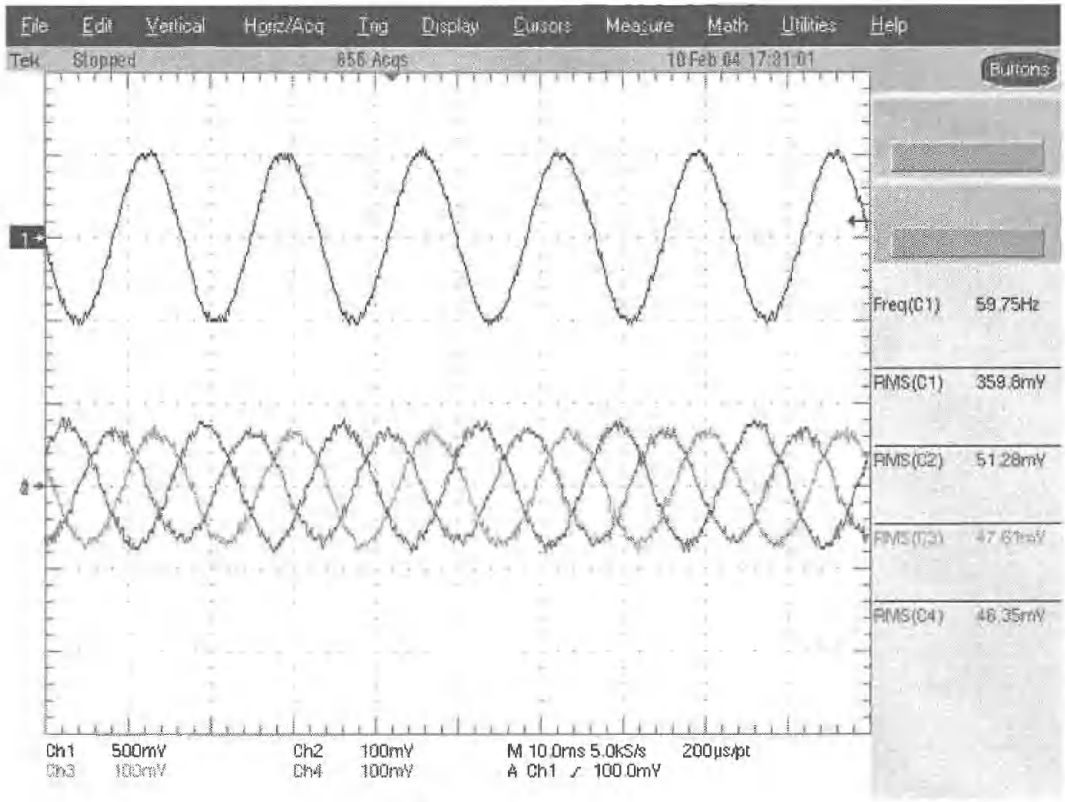

Fig. C.3: PMSG Baseline, 1/2 Load, Full Speed

Table C.4: PMSG Baseline, 1/2 Load, Full Speed

1/2 Load (9.2Nm) Phase Quantities

	A	B	C	Total-Line
Irms (A)	4.81	5.13	5.31	5.08
Vrms (V)	106.18	101.12	100.85	177.96
P (kW)	0.48	0.28	0.29	1.56
Q (kVar)	0.14	0.44	0.45	1.17
S (kVA)	0.51	0.52	0.54	1.57

3/4 Load – 13.7 Nm

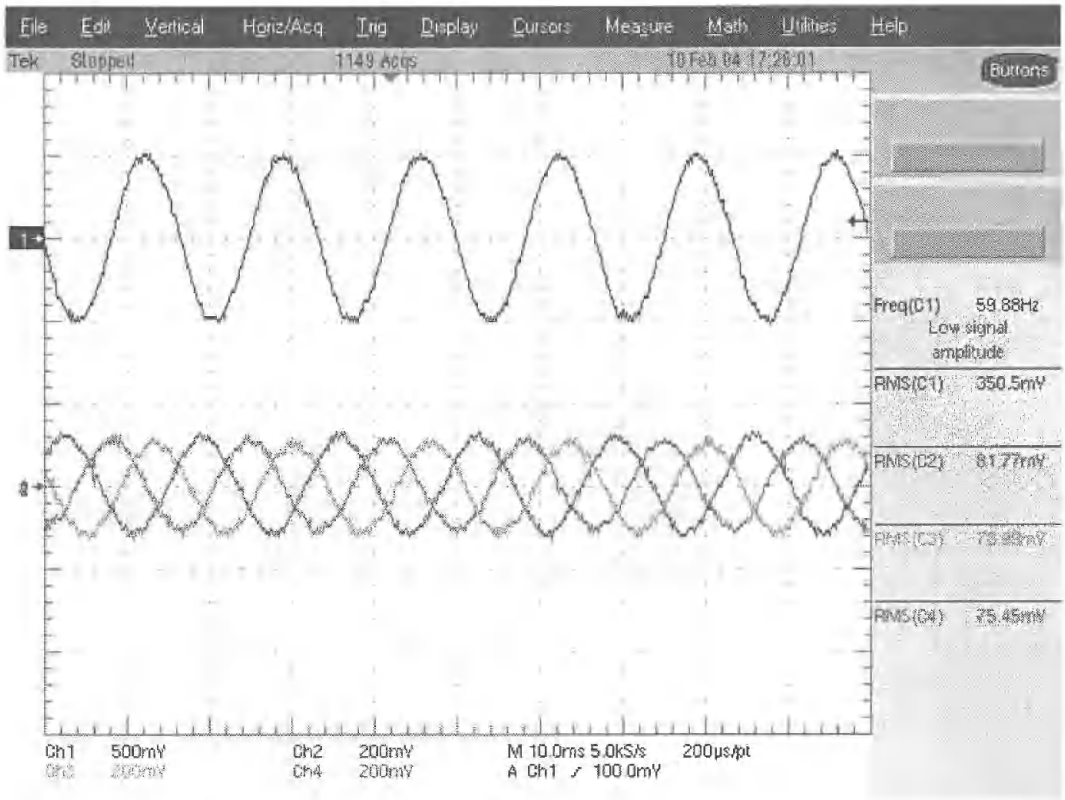

Fig. C.4: PMSG Baseline, 3/4 Load, Full Speed

Table C.5: PMSG Baseline, 3/4 Load, Full Speed

3/4 Load (13.7Nm) Phase Quantities

	A	B	C	Total-Line
Irms (A)	7.63	8.21	8.07	7.97
Vrms (V)	103.78	97.99	97.60	172.91
P (kW)	0.78	0.43	0.45	1.65
Q (kVar)	0.14	0.68	0.65	1.72
S (kVA)	0.79	0.81	0.79	2.39

Full Load – 18.3 Nm

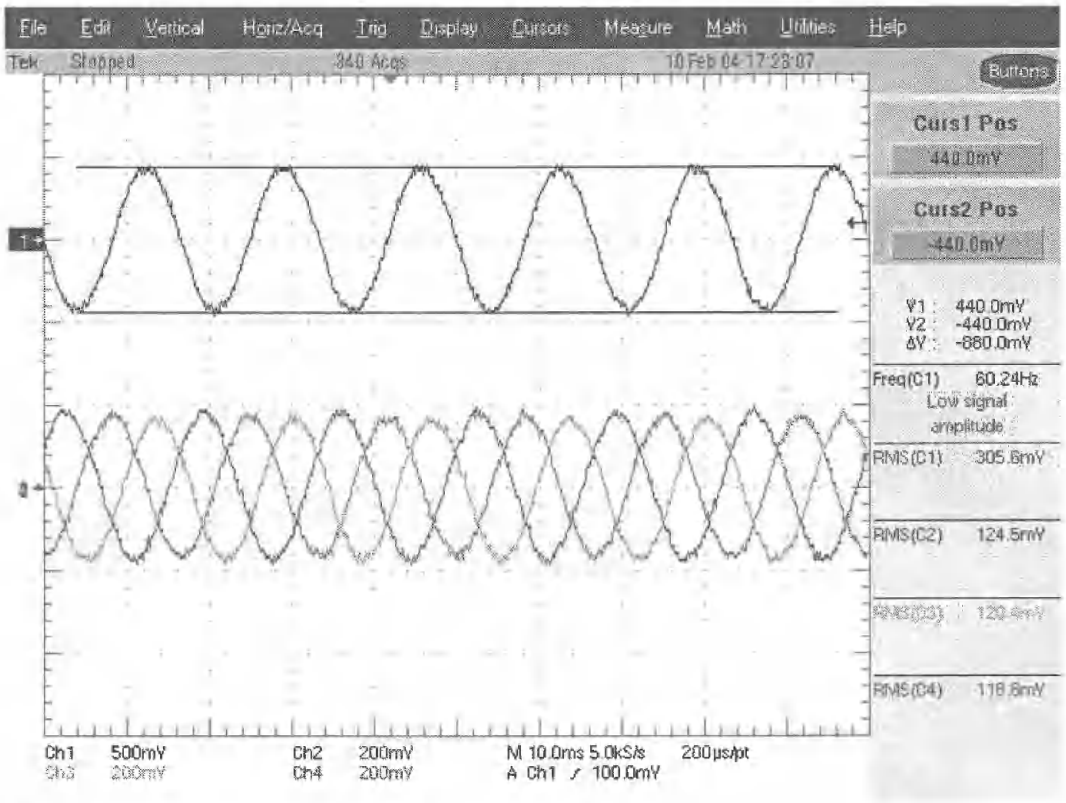

Fig. C.5: PMSG Baseline, Rated Load, Full Speed

Table C.6: PMSG Baseline, Rated Load, Full Speed

Full Load (18.3Nm) Phase Quantities

	A	B	C	Total-Line
Irms (A)	10.77	11.29	10.98	11.01
Vrms (V)	95.78	89.21	89.58	158.61
P (kW)	1.02	0.53	0.56	2.11
Q (kVar)	0.14	0.88	0.83	2.22
S (kVA)	1.06	1.04	1.01	3.12

C.1.1.1. Reduced Speed – 262.5 rpm

No Load – 0 Nm

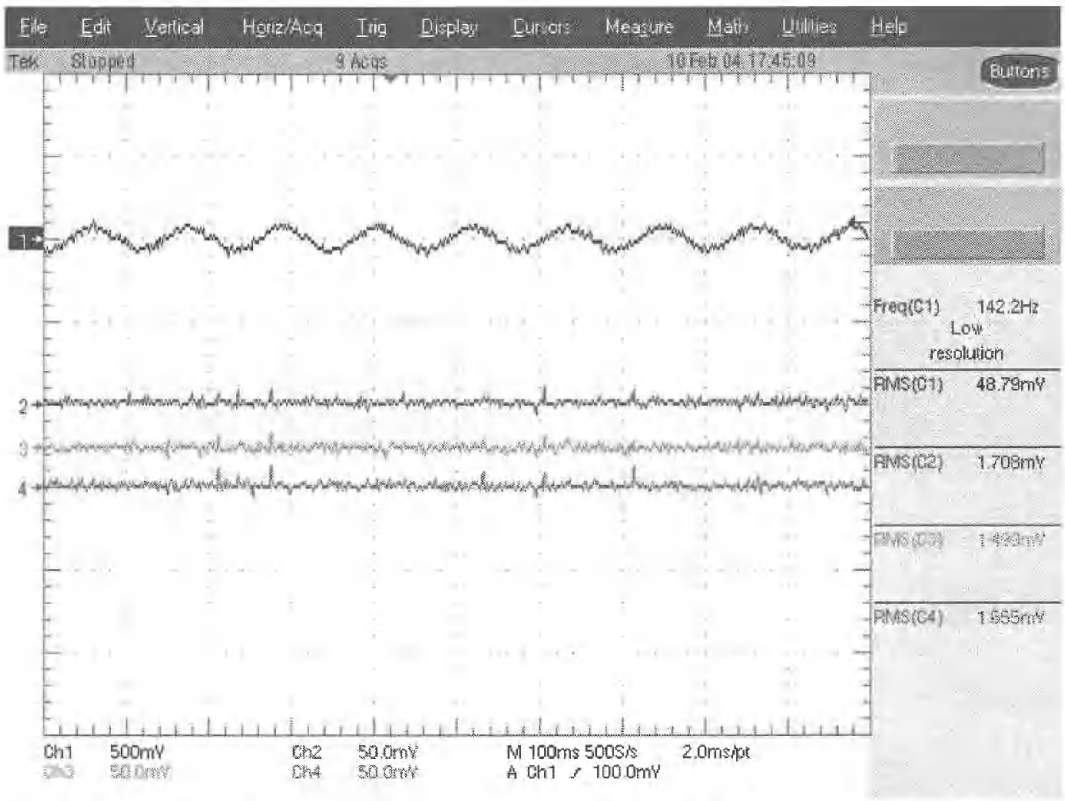

Fig. C.6: PMSG Baseline, No Load, Reduced Speed - 262.5 Rev/Min

Table C.7: PMSG Baseline, No Load, Reduced Speed - 262.5 Rev/Min

No Load (0Nm)	Phase Quantities			
	A	B	C	Total-Line
Irms (A)	0.00	0.00	0.00	0.00
Vrms (V)	13.78	13.41	13.46	23.47

1/4 Load – 3.5 Nm

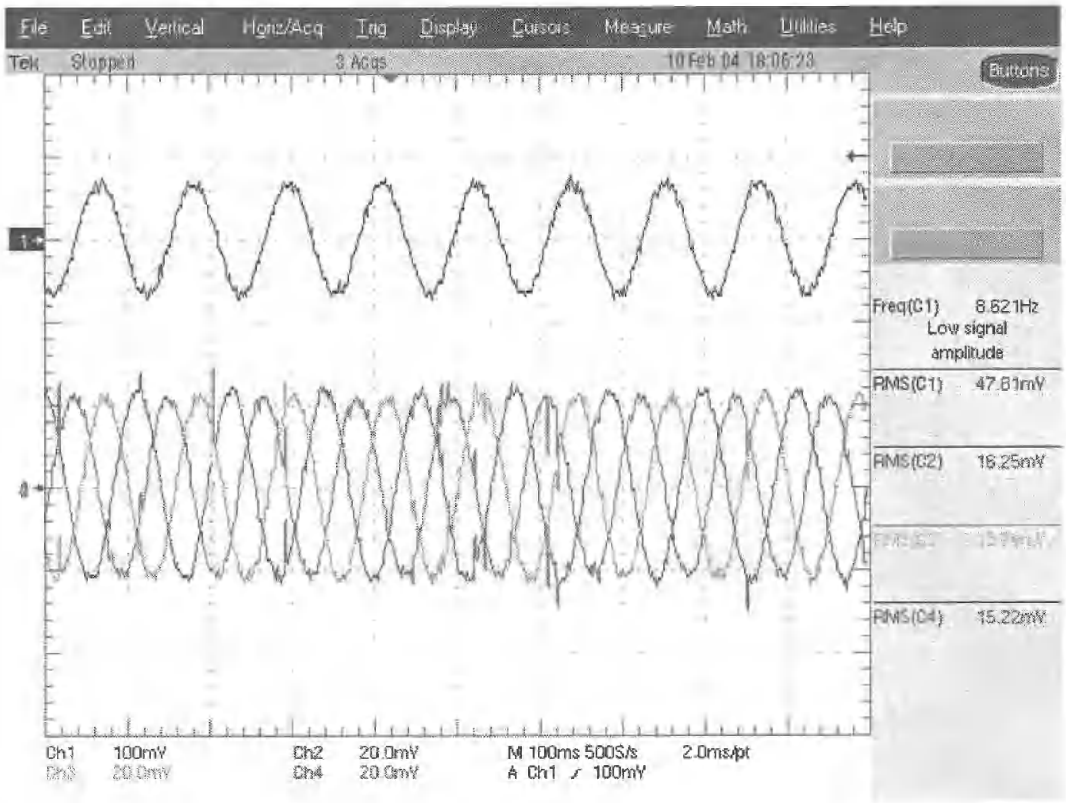

Fig. C.7: PMSG Baseline, 1/4 Load, Reduced Speed - 262.5 Rev/Min

Table C.8: PMSG Baseline, 1/4 Load, Reduced Speed - 262.5 Rev/Min

1/4 Load (3.5Nm)	Phase Quantities			
	A	B	C	Total-Line
Irms (A)	2.12	1.96	2.86	2.31
Vrms (V)	13.92	13.47	13.47	23.65
P (kW)	0.02	0.01	0.01	0.05
Q (kVar)	0.02	0.02	0.04	0.08
S (kVA)	0.03	0.03	0.04	0.10

1/2 Load – 7 Nm

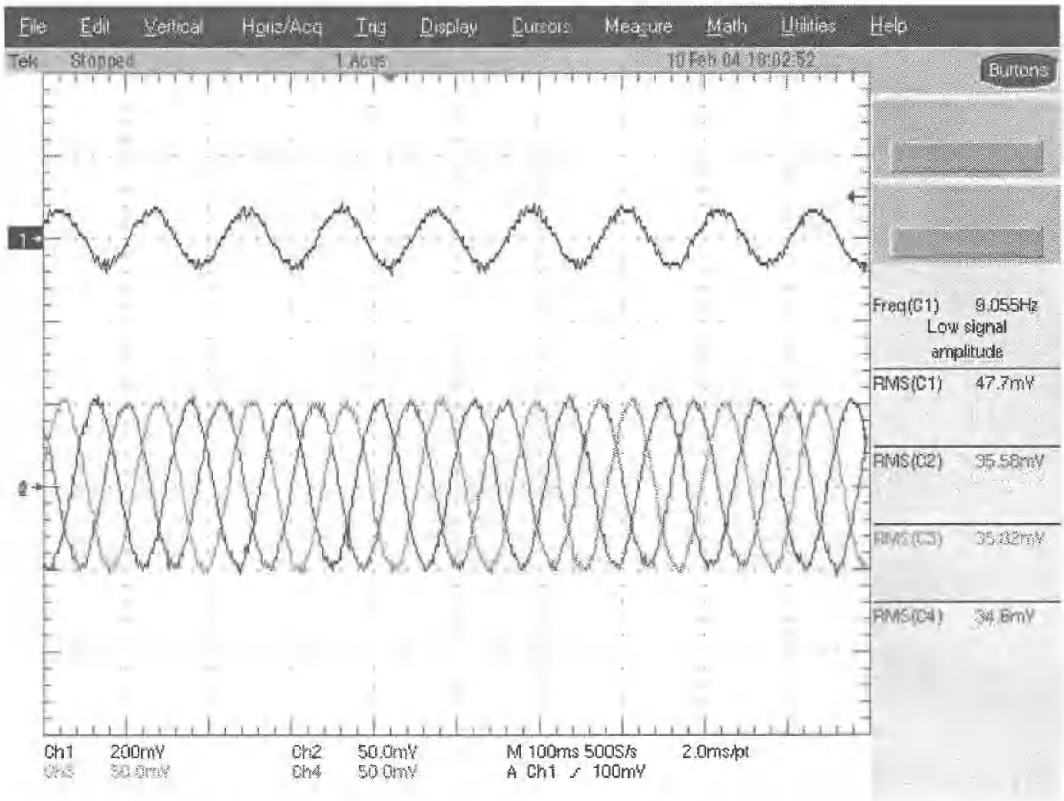

Fig. C.8: PMSG Baseline, 1/2 Load, Reduced Speed - 262.5 Rev/Min

Table C.9: PMSG Baseline, 1/2 Load, Reduced Speed - 262.5 Rev/Min

1/2 Load (7Nm)	Phase Quantities			
	A	B	C	Total-Line
Irms (A)	3.91	3.61	4.51	4.01
Vrms (V)	13.92	13.46	13.34	23.51
P (kW)	0.05	0.02	0.03	0.10
Q (kVar)	0.02	0.04	0.05	0.13
S (kVA)	0.05	0.05	0.05	0.13

3/4 Load – 10.5 Nm

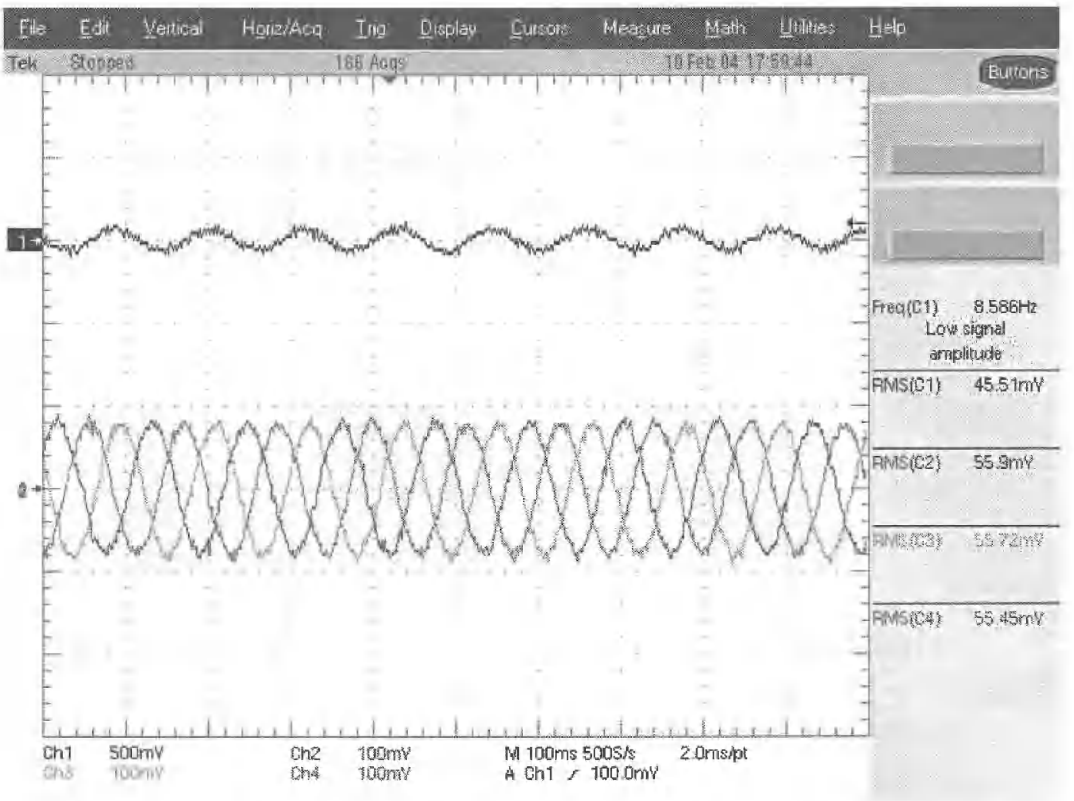

Fig. C.9: PMSG Baseline, 3/4 Load, Reduced Speed - 262.5 Rev/Min

Table C.10: PMSG Baseline, 3/4 Load, Reduced Speed - 262.5 Rev/Min

3/4 Load (10.5Nm)	Phase Quantities			
	A	B	C	Total-Line
Irms (A)	5.91	5.67	6.23	5.94
Vrms (V)	13.27	12.61	12.79	22.33
P (kW)	0.08	0.03	0.04	0.15
Q (kVar)	0.02	0.06	0.07	0.18
S (kVA)	0.08	0.07	0.08	0.23

Full Load – 14 Nm

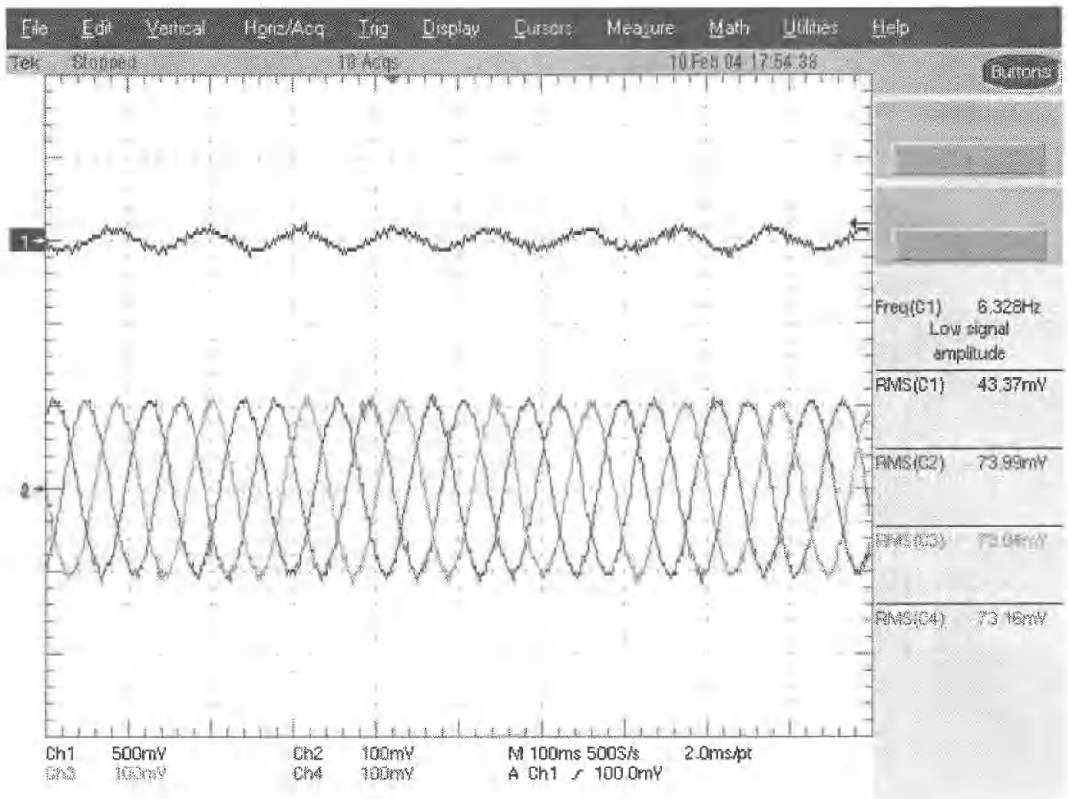

Fig. C.10: PMSG Baseline, Rated Load, Reduced Speed - 262.5 Rev/Min

Table C.11: PMSG Baseline, Rated Load, Reduced Speed - 262.5 Rev/Min

Full Load (14Nm)	Phase Quantities			
	A	B	C	Total-Line
Irms (A)	7.59	7.44	8.12	7.72
Vrms (V)	12.08	12.01	11.75	20.69
P (kW)	0.90	0.04	0.049	0.18
Q (kVar)	0.02	0.08	0.08	0.21
S (kVA)	0.09	0.09	0.10	0.28

C.1.2. Directly Connected Reciprocating Test

No Load – 0 Nm

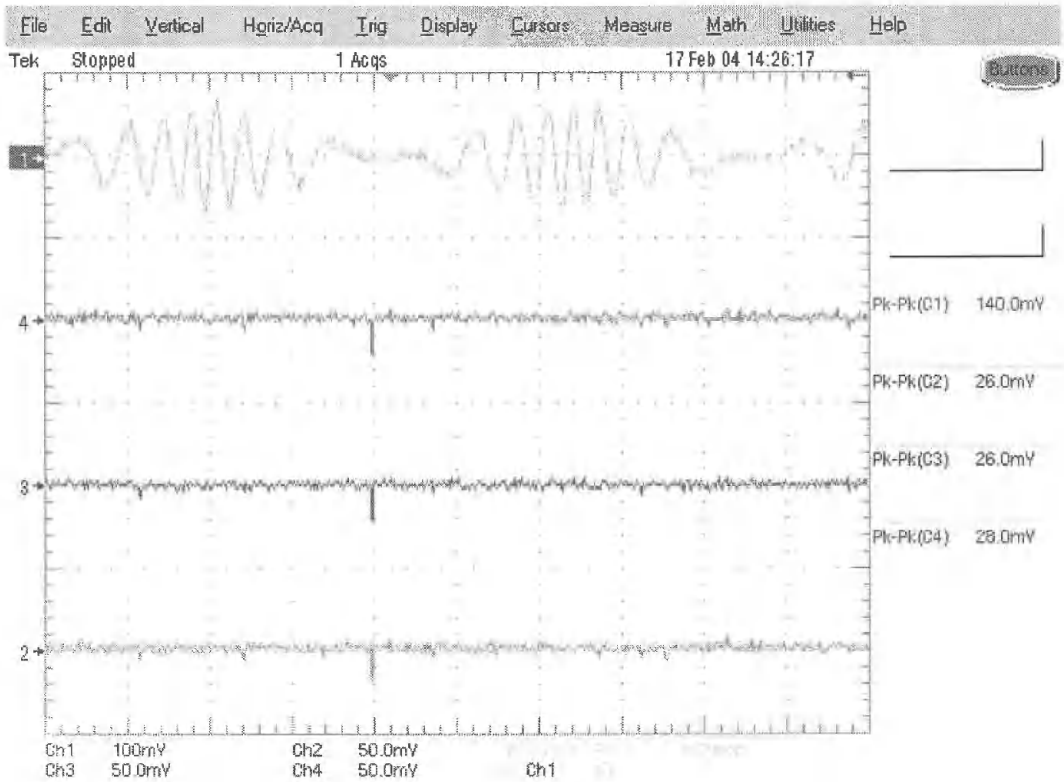

Fig. C.11: PMSG Reciprocating Investigation, No Load

Table C.12: PMSG Reciprocating Investigation, No Load

No Load (0Nm) — Phase Quantities

	A	B	C	Total-Line
Irms (A)	0	0	0	0
Vrms (V)	11.41	11.81	11.70	20.18

1/4 Load – 3.5 Nm

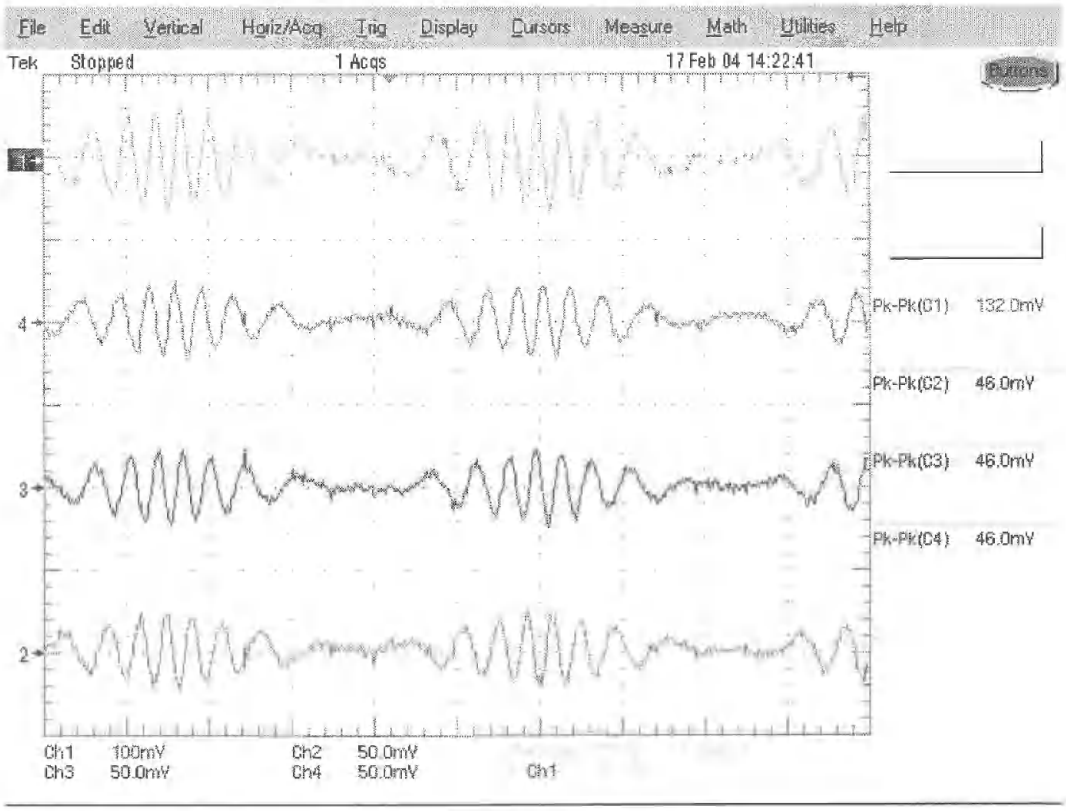

Fig. C.12: PMSG Reciprocating Investigation, 1/4 Load

Table C.13: PMSG Reciprocating Investigation, 1/4 Load

1/4 Load (3.5Nm) Phase Quantities

	A	B	C	Total-Line
Irms (A)	1.96	2.42	2.89	2.43
Vrms (V)	10.70	10.70	10.56	18.49
P (kW)	0.02	0.02	0.01	0.02
Q (kVar)	0.01	0.02	0.03	0.06
S (kVA)	0.02	0.02	0.03	0.06

1/2 Load – 7 Nm

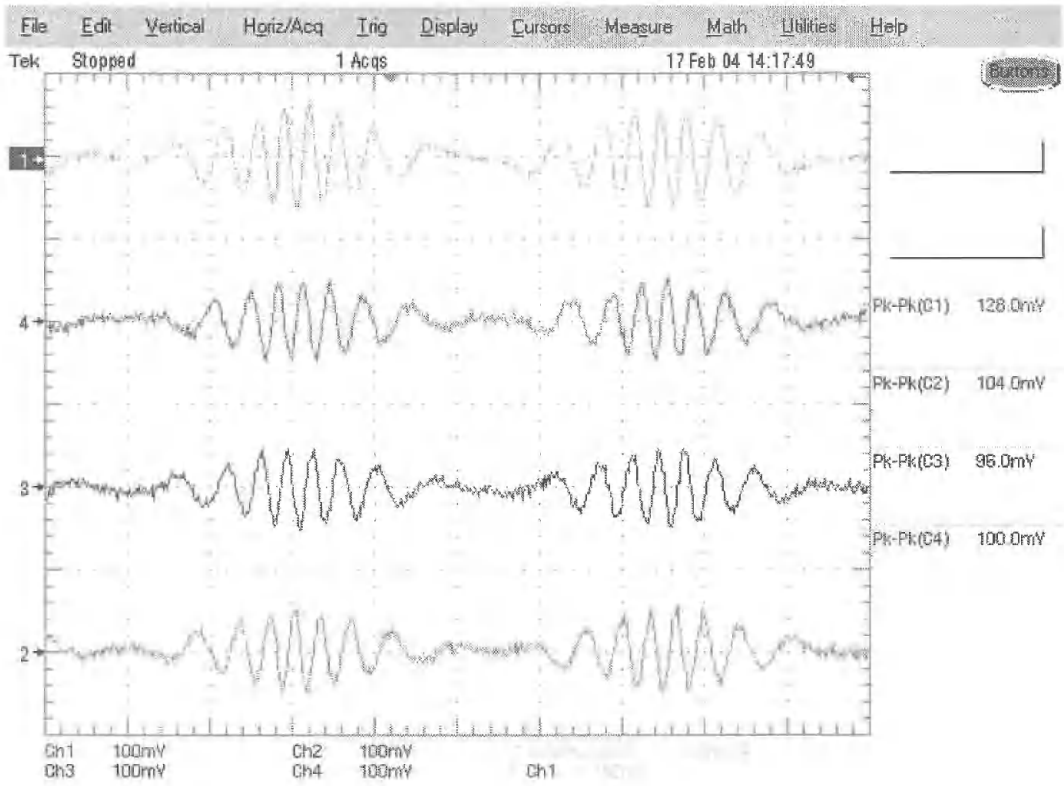

Fig. C.13: PMSG Reciprocating Investigation, 1/2 Load

Table C.14: PMSG Reciprocating Investigation, 1/2 Load

1/2 Load (7Nm)	Phase Quantities			
	A	B	C	Total-Line
Irms (A)	3.15	2.98	3.61	5.64
Vrms (V)	10.76	10.81	10.65	18.60
P (kW)	0.03	0.02	0.01	0.06
Q (kVar)	0.02	0.03	0.04	0.09
S (kVA)	0.03	0.03	0.04	0.10

3/4 Load – 10.5 Nm

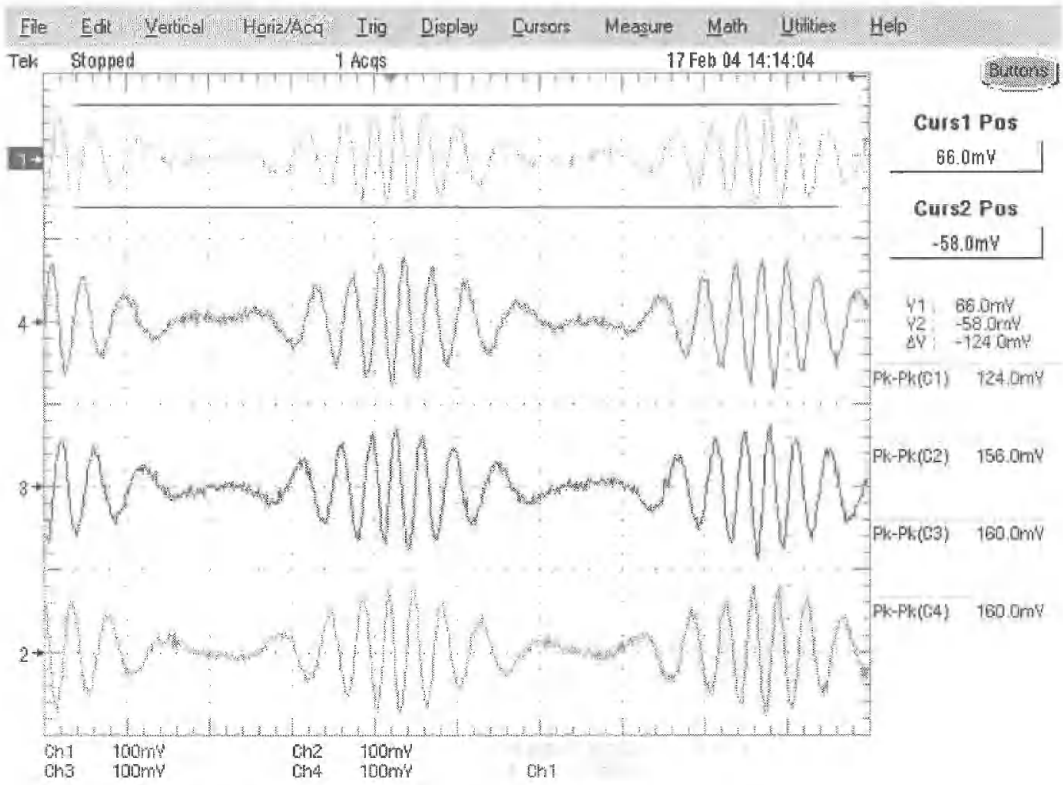

Fig. C.14: PMSG Reciprocating Investigation, 3/4 Load

Table C.15: PMSG Reciprocating Investigation, 3/4 Load

3/4 Load (10.5Nm) Phase Quantities

	A	B	C	Total-Line
Irms (A)	4.64	4.74	5.02	4.80
Vrms (V)	10.52	10.66	10.62	18.36
P (kW)	0.047	0.03	0.024	0.10
Q (kVar)	0.014	0.04	0.048	0.12
S (kVA)	0.049	0.05	0.053	0.15

Full Load – 14 Nm

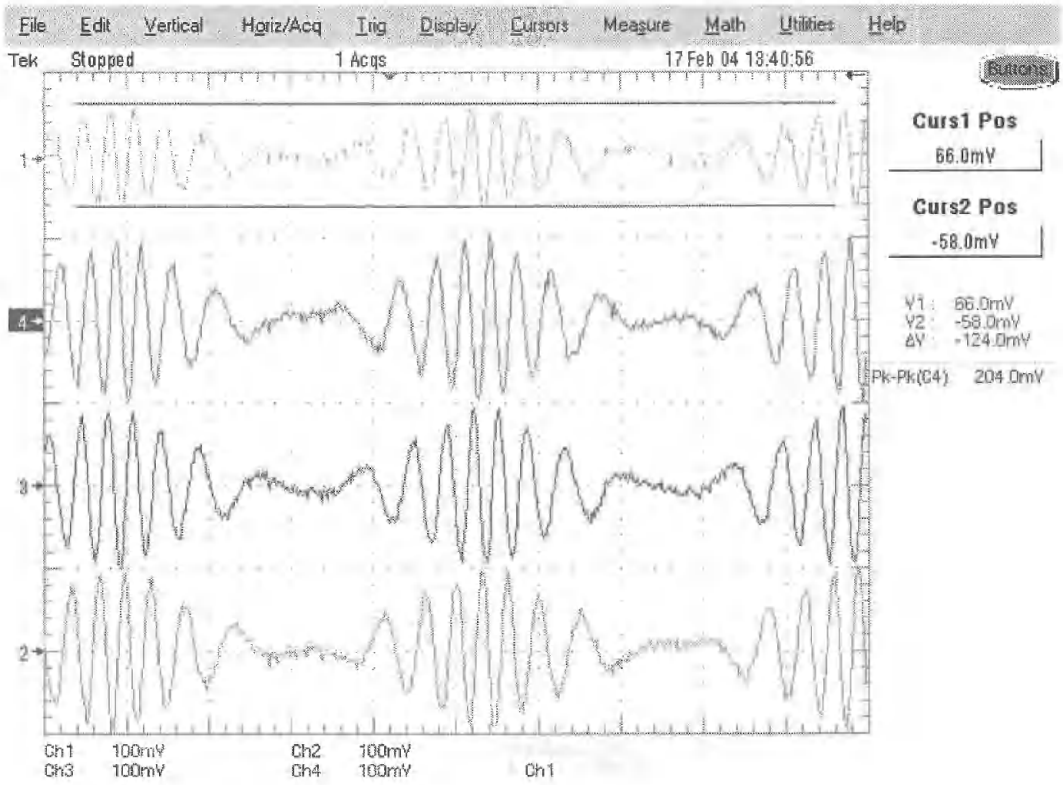

Fig. C.15: PMSG Reciprocating Investigation, Under Load

Table C.16: PMSG Reciprocating Investigation, Under Load

Full Load (14Nm)	Phase Quantities			
	A	B	C	Total-Line
Irms (A)	5.71	5.69	5.89	5.76
Vrms (V)	9.76	9.87	9.89	17.05
P (kW)	0.05	0.03	0.02	0.11
Q (kVar)	0.01	0.05	0.05	0.13
S (kVA)	0.06	0.06	0.06	0.17

C.1.3. Investigation of Reciprocating Drive via Over-Running Clutch

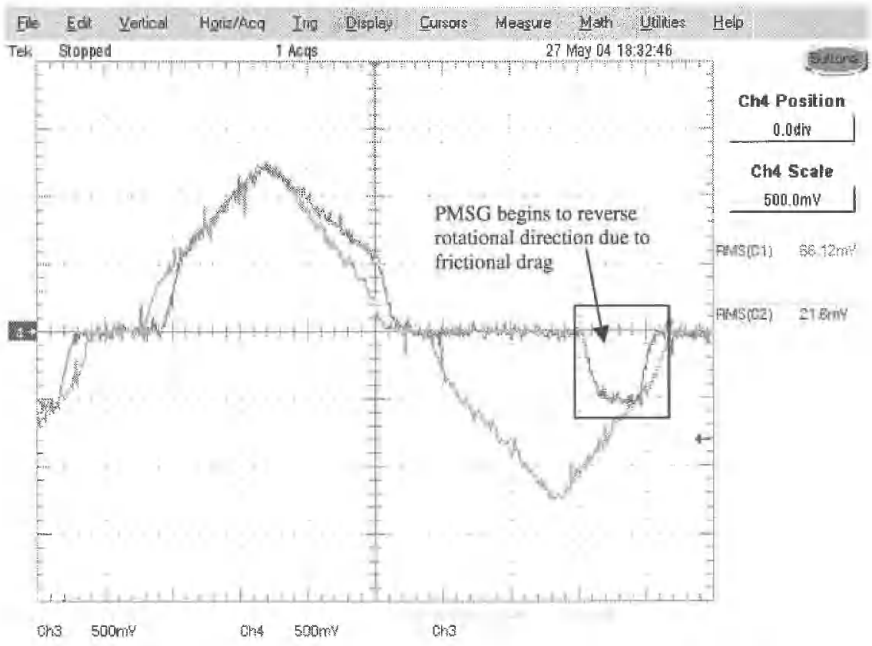

Fig. C.16: Investigation of Reciprocating Drive via Over-Running Clutch, No-Load Speed Output

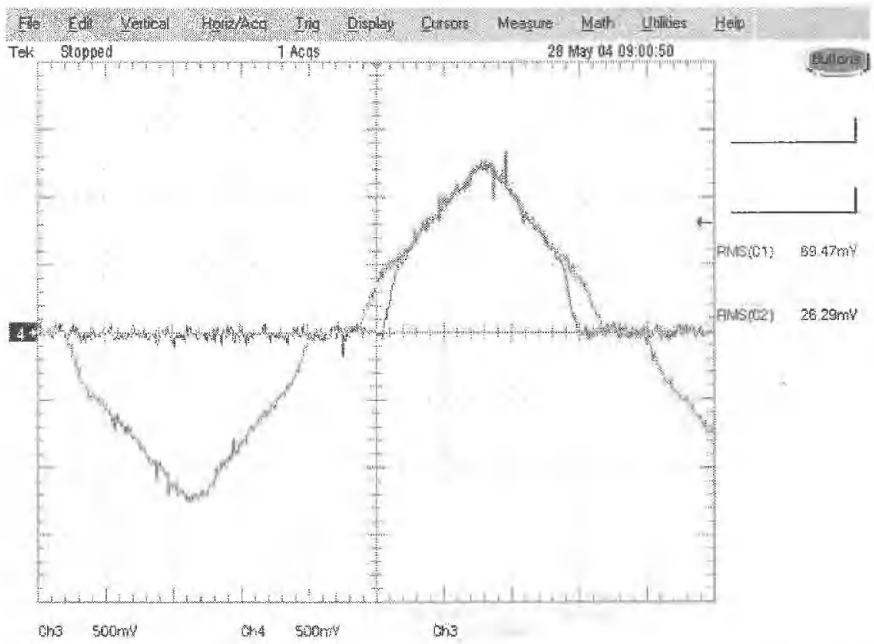

Fig. C.17: Investigation of Reciprocating Drive via Over-Running Clutch, Full Load Speed Output

C.1.3.1. Investigation of Reciprocating Drive via Over-Running Clutch,

Unrectified Output

No Load – 0Nm

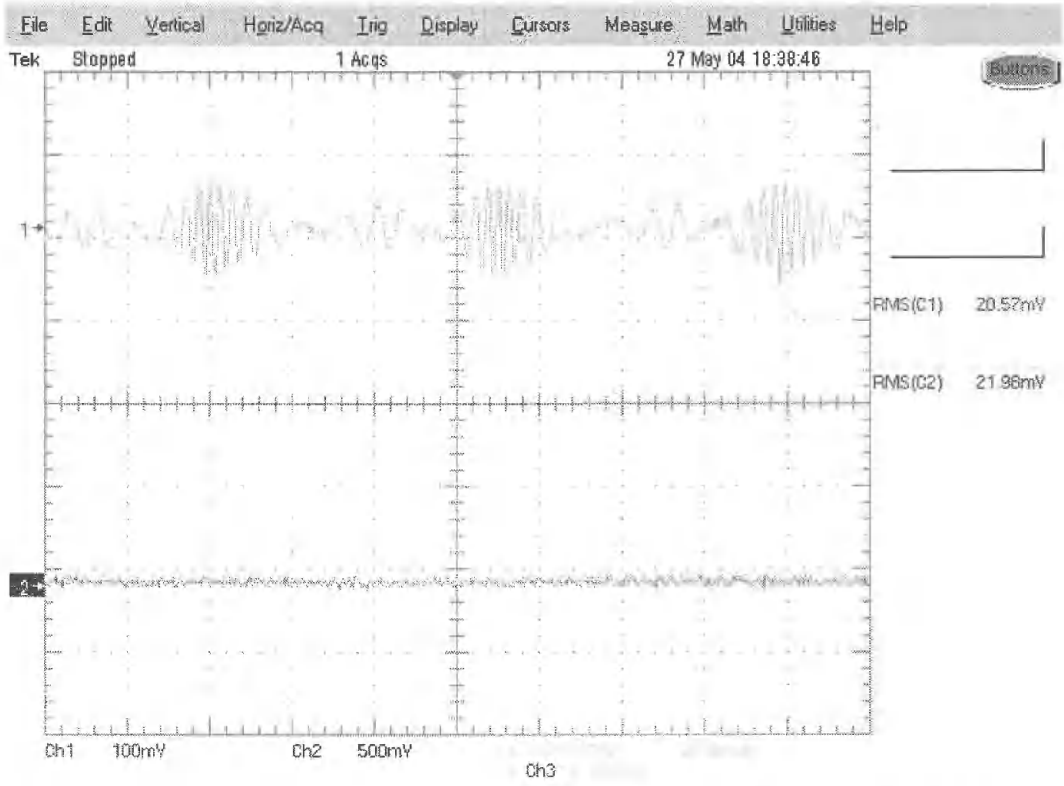

Fig. C.18: Over-Running Clutch Connected Reciprocating Test, No-Load, Unrectified (Ch1: Voltage 500/1, Ch2: Current 100/1)

Table C.17: Quantitative Output for Over-Running Clutch Connected Reciprocating Test, No-Load, Unrectified

No Load (0Nm)	Phase Quantities			
	A	B	C	Total - Line
Irms (A)	0.00	0.00	0.00	0.00
Vrms (V)	10.53	10.59	10.60	18.53

Full Load – 14Nm

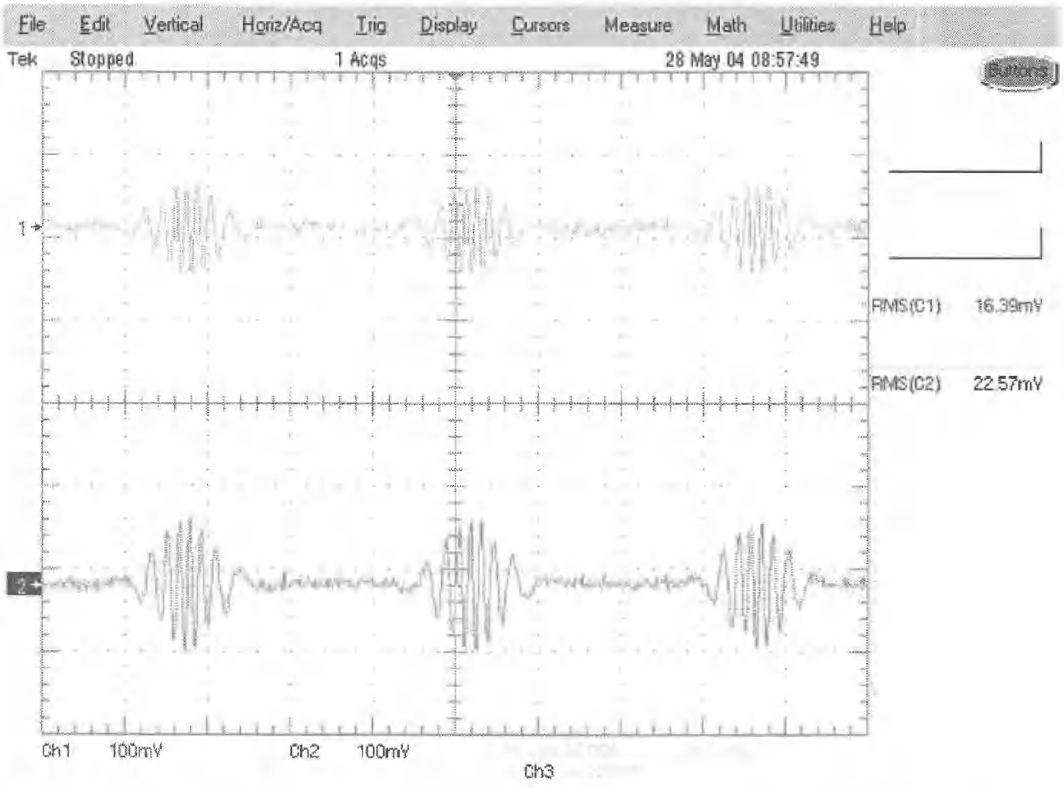

Fig. C.19: Over-Running Clutch Connected Reciprocating Test, Full Load, Unrectified (Ch1: Voltage 500/1, Ch2: Current 100/1)

Table C.18: Quantitative Output for Over-Running Clutch Connected Reciprocating Test, Full Load, Unrectified

Full Load (14Nm) — Phase Quantities

	A	B	C	Total - Line
Irms (A)	5.03	4.99	4.85	8.58
Vrms (V)	9.83	10.10	9.72	17.12
P (kW)	-.05	-.05	-.05	-.15
Q (kVar)	.01	.01	.01	.02
S (kVA)	.05	.05	.05	.15

C.1.3.2. *Investigation of Reciprocating Drive via Over-Running Clutch,*

Rectified Output

No Load – 0 Nm

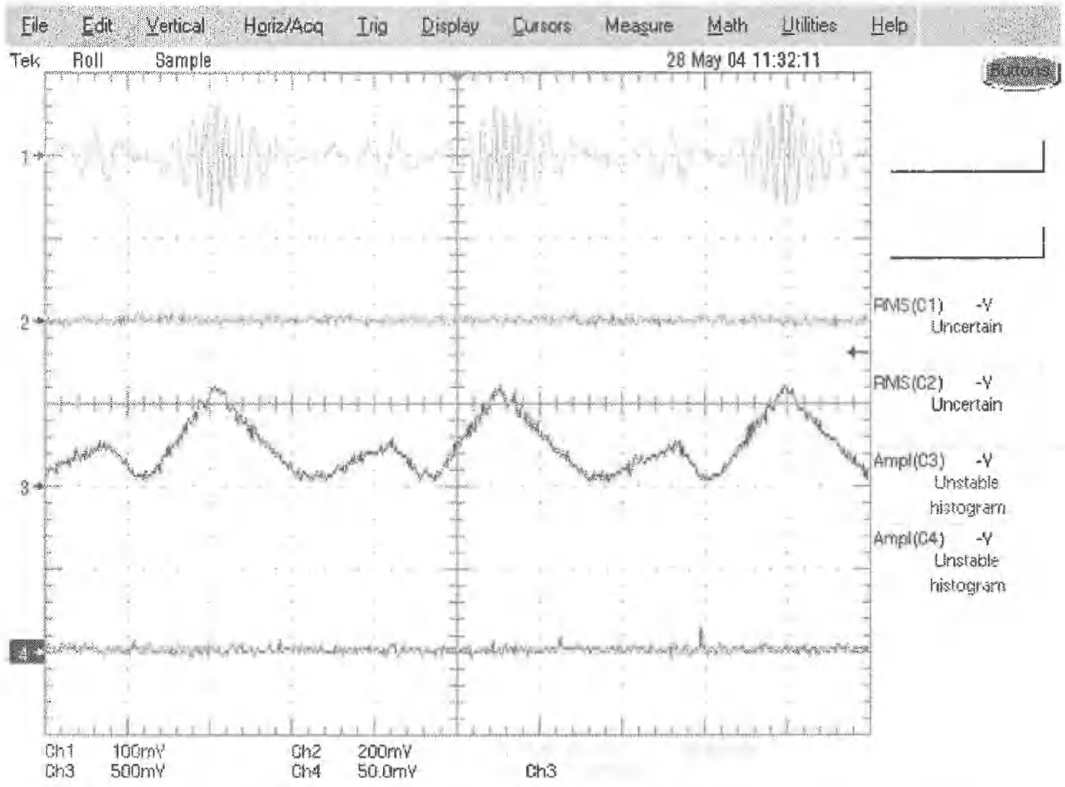

Fig. C.20: No-Load Output with rectifier (Ch1: AC Voltage 500/1, Ch2: AC Current 100/1, Ch3 Rectified Voltage 500/1, Ch4 Rectified Current 100/1)

Table C.19: No-Load Output with rectifier

Full Load (18.3Nm) Phase Quantities

	A		B		C		Total – Line		Rectified Values	
	High	Low	High	Low	High	Low	High	Low	High	Low
Irms (A)	0.00	0.00	0.00	0.00	0.00	0.00	0.00	0.00	0.00	0.00
Vrms (V)	11.33	0.00	11.08	0.00	11.15	0.00	19.38	0.00	24.3	0.00

Full Load – 14 Nm

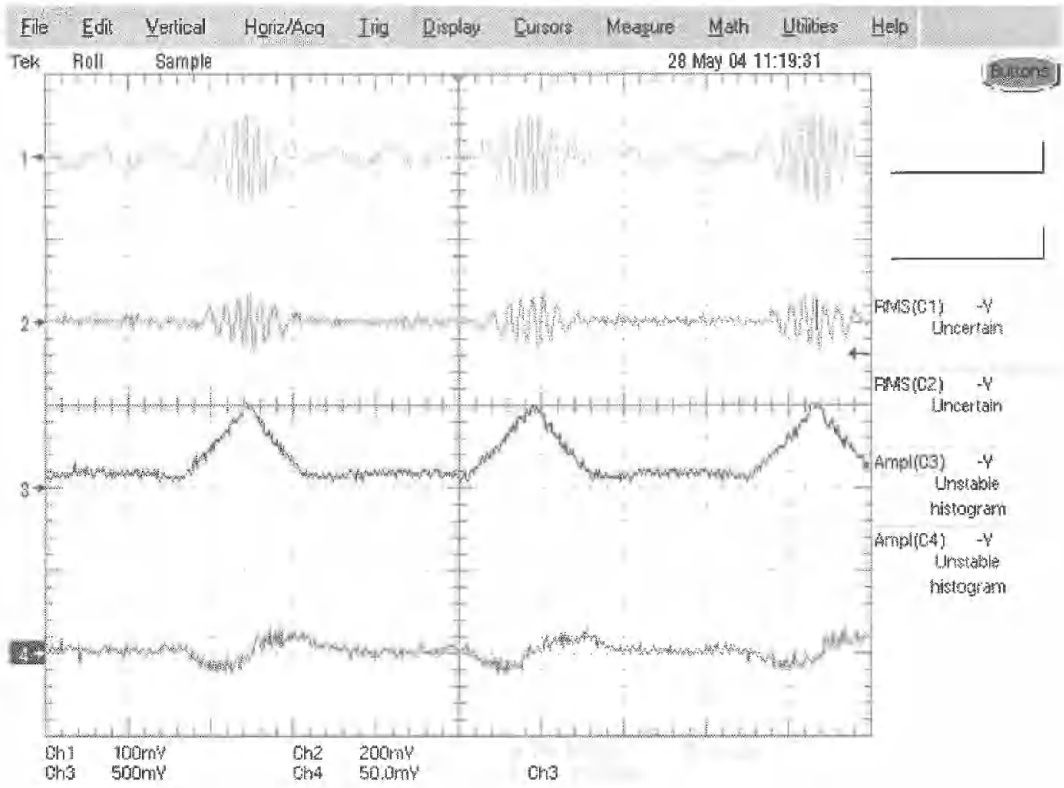

Fig. C.21: Full Load Output with rectifier (Ch1: AC Voltage 500/1, Ch2: AC Current 100/1, Ch3 Rectified Voltage 500/1, Ch4 Rectified Current 100/1)

Table C.20: Full Load Output with rectifier

Full Load (14Nm) Phase Quantities

	A		B		C		Total – Line		Rectified Values	
	High	Low	High	Low	High	Low	High	Low	High	Low
Irms (A)	3.35	0.00	3.23	0.00	3.31	0.00	3.30	0.00	4.67	0.00
Vrms (V)	9.00	0.00	8.90	0.00	8.97	0.00	15.53	0.00	16.34	0.00
P (kW)	-.03	0.00	-.03	0.00	-.03	0.00	-.08	0.00	.08	0.00
Q (kVar)	.01	0.00	.01	0.00	.01	0.00	.03	0.00	-	-
S (kVA)	.03	0.00	.03	0.00	.03	0.00	.09	0.00	-	-

C.1.4. Directly Connected Synchronous Speed with an Added Sine Component

No Load – 0 Nm

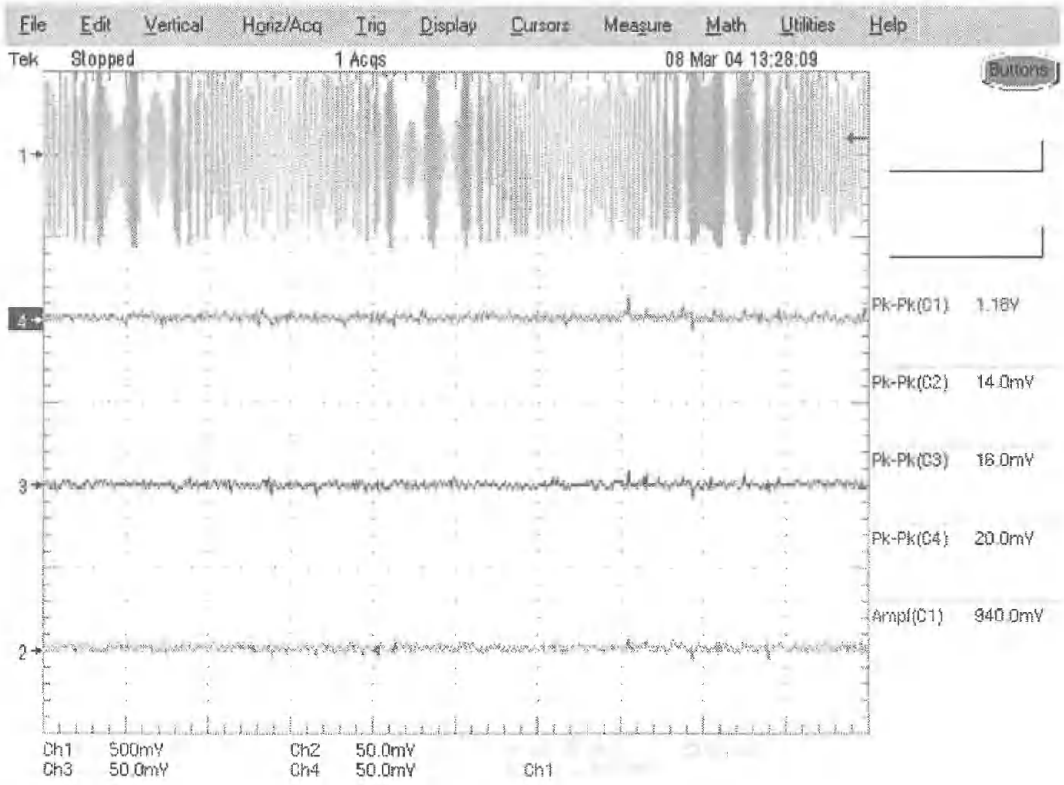

Fig. C.22: PMSG Base Speed with Added Sine, No Load

Table C.21: PMSG Base Speed with Added Sine, No Load

No Load (0Nm) Phase Quantities

	A		B		C		Total-Line	
	High	Low	High	Low	High	Low	High	Low
Irms (A)	0	0	0	0	0	0	0	0
Vrms (V)	112.21	95.77	111.07	94.75	111.11	94.5	193.06	164.56

1/4 Load – 4.6 Nm

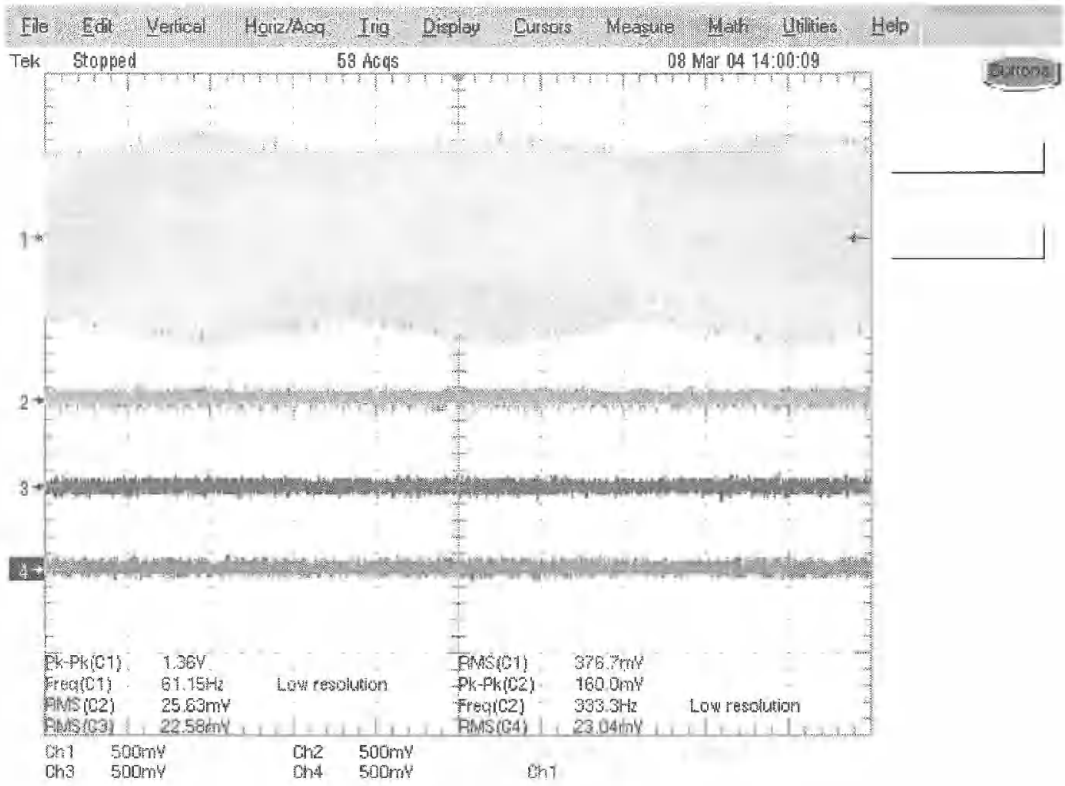

Fig. C.23: PMSG Base Speed with Added Sine, 1/4 Load

Table C.22: PMSG Base Speed with Added Sine, 1/4 Load

1/4 Load (4.6Nm) — Phase Quantities

	A		B		C		Total-Line	
	High	Low	High	Low	High	Low	High	Low
Irms (A)	2.42	2.14	2.49	2.11	3.11	2.85	2.67	2.37
Vrms (V)	128.53	103.13	122.67	98.91	123.08	99.41	216.14	174.08
P (kW)	0.27	0.18	0.16	0.11	0.17	0.11	0.60	0.40
Q (kVar)	0.15	0.13	0.26	0.18	0.35	0.26	0.81	0.60
S (kVA)	0.31	0.22	0.31	0.21	0.38	0.28	1.01	0.72

1/2 Load – 9.2 Nm

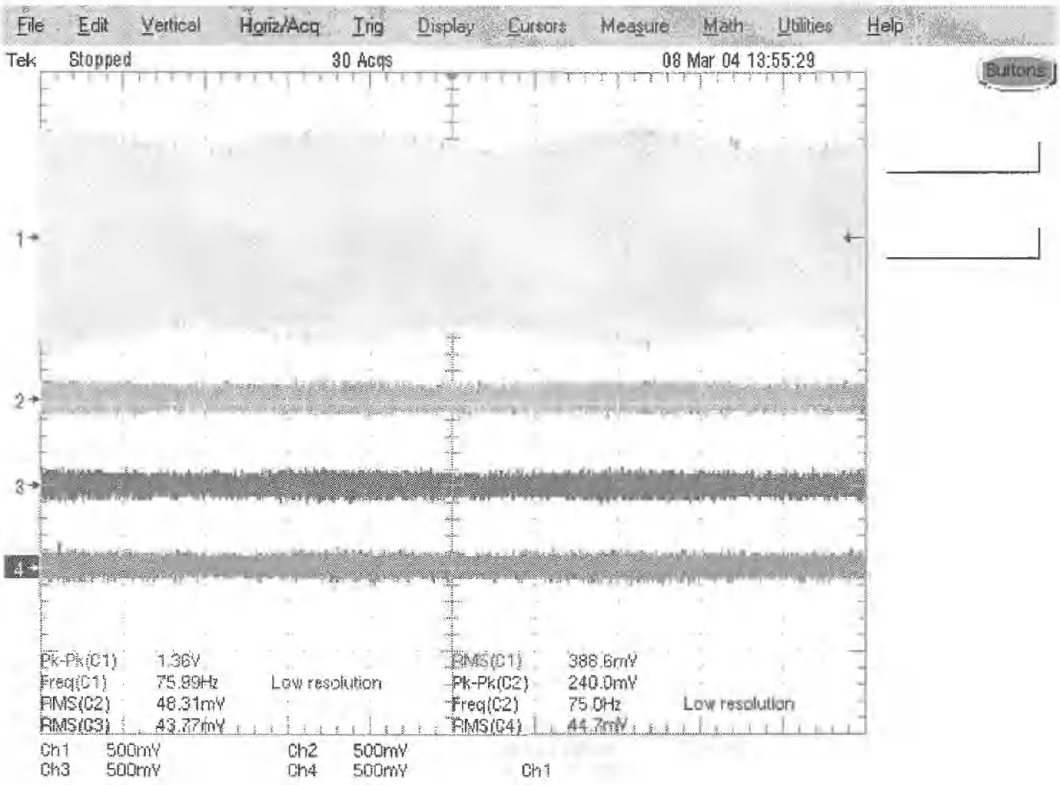

Fig. C.24: PMSG Base Speed with Added Sine, 1/2 Load

Table C.23: PMSG Base Speed with Added Sine, 1/2 Load

1/2 Load (9.2Nm) Phase Quantities

	A		B		C		Total-Line	
	High	Low	High	Low	High	Low	High	Low
Irms (A)	5.1	4.23	5.62	4.61	5.54	4.69	5.42	4.51
Vrms (V)	133.36	108.05	126.56	103.40	125.73	103.22	222.73	181.71
P (kW)	0.66	0.44	0.38	0.25	0.39	0.26	1.43	0.95
Q (kVar)	0.17	0.13	0.60	0.41	0.58	0.41	1.53	1.06
S (kVA)	0.68	0.46	0.71	0.48	0.70	0.48	2.09	1.42

3/4 Load – 13.7 Nm

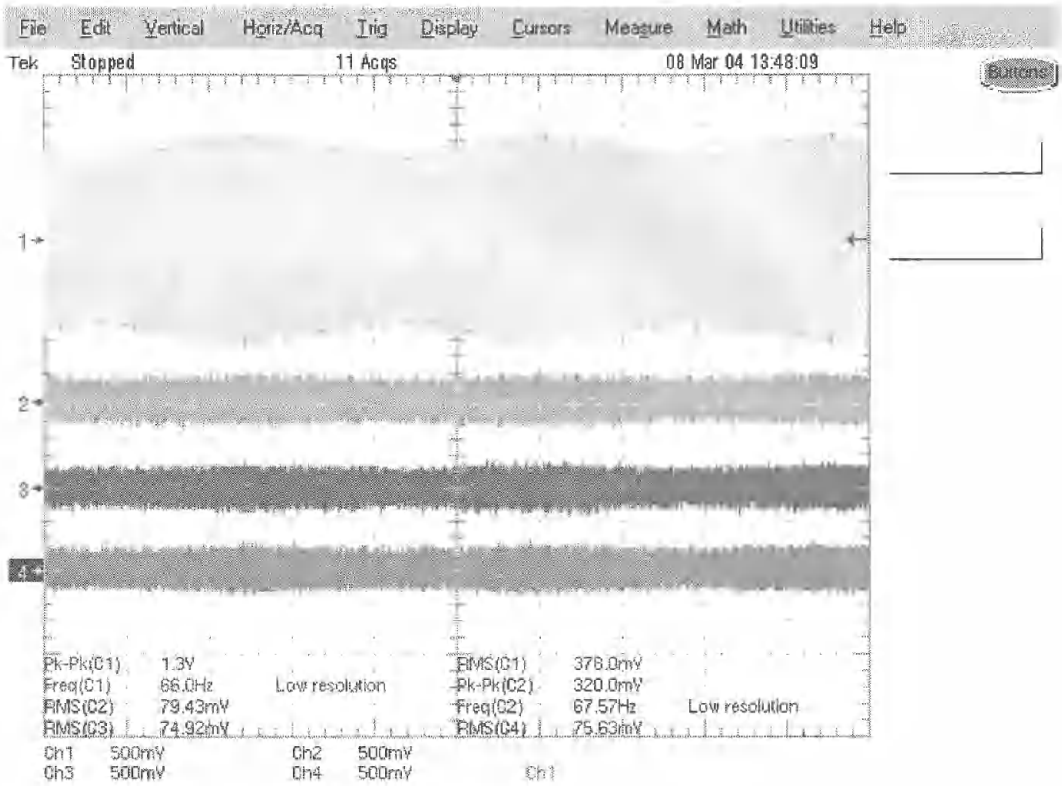

Fig. C.25: PMSG Base Speed with Added Sine, 3/4 Load

Table C.24: PMSG Base Speed with Added Sine, 3/4 Load

3/4 Load (13.7Nm) Phase Quantities

	A		B		C		Total-Line	
	High	Low	High	Low	High	Low	High	Low
Irms (A)	8.25	7.32	8.97	7.94	8.61	7.66	8.61	7.46
Vrms (V)	130.66	106.83	122.65	100.91	122.12	100.92	216.86	178.26
P (kW)	1.07	0.77	0.60	0.43	0.61	0.44	2.27	1.64
Q (kVar)	0.17	0.14	0.93	0.68	0.86	0.64	2.31	1.70
S (kVA)	1.08	0.78	1.10	0.80	1.05	0.77	3.24	2.36

Full Load – 18.3 Nm

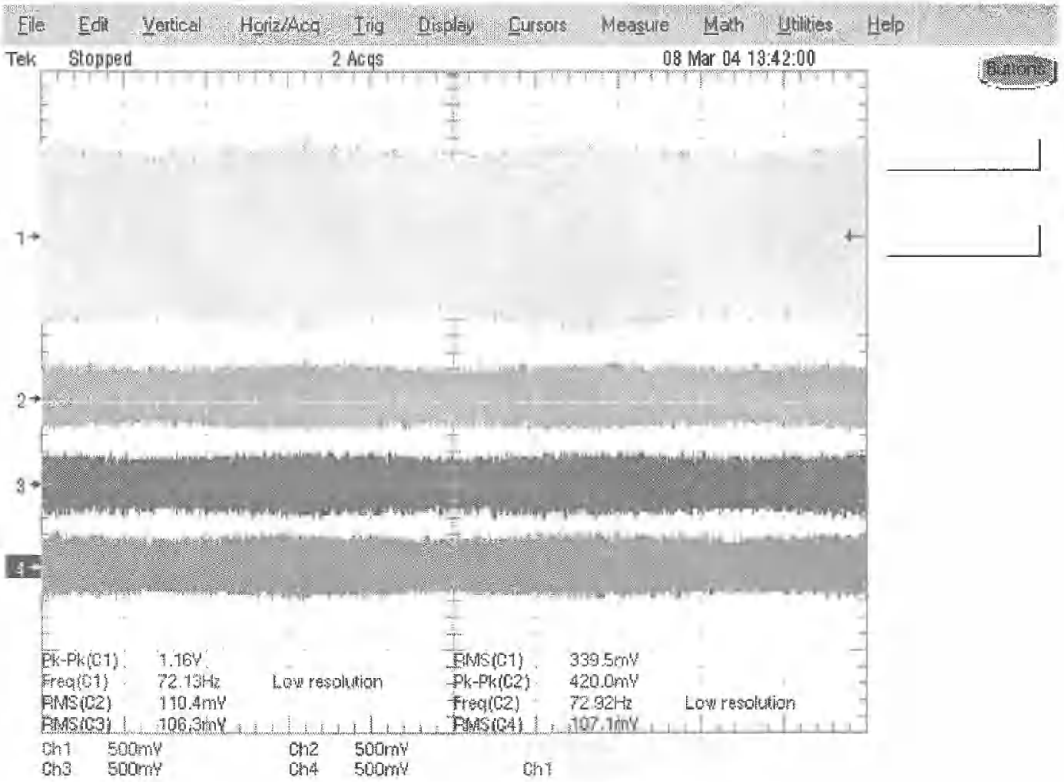

Fig. C.26: PMSG Base Speed with Added Sine, Rated Load

Table C.25: PMSG Base Speed with Added Sine, Rated Load

Full Load (18.3Nm) Phase Quantities

	A		B		C		Total-Line	
	High	Low	High	Low	High	Low	High	Low
Irms (A)	12.18	10.28	12.84	10.88	12.43	10.56	12.48	10.57
Vrms (V)	116.82	101.26	107.95	94.68	107.52	94.56	191.99	167.80
P (kW)	1.41	1.03	0.75	0.55	0.77	0.57	2.94	2.15
Q (kVar)	0.16	0.13	1.17	0.87	1.09	0.82	2.94	2.20
S (kVA)	1.42	1.04	1.39	1.03	1.34	1.00	4.15	3.07

C.1.5. Over-Running Clutch Connected Base Speed with Added Sine

C.1.5.1. Over-Running Clutch Connected Base Speed with Added Sine Investigation, Speed Profile

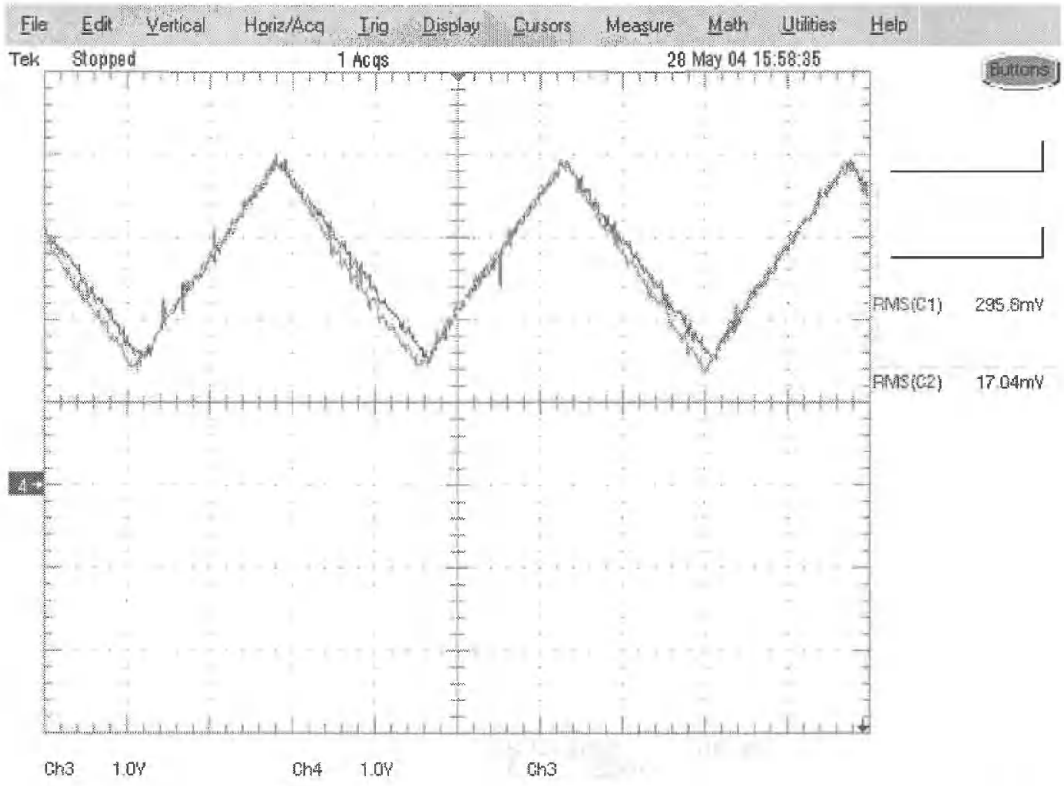

Fig. C.27: Over-Running Clutch Connected Base Speed investigation, Speed Profile, No Load

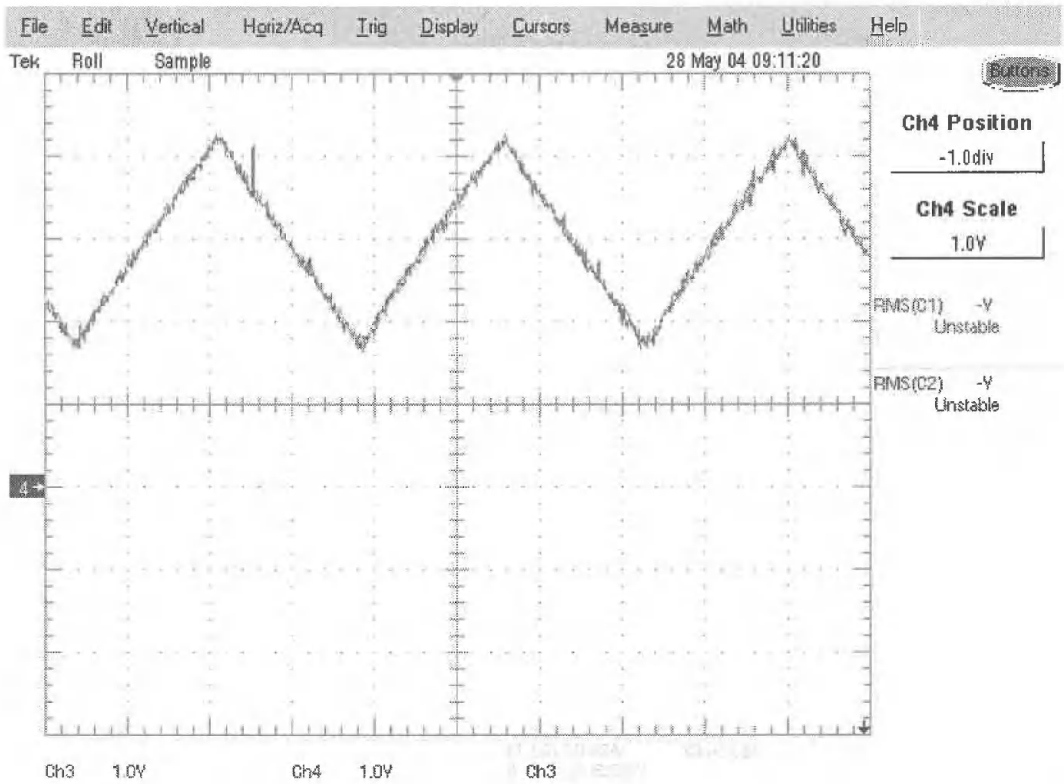

Fig. C.28: Over-Running Clutch Connected Base Speed investigation, Speed Profile, Full Load

6.1.1.1 *Over-Running Clutch Connected Base Speed with Added Sine Investigation, Unrectified Output*

No Load – 0Nm

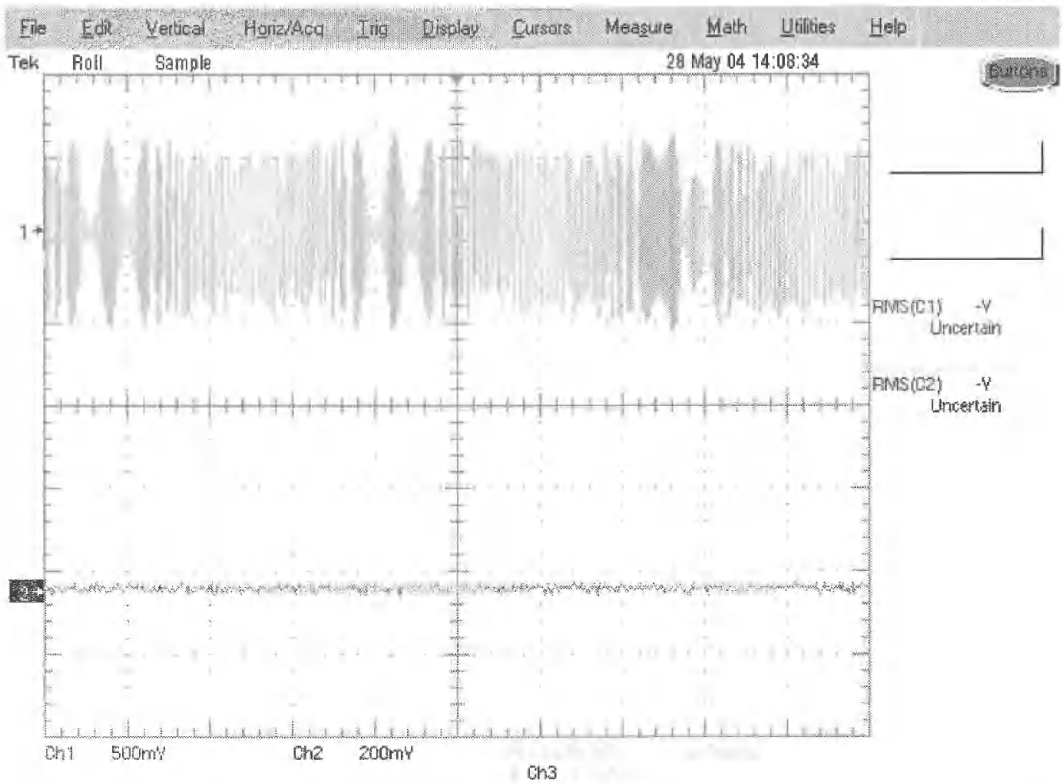

Fig. C.29: No Load Output without Rectifier (Ch1: Voltage 500/1, Ch2: Current 100/1)

Table C.26: No Load Output without Rectifier

No Load
(0 Nm)

	Phase Quantities							
	A		B		C		Total – Line	
	High	Low	High	Low	High	Low	High	Low
Irms (A)	0.00	0.00	0.00	0.00	0.00	0.00	0.00	0.00
Vrms (V)	116.42	94.55	116.2	64.69	115.98	94.78	201.6	163.98

Full Load – 18.3Nm

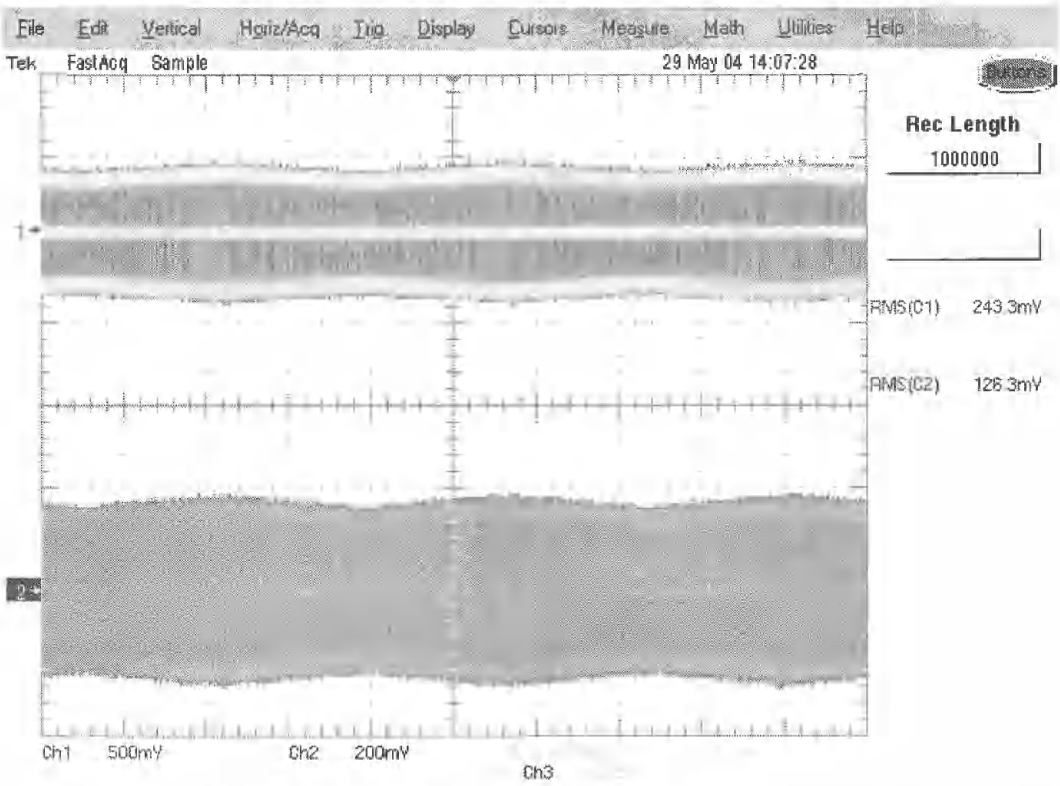

Fig. C.30: Full Load Output without rectifier (Ch1: Voltage 500/1, Ch2: Current 100/1)

Table C.27: Full Load Output without rectifier

Full Load (18.3Nm)	Phase Quantities							
	A		B		C		Total – Line	
	High	Low	High	Low	High	Low	High	Low
Irms (A)	10.64	9.53	9.83	8.77	10.00	8.93	10.16	9.08
Vrms (V)	116.04	98.83	124.92	104.44	117.98	99.71	207.34	174.97
P (kW)	-1.23	-.94	-1.23	-.91	-1.18	-.89	-3.63	-2.74
Q (kVar)	.10	.08	.08	.07	.06	.55	.34	.26
S (kVA)	1.24	.94	1.23	.92	1.18	.89	3.65	2.75

6.1.1.2 *Over-Running Clutch Connected Base Speed with Added Sine Investigation, Rectified Output*

No Load – 0Nm

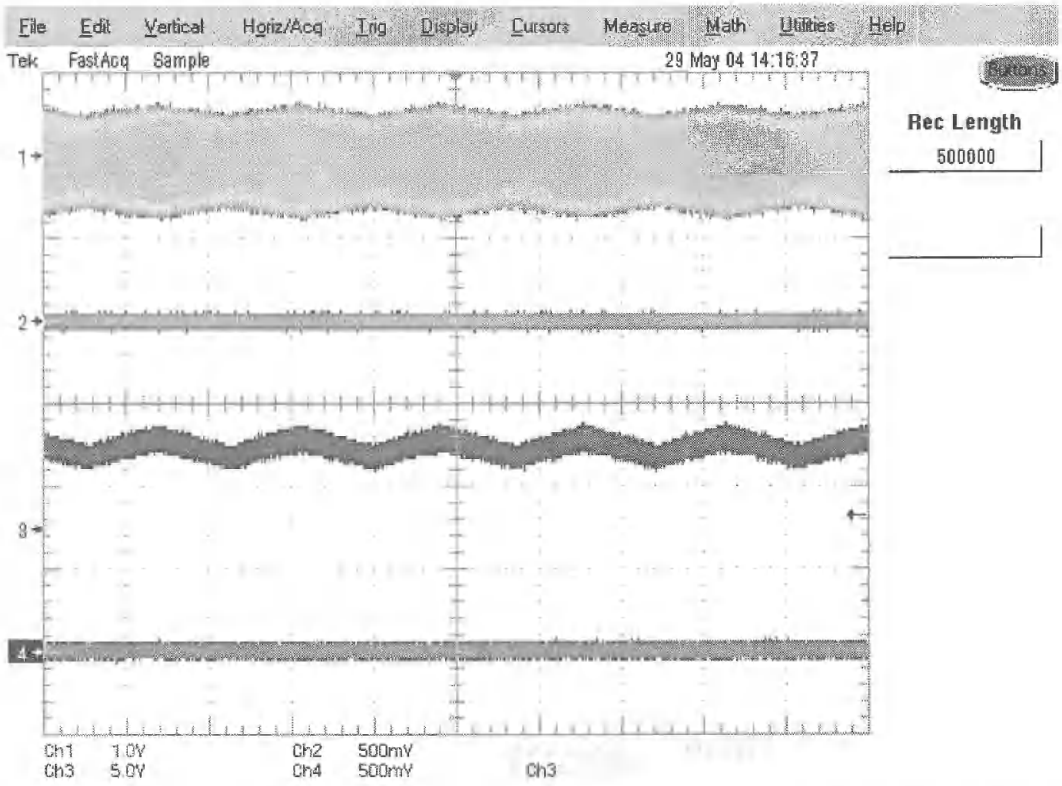

Fig. C.31: No Load Output with rectifier (Ch1: AC Voltage 500/1, Ch2: AC Current 100/1, Ch3 Rectified Voltage 500/1, Ch4 Rectified Current 100/1);

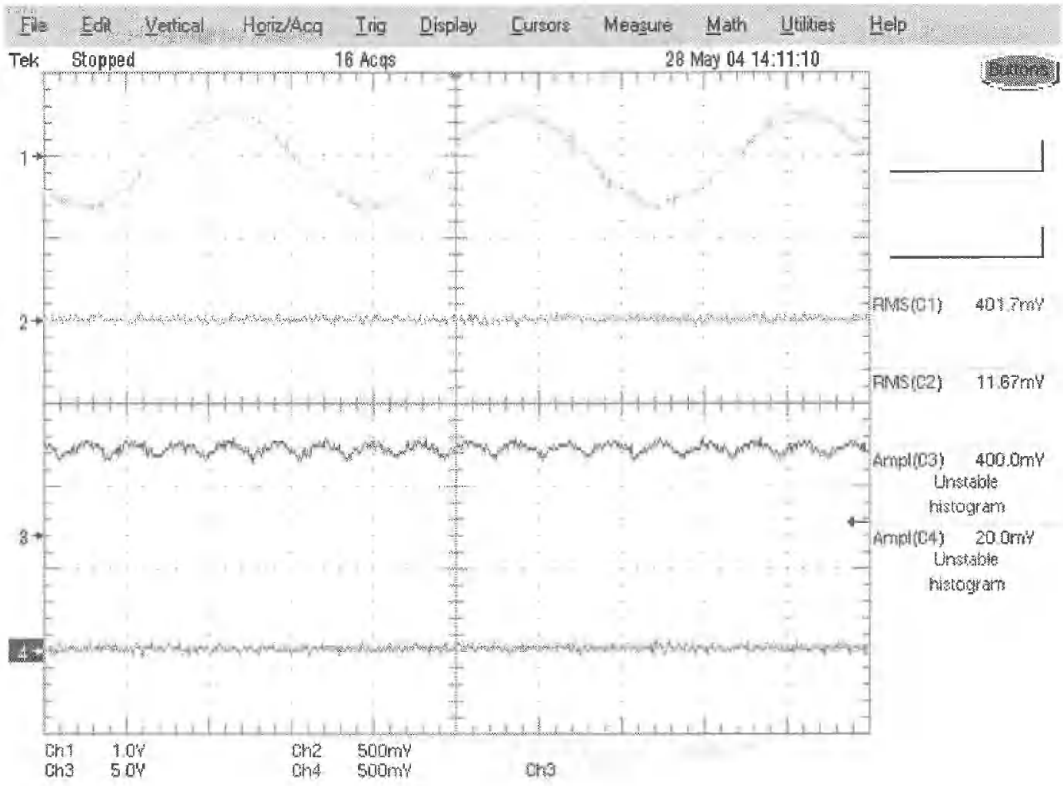

Fig. C.32: Close up of No Load Output with rectifier (Ch1: AC Voltage 500/1, Ch2: AC Current 100/1, Ch3 Rectified Voltage 500/1, Ch4 Rectified Current 100/1)

Table 6.28: No Load Output with rectifier

Full Load (18.3Nm) Phase Quantities

	A		B		C		Total – Line		Rectified Values	
	High	Low	High	Low	High	Low	High	Low	High	Low
Irms (A)	0.00	0.00	0.00	0.00	0.00	0.00	0.00	0.00	0.00	0.00
Vrms (V)	117.11	96.50	116.83	96.03	116.66	96.22	202.42	166.71	268.65	222.01

Full Load – 18.3Nm

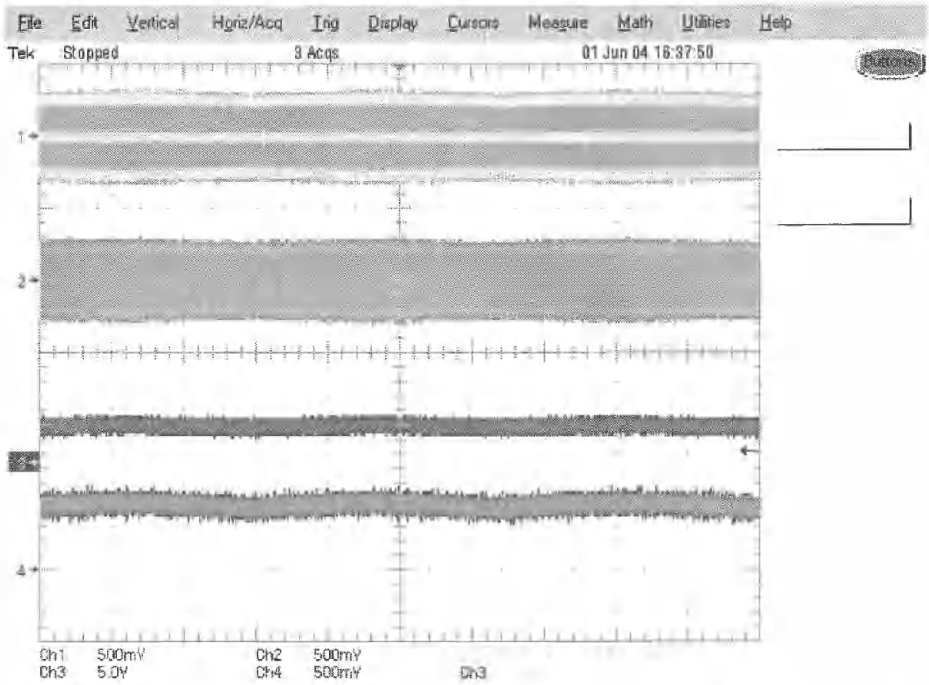

Fig. C.33: Full Load Output with rectifier (Ch1: AC Voltage 500/1, Ch2: AC Current 100/1, Ch3 Rectified Voltage 500/1, Ch4 Rectified Current 100/1)

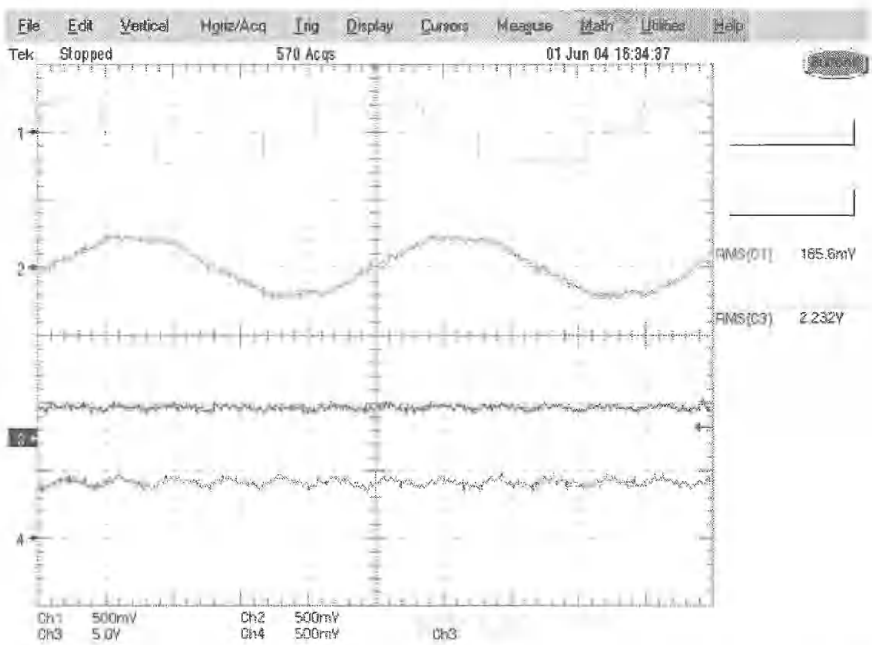

Fig. C.34:Close up of Full Load Output with rectifier (Ch1: AC Voltage 500/1, Ch2: AC Current 100/1, Ch3 Rectified Voltage 500/1, Ch4 Rectified Current 100/1)

Table 6.29: Full Load Output with rectifier

Full Load (18.3Nm) — Phase Quantities

	A		B		C		Total – Line		Rectified Values	
	High	Low	High	Low	High	Low	High	Low	High	Low
Irms (A)	14.48	12.32	14.37	12.23	14.38	12.25	14.41	12.27	19.3	17.1
Vrms (V)	84.87	76.71	84.68	76.5	84.83	76.51	146.87	132.63	176.55	160.10
P (kW)	-1.15	-.88	-1.14	-.87	-1.14	-.87	-3.42	-2.62	-3.41	-2.74
Q (kVar)	.44	.35	.44	.34	.44	.34	1.32	1.03	-	-
S (kVA)	1.23	.95	1.22	.94	1.22	.94	3.67	2.82	-	-

C.2. Wound Rotor Induction Generator

C.2.1. Rotor with Connected External Impedance (External R & L)

C.2.1.1. Baseline Steady State Testing

Steady State 1200 Rev/Min

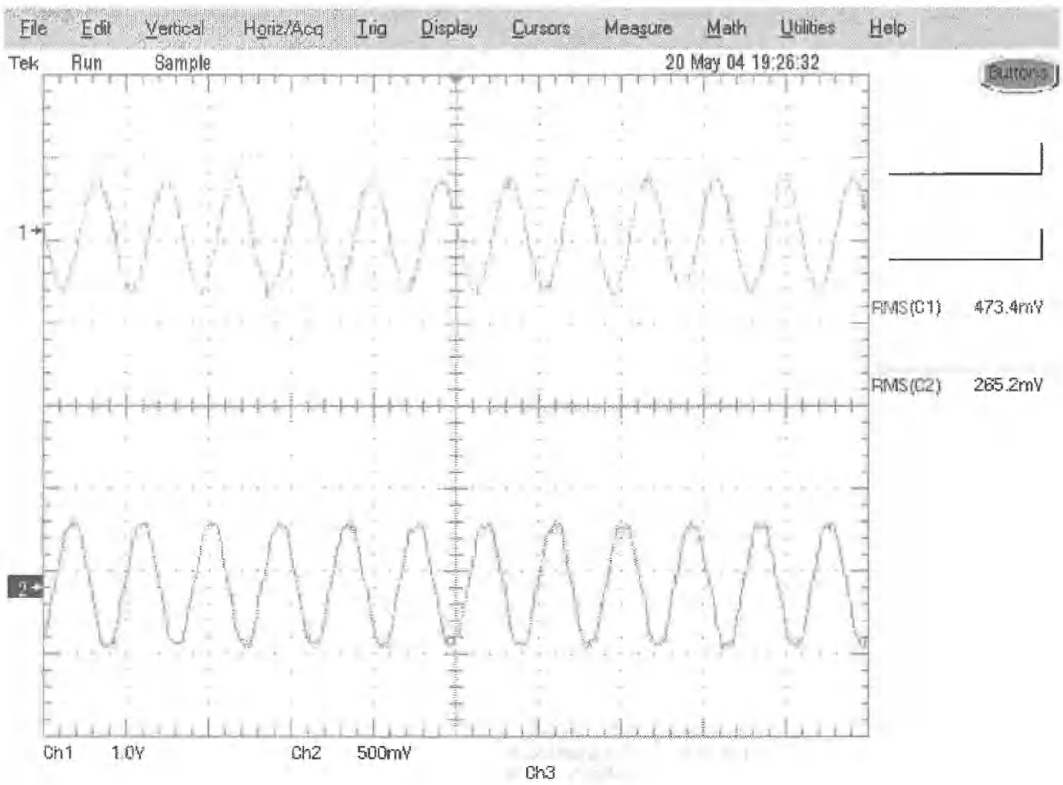

Fig. C.35: Baseline Test for the WRIG at 1200 Rev/Min

Table C.30: Baseline Test for the WRIG at 1200 Rev/Min

Speed: 1200	Phase Quantities			
Torque: 3.3Nm	A	B	C	Total-Line
Irms (A)	26.96	26.37	25.49	26.27
Vrms (V)	233.60	231.60	233.50	232.90
P (kW)	0.38	0.38	0.37	0.93
Q (kVar)	3.66	3.51	3.39	10.56
S (kVA)	3.60	3.53	3.41	10.53

Steady State 1462.5 Rev/Min

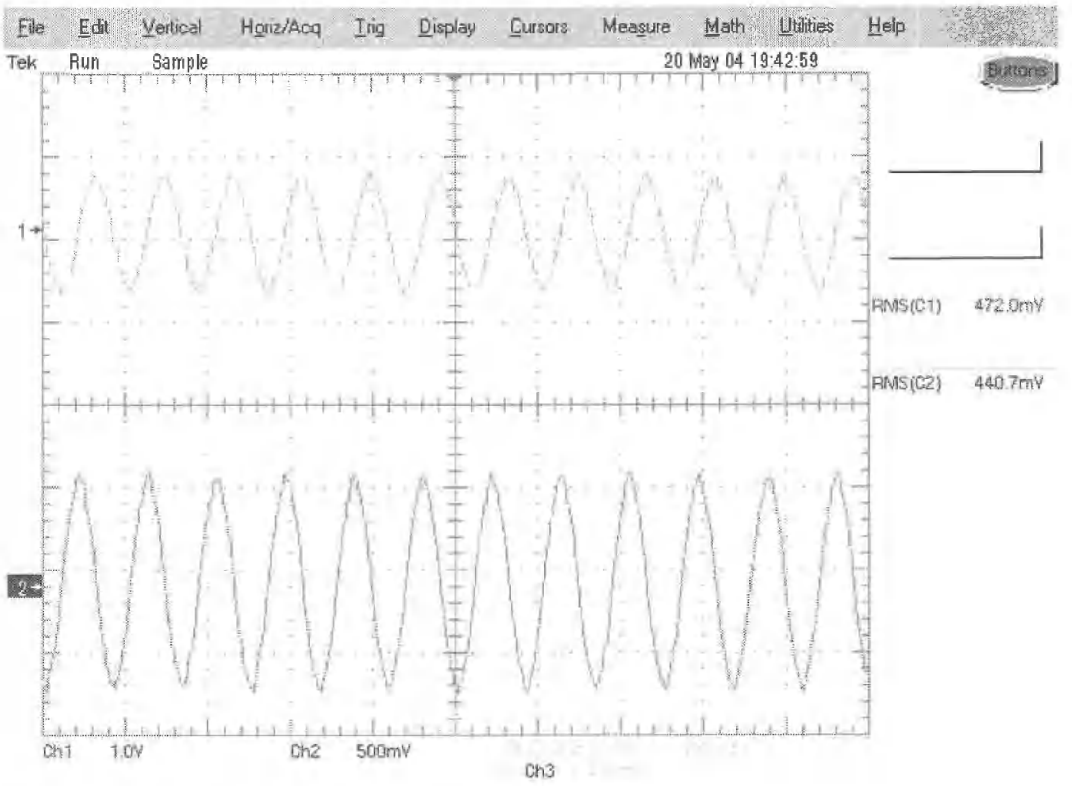

Fig. C.36: Baseline Test for the WRIG at 1462.5 Rev/Min

Table C.31: Baseline Test for the WRIG at 1462.5 Rev/Min

Speed: 1462.5	Phase Quantities			
Torque: 94.4 Nm	A	B	C	Total-Line
Irms (A)	44.97	44.85	43.07	44.29
Vrms (V)	234.00	232.20	234.01	232.20
P (kW)	-3.21	-3.36	-3.09	-9.68
Q (kVar)	5.25	4.95	4.88	15.07
S (kVA)	5.99	5.97	5.81	17.75

Steady State 1550 Rev/Min

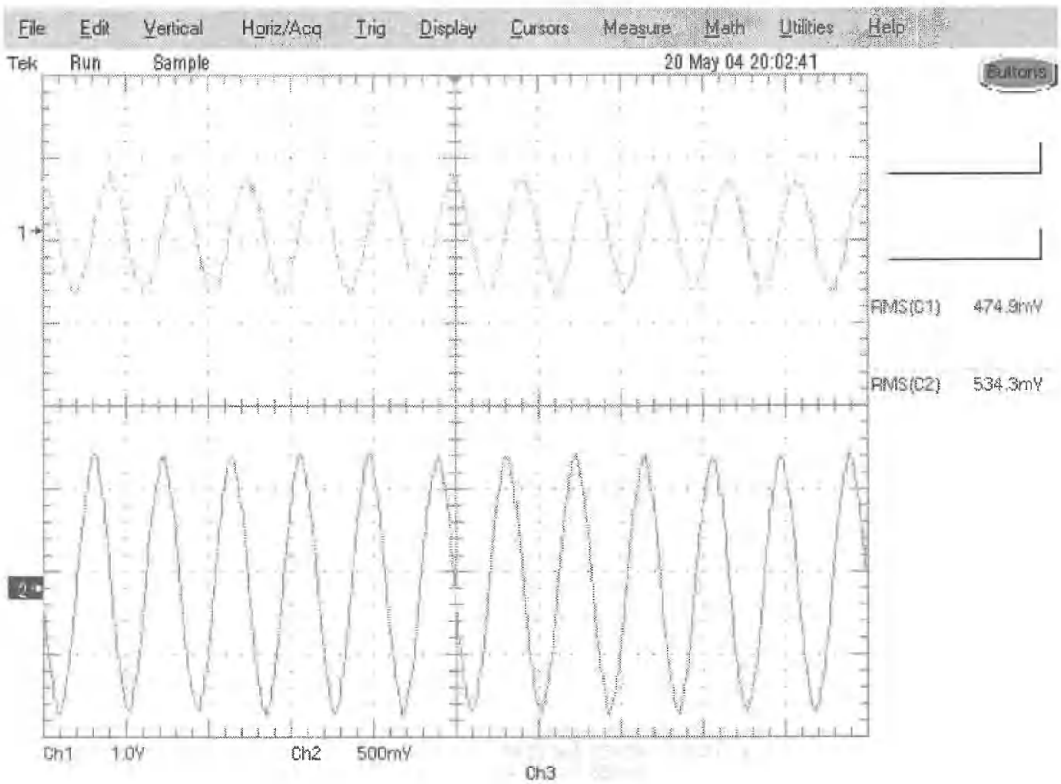

Fig. C.37: Baseline Test for the WRIG at 1550 Rev/Min

Table C.32: Baseline Test for the WRIG at 1550 Rev/Min

Speed: 1550	Phase Quantities			
Torque:126 Nm	A	B	C	Total-Line
Irms (A)	53.14	54.06	52.19	53.13
Vrms (V)	234.40	231.80	233.80	233.30
P (kW)	-4.29	-4.47	-4.22	-12.99
Q (kVar)	5.84	5.65	5.56	17.05
S (kVA)	6.91	6.23	6.77	19.89

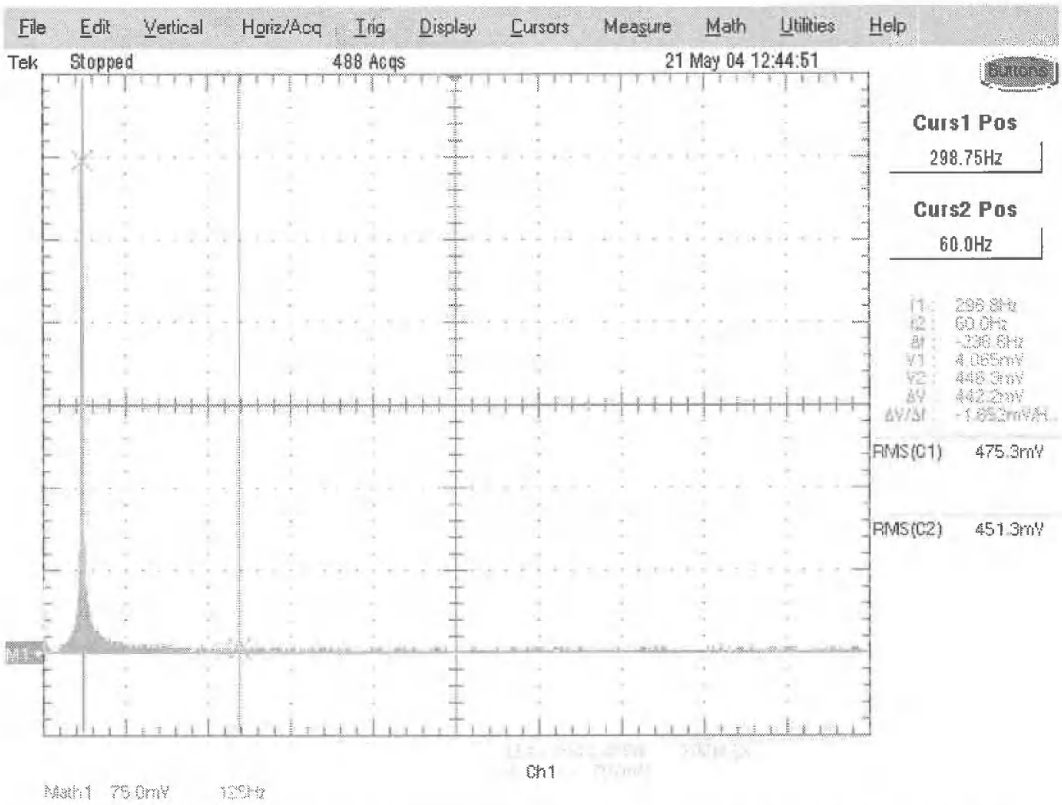

Fig. C.38: Spectral Analysis (FFT) of the Baseline Test for the WRIG at 1462.5 Rev/Min

C.2.1.2. *Over-Running Clutch Base Speed with an Added Sine Component*

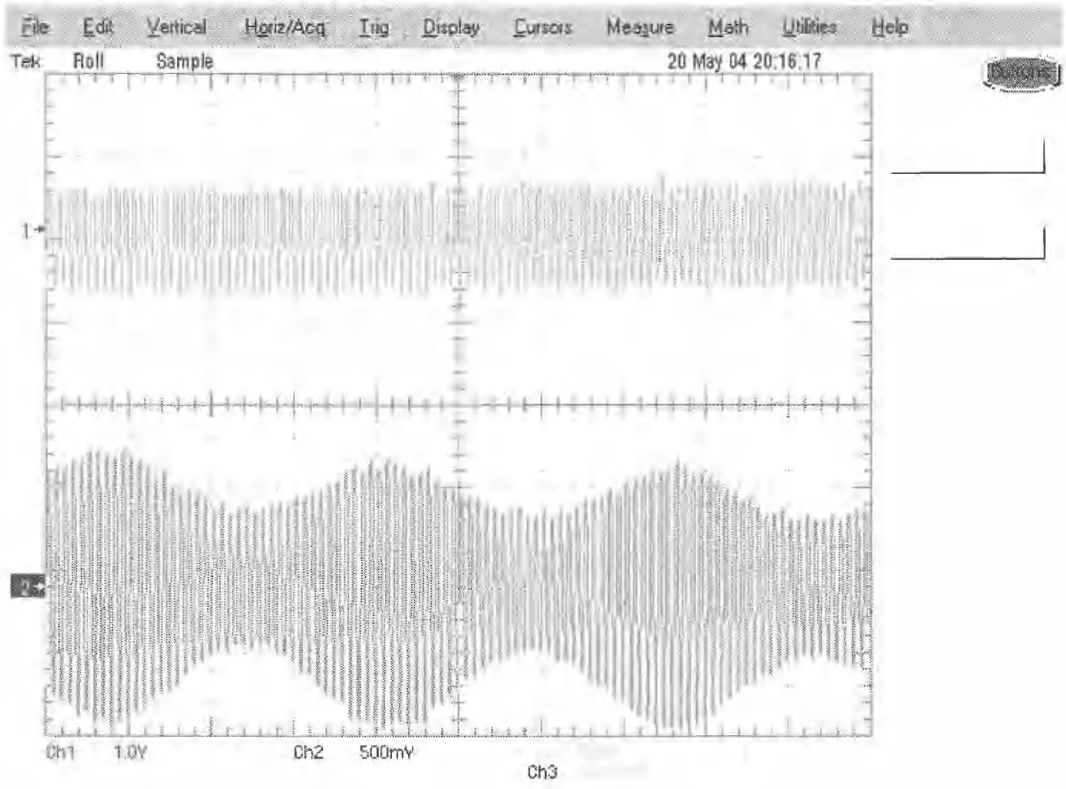

Fig. C.39: Over-Running Clutch Connected Base Speed with an Added Sine Component

Table C.33: Over-Running Clutch Connected Base Speed with an Added Sine Component

Speed: Recip.	Phase Quantities - Grid Connected							
Torque: Recip.	A		B		C		Total-Line	
	High	Low	High	Low	High	Low	High	Low
Irms (A)	57.84	32.29	59.09	32.40	57.24	31.33	58.05	32.00
Vrms (V)	235.00	234.50	231.90	232.30	234.00	233.90	233.60	233.60
P (kW)	-4.85	-1.24	-5.01	-1.37	-4.77	-1.23	-14.60	-3.85
Q (kVar)	6.23	4.23	6.07	4.10	5.99	4.01	18.29	12.35
S (kVA)	7.89	4.41	7.87	4.32	7.65	4.20	23.40	12.93

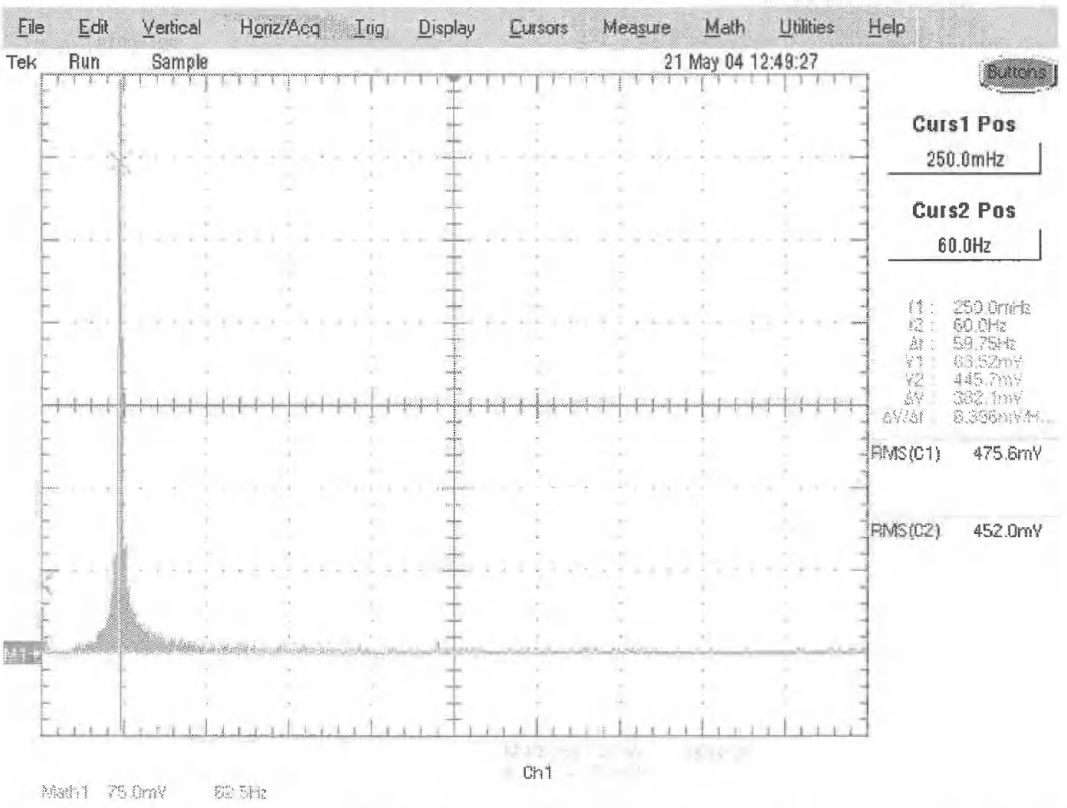

Fig. C.40: Spectral Analysis (FFT) of the Over-Running Clutch Connected Base Speed with an Added Sine Component

D. APPENDIX D: Analytical Approach to External Rotor Components

Anthony Schacher

```
> restart;
```

Parameter Values for the Per-Phase equivalent circuit

Rated Voltage

```
> V:=230;
```

$$V := 230$$

Rated Stator Current (from Nameplate)

```
> Is:=Is;
```

$$Is := Is$$

Frequency

```
> f:=60;
```

$$f := 60$$

Rated Power

```
> P:=11190;
```

$$P := 11190$$

Poles

```
> p:=6;
```

$$p := 6$$

Rated Slip

```
> slip:=.01;
```

$$slip := .01$$

Winding Ratio Rotor:Stator

```
> a:=1.1061;
```

$$a := 1.1061$$

Rotor Current (Ns*Is=Nr*Ir)

```
> Ir:Is/a;
```

$$.9040773890\ Is$$

Stator Resistance

```
> R1:=.18;
```

$$R1 := .18$$

Stator referred rotor resistance

```
> R2:=.33;
```

$$R2 := .33$$

Core Loss Resistance

```
> Rc:=93.63;
```

$$Rc := 93.63$$

Stator Reactance

```
> X1:=.4;
```

$$X1 := .4$$

Stator Referred Rotor Reactance

```
> X2:=.40;
```

$$X2 := .40$$

Core Reactance

```
> Xm:=4.65;
```

$$Xm := 4.65$$

Intrinsic resistance of the external inductor

```
> #Rlex:=.684;
```

Required slip

```
> s_required:=.22;
```

$$s\_required := .22$$

Calculations for the Required External Resistance for the Per-Phase Equivalent circuit

Synchronous Frequency (rpm)

```
> n_s:=120*f/p;
```

$$n\_s := 1200$$

Synchronous frequency (rad/s)

```
> omega:=4*Pi*f/p;
```

$$\omega := 40\,\pi$$

Required Torque

```
> T_required:=evalf((P/(3*(1-slip)*omega)));
```

$$T\_required := 29.98221906$$

Thevanin Impedance

Magnetizing Core Impedance

```
> Zc:=Rc*I*Xm/(Rc+I*Xm);
```

$$Zc := .2303674032 + 4.638559132\ I$$

```
> Zc_mag:=abs(Zc);
```

$$Zc\_mag := 4.644276043$$

Thevanin Impedance = R+Xi

```
> Zth := Zc*(R1+I*X1)/(R1+I*X1+Zc);
```

$$Zth := .1536577185 + .3725298423\ I$$

Thevanin Resistance

```
> Rth:=Re(Zth);
```

$$Rth := .1536577185$$

Thevanin Reactance

```
> Xth:=Im(Zth);
```

$$Xth := .3725298423$$

Thevanin Voltage

Rated Voltage Phase the line to line

```
> V1:=V/sqrt(3);
```

$$V1 := \frac{230}{3}\sqrt{3}$$

Thevenin Voltage

```
> Vth:=V1*(Zc/(I*X1+R1+Zc));
```

$$Vth := (70.39877867 + 2.228387677\ I)\sqrt{3}$$

evaluate only the magnitude of the thevanin voltage

```
> Vth:=abs(Vth);
```

$$Vth := 70.43403829\ \sqrt{3}$$

General Torque Output

```
>
Torque_general:=(1/omega)*((Vth^2)/((((R2)/s)+Rth)^2+(Xth
+X2)^2)*((R2)/s));
```

$$Torque\_general := 122.7836054\ \frac{1}{\pi\left(\left(.33\ \frac{1}{s} + .1536577185\right)^2 + .5968023572\right)s}$$

Plot the general torque output

```
> plot(Torque_general, s=-1..1);
```

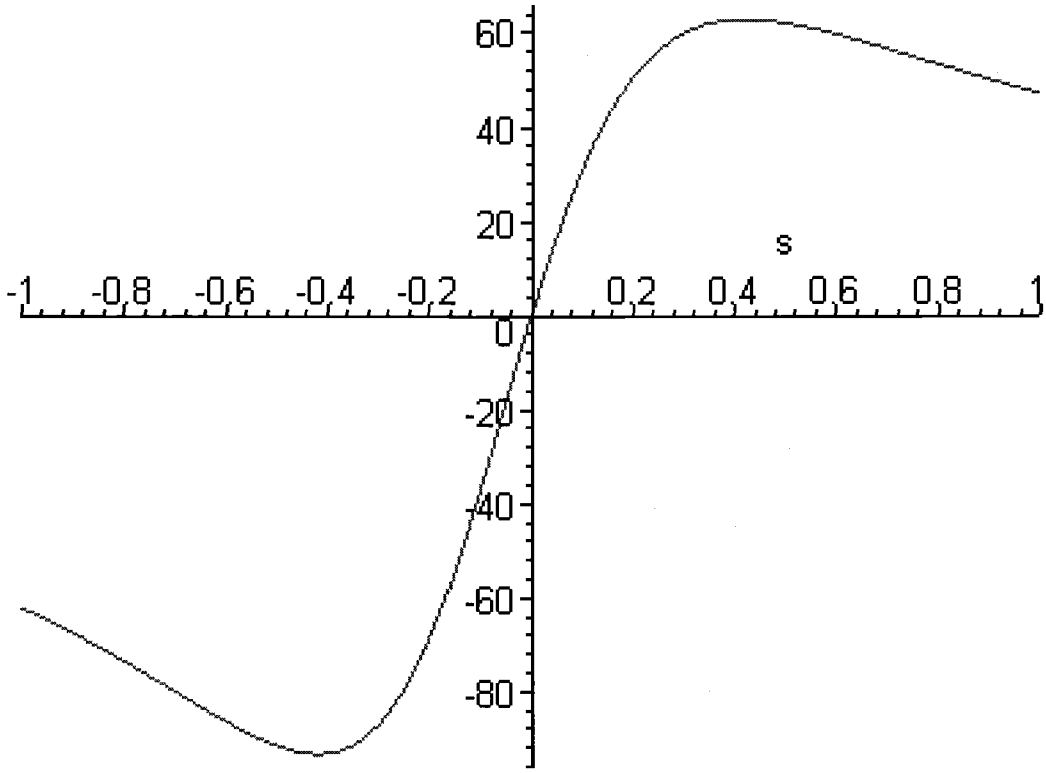

Plot the torque-speed profile

```
> slip_chg:=(n_s-n_m)/n_s;
```

$$slip\_chg := 1 - \frac{1}{1200}\, n\_m$$

```
>
Torque_speed:=(1/omega)*((Vth^2)/((((R2)/slip_chg)+Rth)^2
+(Xth+X2)^2)*((R2)/slip_chg));
```

$$Torque\_speed := 122.7836054$$

$$\frac{1}{\pi\left(\left(.33\,\frac{1}{1-\frac{1}{1200}\,n\_m}+.1536577185\right)^2+.5968023572\right)\left(1-\frac{1}{1200}\,n\_m\right)}$$

```
> plot(Torque_speed, n_m=-1500..4500);
```

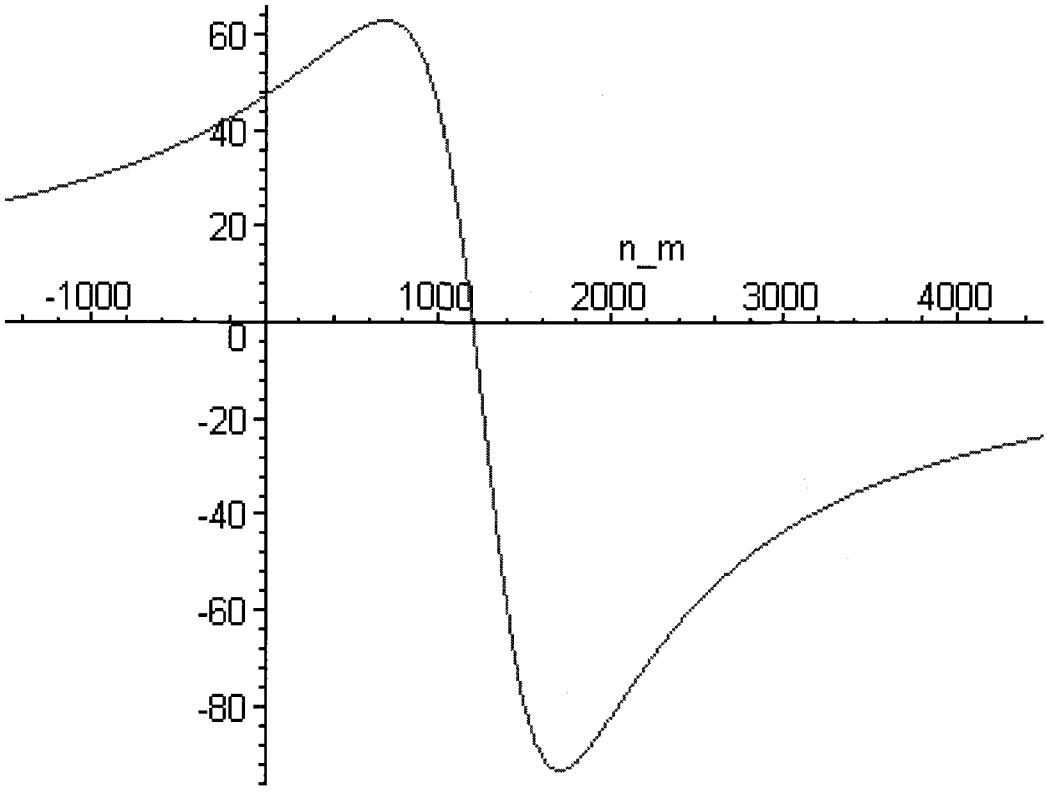

Torque output at the required slip if no additional rotor impedance is put into the rotor

```
>
T_out:=(1/omega)*((Vth^2)/((((R2)/s_required)+Rth)^2+(Xth
+X2)^2)*((R2)/s_required));
```

$$T\_out := 167.5300499\,\frac{1}{\pi}$$

slip at the maximum Torque value

```
> s_Tmaxgeneral:=(R2)/sqrt((Rth^2+(Xth+X2)^2));
```

$$s\_Tmaxgeneral := .4189608839$$

Maximum Torque

```
> T_maxgeneral:=(1/(2*omega))*(Vth^2/(Rth+sqrt((Rth^2)+(Xth
+X2)^2)));
```

$$T\_maxgeneral := 197.6327045\ \frac{1}{\pi}$$

Solve for Equivalent Impedance Magnitude of the External Components

When the torque equation is solved for Rext a quadratic is formed and therefore the quadratic formula must be used to find the solutions to the roots.

Using direct values

```
> A:=1;
```

$$A := 1$$

```
> B:=evalf(2*R1*s_required+2*R2-
(s_required*V1^2)/(T_required*(1-s_required)*omega));
```

$$B := -.580845371$$

```
> C:=evalf(2*R1*R2*s_required+R2^2+s_required^2*R1^2+s_requ
ired^2*(X1+X2)^2-s_required*V1^2*R2/(T_required*(1-
s_required)*omega));
```

$$C := -.2680348123$$

```
> Req1_prime :=evalf((-B+(sqrt(B^2-4*A*C)))/(2*A));
```

$$Req1\_prime := .8840388480$$

```
> Req1:=a^2*Req1_prime;
```

$$Req1 := 1.081583703$$

```
> Req2_prime:=evalf((-B-(sqrt(B^2-4*A*C)))/(2*A));
```

$$Req2\_prime := -.3031934770$$

```
> Req2:=a^2*Req2_prime;
```

$$Req2 := -.3709442455$$

Using Thevanin Equivalents

```
> A:=1;
```

$$A := 1$$

```
> B:=evalf(2*Rth*s_required+2*R2-
(s_required*Vth^2)/(T_required*(1-s_required)*omega));
```

$$B := -.3865334449$$

```
> C:=evalf(2*Rth*R2*s_required+R2^2+s_required^2*Rth^2+s_re
quired^2*(Xth+X2)^2-s_required*Vth^2*R2/(T_required*(1-
s_required)*omega));
```

$$C := -.2064280450$$

```
> Req1_prime :=evalf((-B+(sqrt(B^2-4*A*C)))/(2*A));
```

$$Req1\_prime := .6870076170$$

```
> Req1:=a^2*Req1_prime;
```

$$Req1 := .8405244223$$

```
> Req2_prime:=evalf((-B-(sqrt(B^2-4*A*C)))/(2*A));
```

$$Req2\_prime := -.3004741722$$

```
> Req2:=a^2*Req2_prime;
```

$$Req2 := -.3676172924$$

Torque output with Rext1

```
>
Torque_Rated1:=evalf(1/omega)*((Vth^2)/((((R2+Req1_prime)
/s)+Rth)^2+(Xth+X2)^2)*((R2+Req1_prime)/s));
```

$$Torque\_Rated1 := 120.4483276 \frac{1}{\left(\left(1.017007617 \frac{1}{s} + .1536577185\right)^2 + .5968023572\right) s}$$

```
> plot(Torque_Rated1, s=-1..1);
```

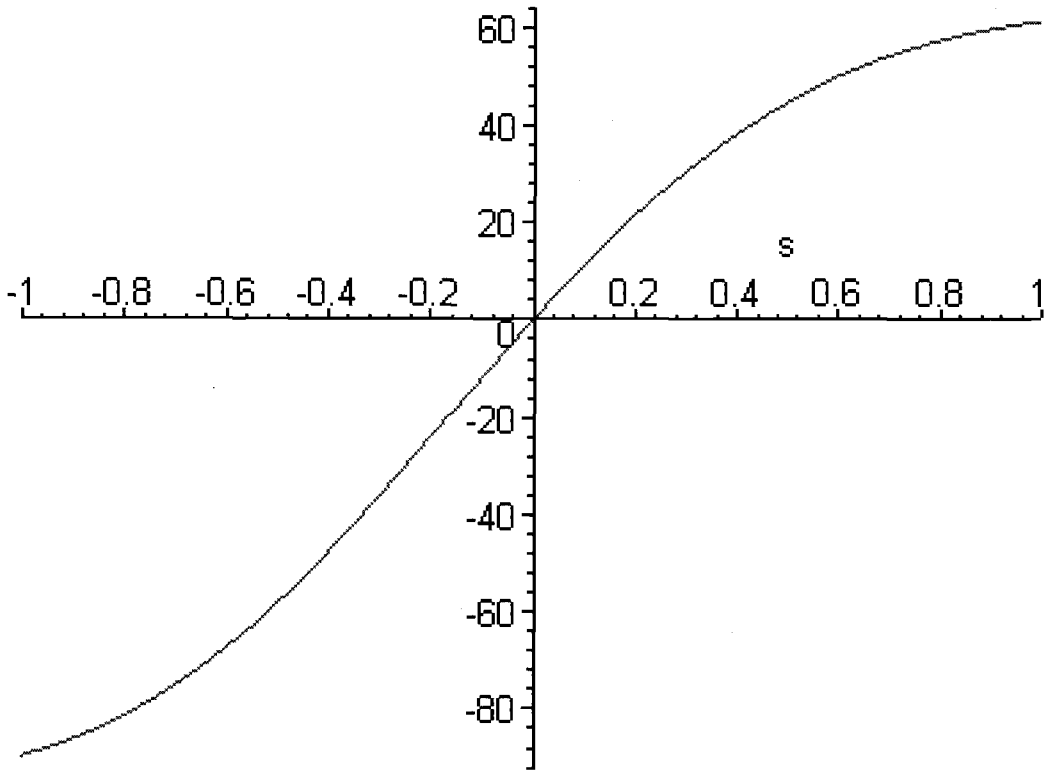


```
>
Torque_out1:=evalf(1/omega)*((Vth^2)/((((R2+Req1_prime)/s
_required)+Rth)^2+(Xth+X2)^2)*((R2+Req1_prime)/s_required
));
```

$$Torque\_out1 := 23.38613085$$

```
> s_TmaxExt1:=(R2+Req1_prime)/sqrt((Rth^2+(Xth+X2)^2));
```

$$s\_TmaxExt1 := 1.291170940$$

```
> T_maxExt1 :=
evalf(1/(2*omega)*Vth^2/(Rth+sqrt(Rth^2+(Xth+X2)^2)));
```

$$T\_maxExt1 := 62.90844366$$

Torque-Speed Profile

```
> slip_chg2:=(n_s-n_m2)/n_s;
```

$$slip\_chg2 := 1 - \frac{1}{1200}\, n\_m2$$

```
>
Torque_speed2:=(1/omega)*((Vth^2)/((((R2)/slip_chg2)+Rth)
^2+(Xth+X2)^2)*((R2)/slip_chg2));
```

$$Torque\_speed2 := 122.7836054$$

$$\frac{1}{\pi\left(\left(.33\,\frac{1}{1-\frac{1}{1200}\, n\_m2}+.1536577185\right)^2+.5968023572\right)\left(1-\frac{1}{1200}\, n\_m2\right)}$$

```
> plot(Torque_speed2, n_m2=-1500..2500);
```

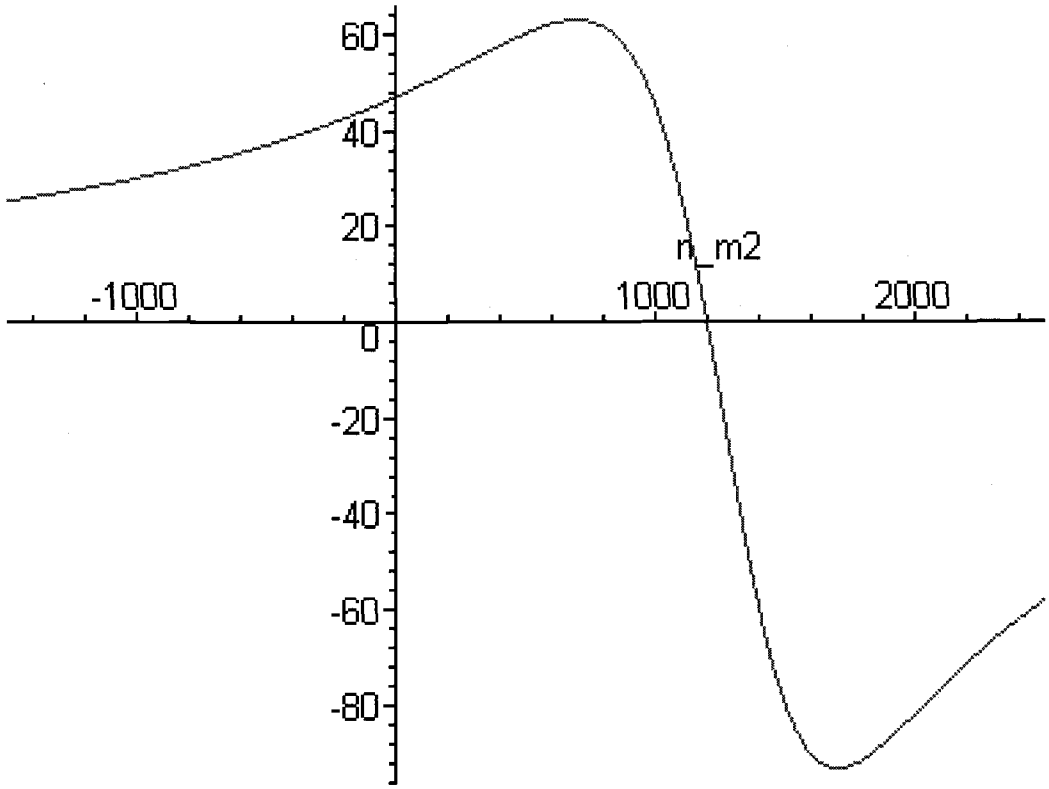

Torque output with Rext2

```
>
Torque_Rated2:=evalf(1/omega)*((Vth^2)/((((R2+Req2_prime)
/s)+Rth)^2+(Xth+X2)^2)*((R2+Req2_prime)/s));
```

$$Torque\_Rated2 := 3.496863269 \frac{1}{\left(\left(.0295258278\ \frac{1}{s} + .1536577185\right)^2 + .5968023572\right) s}$$

```
>plot(Torque_Rated2, s=-1..1);
```

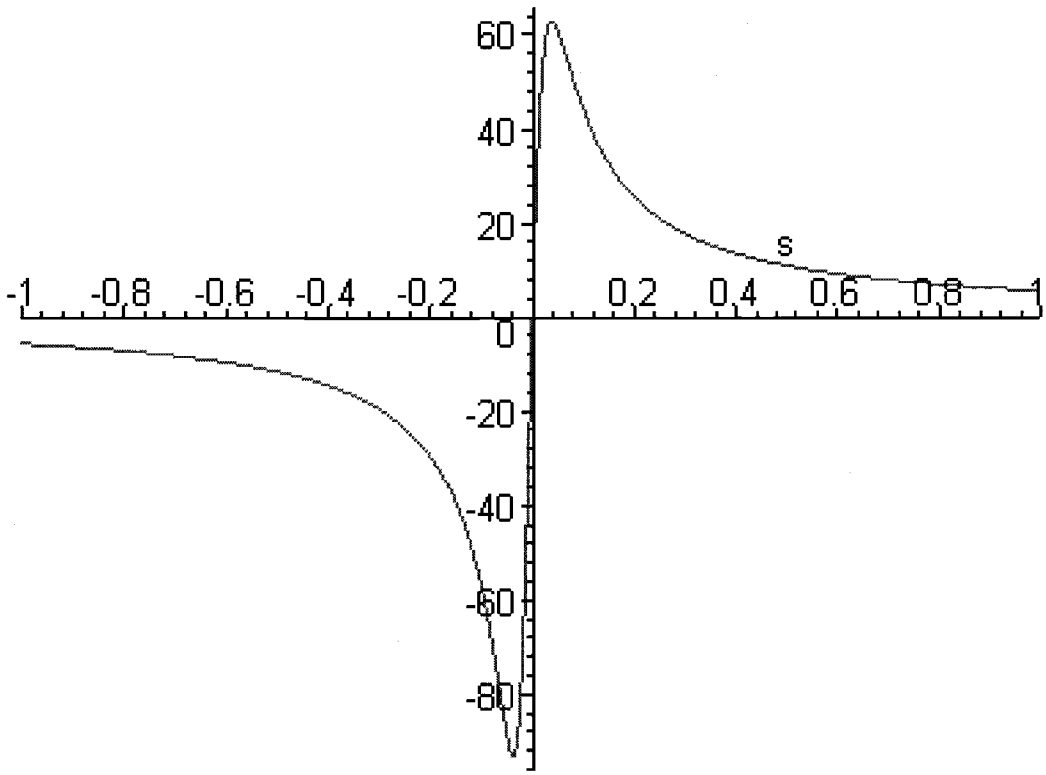


```
>
Torque_out2:=abs(evalf((1/omega)*((Vth^2)/((((R2+Req2_pri
me)/s_required)+Rth)^2+(Xth+X2)^2)*((R2+Req2_prime)/s_req
uired))));
```

$$Torque\_out2 := 23.38613093$$

```
>
s_TmaxExt2:=evalf((R2+Req2_prime)/sqrt((Rth^2+(Xth+X2)^2)
));
```

$$s\_TmaxExt2 := .03748535428$$

```
>
T_maxExt2:=evalf((1/(2*omega))*(Vth^2/(Rth+sqrt((Rth^2)+(
Xth+X2)^2))));
```

$$T\_maxExt2 := 62.90844366$$

Torque-Speed Profile

```
> slip_chg3:=(n_s-n_m3)/n_s;
```

$$slip\_chg3 := 1 - \frac{1}{1200}\, n\_m3$$

```
>
Torque_speed3:=(1/omega)*((Vth^2)/((((R2)/slip_chg3)+Rth)
^2+(Xth+X2)^2)*((R2)/slip_chg3));
```

$$Torque\_speed3 := 122.7836054 \frac{1}{\pi\left(\left(.33\frac{1}{1-\frac{1}{1200}\, n\_m3}+.1536577185\right)^2+.5968023572\right)\left(1-\frac{1}{1200}\, n\_m3\right)}$$

```
> plot(Torque_speed3, n_m3=-1550..4500);
```

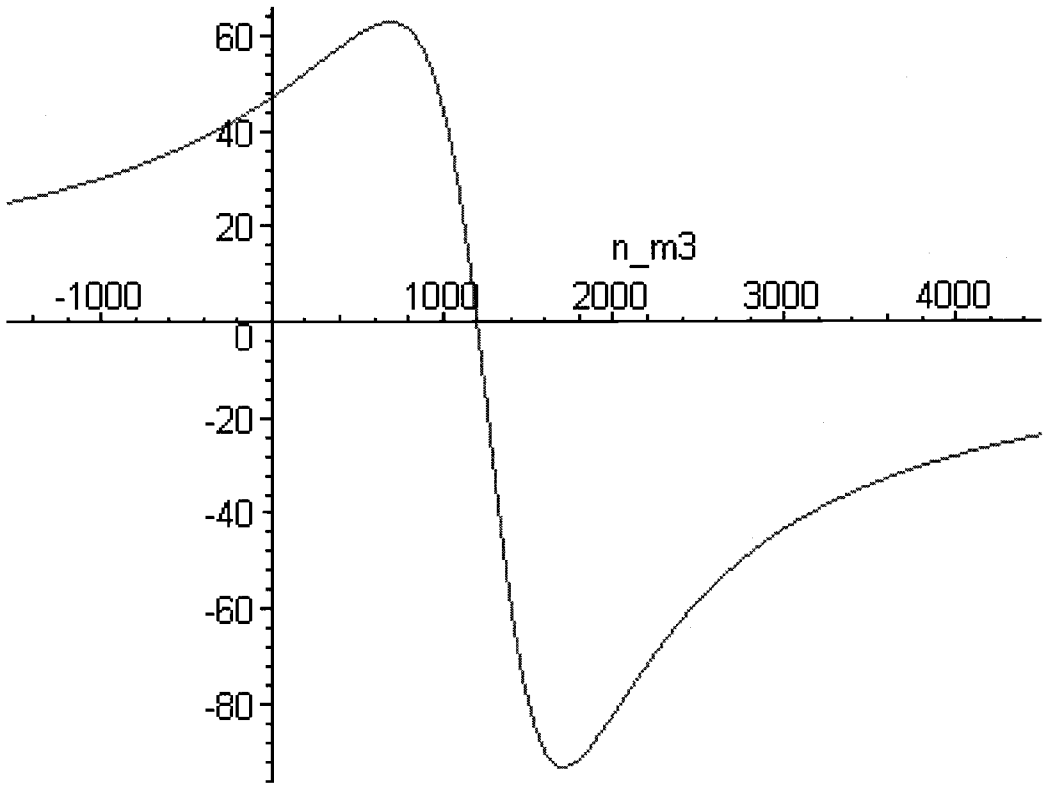

Required External Inductance

Rotor Frequency

```
> f_rot:=f;#*s_required;
```

$$f\_rot := 60$$

Intrinsic Inductor Resistance

```
> Rlex:=.638;
```

$$Rlex := .638$$

Additional Required Series Resistance

```
> Rser:=1.04;
```

$$Rser := 1.04$$

Final required Inductor Resistance

```
> Rlex:=Rlex+Rser;
```

$$Rlex := 1.678$$

>

Equivalent Resistance using Req1 above

```
> Rext1:=(Rlex*Req1)/(Rlex-Req1);
```

$$Rext1 := 1.684108789$$

Equivalent Resistance using Req2 above

```
> Rext2:=(Rlex*Req2)/(Rlex-Req2);
```

$$Rext2 := -.3015528951$$

Equivalent Reactance from Req1

```
> Xlex1:=99*Rext1;
```

$$Xlex1 := 166.7267701$$

Equivalent Reactance from Req2

```
> Xlex2:=99*Rext2;
```

$$Xlex2 := -29.85373661$$

Convert Xlex to Lext

```
> Lex:=evalf(Xlex1/(2*Pi*f_rot));
```

$$Lex := .4422564934$$

E. APPENDIX E: MATLAB Code for Per-Phase Equivalent Circuit Parameter Values and their Solutions

The Code

```
% Anthony Schacher

clear all

clc

%dc Measurements

a=1.106;                % Rotor to Stator Turns Ratio

Rs1=.3964;              %Phase 1 Stator Resitance

Rs2=.3121;              %Phase 2 Stator Resitance

Rs3=.3613;              %Phase 3 Stator Resitance

Rs=(Rs1+Rs2+Rs3)/3;     %Average Stator Resitance

R1=Rs/2;                %Average Stator Resistance per Phase

R2=.8;                  %Measured Stator Resistance

R2=R2/2;

R2=R2/(a^2);

ns=1200;                %Synchronous Motor Speed


% Blocked Rotor Test Results

Tbr=9.2;                %Blocked Rotor Torque

V1br=37.85;             %Blocked Rotor Voltage Phase 1

V2br=35.02;             %Blocked Rotor Voltage Phase 2

V3br=37.5;              %Blocked Rotor Voltage Phase 3
```

```
Vbr=(V1br+V2br+V3br)/3*sqrt(3);  %Blocked Rotor Average Voltage
Vbrp=Vbr/sqrt(3);            %Blocked Rotor Average Phase Voltage
I1br=47.44;                  %Blocked Rotor Current Phase 1
I2br=37.03;                  %Blocked Rotor Current Phase 2
I3br=42.49;                  %Blocked Rotor Current Phase 3
Ibr=(I1br+I2br+I3br)/3;        %Average Blocked Rotor Current
P1br=382.59;                 %Blocked Rotor Power Phase 1
P2br=478.03;                 %Blocked Rotor Power Phase 2
P3br=907.6;                  %Blocked Rotor Power Phase 3
Pbr=(P1br+P2br+P3br);          %Average Blocked Rotor Power
Pbrp=Pbr/3;                  %Average Blocked Rotor Power per Phase
PF1br=.2105;                 %Blocked Rotor Power Factor Phase 1
PF2br=.3686;                 %Blocked Rotor Power Factor Phase 2
PF3br=.5697;                 %Blocked Rotor Power Factor Phase 3
PFbr=.3829;                  %Average Blocked Rotor Power Factor
fbr=60;                    %Blocked Rotor Frequency

% No Load Test Results

nnl=1197.5;                  %No Load Rotor Speed
Tnl=0;                     %No Load Torque
V1nl=133.22;                 %No Load Voltage Phase 1
V2nl=132.05;                 %No Load Voltage Phase 2
```

```
V3nl=132.38;                %No Load Voltage Phase 3

Vnl=(V1nl+V2nl+V3nl)/3*sqrt(3);  %Average No Load Voltage

Vnlp=Vnl/sqrt(3);           %Average No Load Phase Voltage

I1nl=24.41;                 %No Load Current Phase 1

I2nl=26.39;                 %No Load Current Phase 2

I3nl=27.96;                 %No Load Current Phase 3

Inl=(I1nl+I2nl+I3nl)/3;     %Average No Load Current

P1nl=581;                   %No Load Power Phase 1

P2nl=308;                   %No Load Power Phase 2

P3nl=236;                   %No Load Power Phase 3

Pnl=(P1nl+P2nl+P3nl);       %Average No Load Power

Pnlp=Pnl/3;                 %Average No Load Power per Phase

PF1nl=.1597;                %No Load Power Factor Phase 1

PF2nl=.2081;                %No Load Power Factor Phase 2

PF3nl=.0323;                %No Load Power Factor Phase 3

PFnl=(PF1nl+PF2nl+PF3nl)/3;  %Average No Load Power Factor

fnl=60;                     %No Load Frequency


%Parameter Calculations


Req=Pbrp/Ibr^2;             %Equivalent Blocked Rotor Resistance

Zbr=Vbrp/Ibr;               %Equivalent Blocked Rotor Impedance

Xbr=sqrt(Zbr^2-Req^2);      %Equivalent Blocked Rotor Reactance
```

```
Znl=Vnlp/Inl;              %No Load Impedance

Rnl=Pnlp/(Inl^2);          %No Load Resistance

Xnl=sqrt(Znl^2-Rnl^2);     %No Load Reactance

X1=.5*Xbr;                 %Stator Reactance

X2=.5*Xbr;                 %Referred Rotor Reactance

thetanl=acos(Pnlp/(Vnlp*Inl));  %Phase angle

thetanl_degrees=thetanl*(180/pi);%converting phase angle into degrees

E1=Vnlp-(Inl*exp(-j*thetanl))*(R1+j*X1);          %Magnetizing Voltage

snl=(ns-nnl)/ns;           %motor Slip at no Load

Rr=R2/snl;                 %Rotor Resistance acounting for slip

Zr=(Rr+j*X2);              %Rotor Impedance accounting for slip

I2=E1/Zr;                  %Reflected Secondary Current

I2=abs(I2);

Pc=Pnlp-(Inl^2*R1)-(I2^2*Rr);  %Power Dissipated in Magnetizing Resistance

Rc=abs(E1)^2/Pc;               %Solve For the Magnetizing Resistance

Qm=Vnlp*Inl*sin(thetanl)-(Inl^2*X1)-(abs(I2)^2*X2);

Xm=abs(E1)^2/Qm;


Output_Parameters_From_Parameter_File=['R1';
        'R2';
        'X1';
        'X2';
        'Rc';
```

```
        'Xm']
format short e
[R1;
 R2;
 X1;
 X2;
 Rc;
 Xm]
```

The Output

```
>>
Output_Parameters_From_Paramete =
R1 = 1.7830e-001
R2 =  3.2700e-001
X1 =  4.0231e-001
X2 =  4.0231e-001
Rc = 9.3632e+001
Xm =  4.6465e+000
```